NAVAL POSTGRADUATE SCHOOL
Monterey, California

AD-A257 563

DTIC
S ELECTE
DEC 1 1992
C D

THESIS

COUPLED ROLL AND DIRECTIONAL STABILITY
CHARACTERISTICS OF SURFACE SHIPS

by

Mary J. Logsdon

June, 1992

Thesis Advisor: Anthony J. Healey

92-30422

REPORT DOCUMENTATION PAGE		Form Approved OMB No. 0704-0188

1a. REPORT SECURITY CLASSIFICATION UNCLASSIFIED	1b. RESTRICTIVE MARKINGS

2a. SECURITY CLASSIFICATION AUTHORITY	3. DISTRIBUTION/AVAILABILITY OF REPORT Approved for public release; distribution is unlimited.
2b. DECLASSIFICATION/DOWNGRADING SCHEDULE	

4. PERFORMING ORGANIZATION REPORT NUMBER(S)	5. MONITORING ORGANIZATION REPORT NUMBER(S)

6a. NAME OF PERFORMING ORGANIZATION Naval Postgraduate School	6b. OFFICE SYMBOL (If applicable) ME	7a. NAME OF MONITORING ORGANIZATION Naval Postgraduate School

6c. ADDRESS (City, State, and ZIP Code) Monterey, California 93943-5000	7b. ADDRESS (City, State, and ZIP Code) Monterey, California 93943-5000

8a. NAME OF FUNDING/SPONSORING ORGANIZATION	8b. OFFICE SYMBOL (If applicable)	9. PROCUREMENT INSTRUMENT IDENTIFICATION NUMBER

8c. ADDRESS (City, State, and ZIP Code)	10. SOURCE OF FUNDING NUMBERS

PROGRAM ELEMENT NO.	PROJECT NO.	TASK NO.	WORK UNIT ACCESSION NO.

11. TITLE (Include Security Classification)
COUPLED ROLL AND DIRECTIONAL STABILITY CHARACTERISTICS OF SURFACE SHIPS

12. PERSONAL AUTHOR(S)
Logsdon, Mary J.

13a. TYPE OF REPORT Engineer's Thesis	13b. TIME COVERED FROM _____ TO _____	14. DATE OF REPORT (Yr., Mo., Day) 1992, June	15. PAGE COUNT 116

16. SUPPLEMENTARY NOTATION: The views expressed in this thesis are those of the author and do not reflect the official policy or position of the Department of Defense or the U.S. Government.

17.	COSATI CODES		18. SUBJECT TERMS (Continue on reverse if necessary and identify by block number) Surface Ship, Directional Stability, Coupled Roll
FIELD	GROUP	SUB-GROUP	

19. ABSTRACT (Continue on reverse if necessary and identify by block number)

The problem of roll, sway and yaw motions of surface ships is considered. A mathematical model is developed which consists of the nonlinear maneuvering equations and incorporates cross coupling between sway force, yaw moment and the roll angle induced during a steady turn. The hydrodynamic derivatives and coefficients of a typical container ship were used as the base-line study model. The coupled system of nonlinear algebraic equations is formulated and solved to predict the steady state roll angle, sway velocity and turning rate as a function of the rudder angle and compared to the decoupled systems currently employed. A local perturbation is implemented in the vicinity of the above steady states to investigate dynamic stability of motion. Sensitivity analysis with respect to important design parameters such as speed loss during turing, approach speed, transverse metacentric height and trim is performed. Results demonstrate the significance of the coupling between roll, sway and yaw and the need to incorporate similar studies in the ship design and analysis process.

20. DISTRIBUTION/AVAILABILITY OF ABSTRACT [XX] UNCLASSIFIED/UNLIMITED [ ] SAME AS RPT. [ ] DTIC USERS	21. ABSTRACT SECURITY CLASSIFICATION Unclassified

22a. NAME OF RESPONSIBLE INDIVIDUAL Anthony J. Healey	22b. TELEPHONE (Include Area Code) (408) 646-3462	22c. OFFICE SYMBOL ME/Hy

Coupled Roll and Directional Stability
Characteristics of Surface Ships

by

Mary J. Logsdon
Lieutenant, United States Navy
M.S., Murray State University, 1974

Submitted in partial fulfillment
of the requirements for the degree of

MASTER OF SCIENCE IN MECHANICAL ENGINEERING

and

MECHANICAL ENGINEER
from the

NAVAL POSTGRADUATE SCHOOL
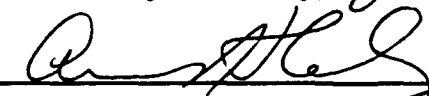June, 1992

Author: _____
Mary J. Logsdon

Approved by: _____
Anthony J. Healey, Thesis Advisor

_____
Anthony J. Healey, Chairman
Department of Mechanical Engineering

_____
Richard S. Elster, Dean of Instruction

ABSTRACT

The problem of roll, sway and yaw motions of surface ships is considered. A mathematical model is developed which consists of the nonlinear maneuvering equations and incorporates cross coupling between sway force, yaw moment and the roll angle induced during a steady turn. The hydrodynamic derivatives and coefficients of a typical container ship were used as the base-line study model. The coupled system of nonlinear algebraic equations is formulated and solved to predict the steady state roll angle, sway velocity and turning rate as a function of the rudder angle. The results are then compared to that of the decoupled systems currently employed. A local perturbation is implemented in the vicinity of the above steady states to investigate dynamic stability of motion. Sensitivity analysis with respect to important design parameters such as speed loss during turning, approach speed, transverse metacentric height and trim is performed. Results demonstrate the significance of the coupling between roll, sway and yaw and the need to incorporate similar studies in the ship design and analysis process.

iii

TABLE OF CONTENTS

LIST OF TABLES

LIST OF FIGURES

I. INTRODUCTION

A. GENERAL

Any study of the motion of a ship through water requires the use of models. The model could be a mathematical representation which attempts to describe the situation symbolically, searching for a quantitative solution, or a physical model which strives to replicate or simulate the actual conditions for the purpose of collecting empirical data. The two can be combined such that they complement each other, or most often, physical models are used to test the validity and accuracy of mathematical models. However, both models fail to completely describe the physical phenomenon. The physical model falls short by the inability to simultaneously satisfy all the parameters describing the problem. The mathematical model suffers by departures from the true state through assumptions made during the development of the equations [Ref. 1]. Notwithstanding these shortcomings, the use of models in predicting a ships response to its environment, i.e., wind and waves, and its own propulsive and control systems is essential in the design process to ensure safety of the ship, performance of its mission, its survivability in extreme conditions and its efficiency during normal operating conditions. [Ref. 1]

In general, the examination of ship motions is separated into: 1) steering and maneuverability (calm water), and 2) seakeeping (waves, current), with motion

1

stability (absence of external excitation) and control (external excitation) some of the primary concerns. [Ref. 1]

The basis of the mathematical model is rigid body dynamics, hence Newton's laws of motion: [Ref. 2]

$$\vec{F} = \frac{d}{dt} x \; (\overrightarrow{linear \; momentum})$$
$$\vec{M} = \frac{d}{dt} x \; (\overrightarrow{angular \; momentum})$$

(1.1)

The ship is free to rotate (roll, pitch, yaw) and translate (surge, sway, heave) in all six degrees of freedom and the forces and moments acting on the vehicle are comprised of: [Ref. 2]

1. Hydrodynamic forces and moments on the bare hull, appendages, rudder and propeller.

2. Inertial reaction forces and moments.

3. Wind, waves and currents.

4. External forces.

Moreover, these forces and moments are dependent upon properties of the rigid body (e.g., geometry, mass, center of gravity), its orientation (i.e., to inertial frame of reference and to the body fixed frame of reference), its dynamics (velocities, accelerations, propeller speed, rudder deflection and deflection rate), and the fluid properties (e.g., density, viscosity, pressure, energy). [Ref. 1]

At this point, the mathematical model has rapidly developed into a very complex and cumbersome system and requires simplification in order to be of practical use. Choice of the body fixed coordinate system to take advantage of any symmetries is one simplification used almost exclusively. Eda, et al, [Ref. 3] found in one study of bulbous bow type ships that the slight asymmetry of the underwater hull form increased significantly in roll such that this simplification was not valid. Another reduction in complexity often used is to separate the lateral motions (sway, yaw, roll) from the longitudinal motions (surge, pitch, heave) [Refs. 4, 5, 6]. Later studies [Refs. 3, 7, 8, 9, 10] account for the loss of speed during a turn by including the surge equation with the lateral motions for maneuvering studies. Seakeeping studies [Refs. 8, 11, 12, 13] heretofore have separated out the roll equations using a one degree of freedom system only, coupling effects were neglected as very small or incorporated as forcing terms. Rutgersson and Ottosson [Ref. 8] superimposed the maneuvering model motions with the seakeeping motions.

As can be ascertained from this discussion, the forces, moments, velocities and accelerations acting upon the vessel are highly nonlinear, involving complex coupling of terms. Linear theory has been successful in predicting and analyzing directionally stable ships with controls fixed for small perturbations [Ref. 14]. In addition, the linear hydrodynamic forces and moments have been reduced to semi-empirical equations based on ship design characteristics such as block coefficient, length,

breadth and draft [Refs. 2, 15]. However, there has been no completely analytical procedure which predicts the nonlinear hydrodynamic forces and moments [Ref. 2].

It is necessary therefore, to combine the mathematical model with the physical model such that the physical model is used to measure these nonlinear forces and moments and incorporate the results in the mathematical model. "The functions that may approximate the hydrodynamic forces and moments can be expressed formally by Taylor expansion around the state of equilibrium with respect to the quantities affecting the different motions, such as the axial speed u, turning rate r, rudder angle δ, etc. The polynomial coefficients thus describing the hydrodynamic forces and motions can be determined from captive model tests at different kinds of basic motions [Ref. 8]. " A complete treatment of the captive model test procedure can be found in *Principals of Naval Architecture, Vol. III* [Ref. 2], and will not be discussed here. The Taylor expansion and subsequent model development is elaborated in the following Chapters.

Captive model tests for the lateral motions are more difficult than for the longitudinal motions due to the large sizes required to adequately represent the physical model. Consequently, there exists little data for the third order coefficients necessary to produce semi-empirical equations for the nonlinear hydrodynamic forces and moments arising from these lateral motions similar to those which exist for the first order terms. One study by Inoue, et al, [Ref. 15] has produced formulations for limited nonlinear terms in yaw and sway based on drift angle and turning rate. The yaw moment coefficients so produced are not in good agreement with the model test

4

data under all conditions of loading and motions induced. Another study done by Son and Nomoto [Ref. 9], utilizes model test data for the third order hydrodynamic coefficients of a SR-108 container ship. In the absence of such semi-empirical formulations for the forces and moments in the equations of motion and access to model test facilities, the aforementioned data, together with vehicle design characteristics, can be used in a mathematical model to ascertain particular information about the coupling of yaw, sway and roll motions.

B.   SCOPE OF THIS THESIS

This research is intended as a bridge between the static roll restoring moment, controls fixed analysis of the coupled lateral motion problem and a fully coupled treatment of a ships roll response to maneuvering in a seaway. As discussed previously, current studies in the area of maneuvering and steering range from three degree of freedom models, to four degree of freedom models which account for the speed loss during a turn. These studies, however, use the equilibrium point in the Taylor expansion of the representative hydrodynamic forces and moments, as straight upright, zero rudder deflection, such that $v_0 = r_0 = \phi_0 = \delta_0 = 0$ and all perturbations and nonlinearity effects are evaluated based on this single nominal point. This research has as its basic premise that the nominal point for the Taylor expansion changes significantly with rudder angle. As a result of this change, the stability characteristics of the ship may also change appreciably, a fact which needs to be established for successful prediction of ship maneuvering response in a seaway.

5

Therefore, the objective is to determine the significance of the coupling of roll into sway and yaw motions as a function of rudder angle. In analyzing this coupled problem, the effects of roll into sway/yaw and conversely, sway/yaw into roll were investigated.

Development of the mathematical model for the coupled yaw, sway, and roll equations of motion along with models for the rudder forces and moments, the righting moment, and the hydrodynamic forces and moments is presented in Chapter II. The final form of the model being reduced to a set of four nonlinear, coupled, first order differential equations. The additional equation is derived from kinematics to relate the roll angle and the roll rate.

In order to utilize Taylor expansion for formulation of the functions which approximate the hydrodynamic forces and moments, the state of equilibrium for the motion parameters, v, r, and ϕ, is established. This is accomplished through steady state analysis. In Chapter III, this analysis is first done for the linear case to obtain an initial approximation for the case of near zero rudder deflection ($\delta \approx 0$). This linear steady state solution is incorporated into the nonlinear steady state analysis in an iterative process which produced the equilibrium values for yaw rate, sway velocity, and roll angle as a function of the rudder deflection in a steady turn. As the rudder angle is incrementally increased, the steady state values from the previous rudder angle are used as the initial approximations to initiate the iterations for the current rudder deflection.

Once the steady state solutions have been computed, their stability properties are established by local perturbation of the coupled equations of motion in the neighborhood of each nominal point. This procedure, described in Chapter IV, yields a generalized eigenvalue problem. The solutions to the eigenvalue problem provide information as to the stability properties of the nominal points and thus characterizes the stability of the coupled sway, yaw and roll motions. Demonstration of the coupling effect on the lateral motions, is shown utilizing comparison to two independent systems:

1. A sway/yaw model represented by two nonlinear equations decoupled from roll in that the hydrodynamic forces and moments are functions of sway velocity (v) and yaw rate (r) only.

2. A roll model represented by the nonlinear roll equation and the kinematic roll rate equation decoupled from sway and yaw in that the hydrodynamic forces and moments are functions of roll angle (ϕ) and roll rate (p) only.

The directional and roll stability characteristics in a steady turn are established by the degree to which the real part of the complex eigenvalues is negative and the magnitude of the roll damping ratio.

Chapter V relates the sensitivity and stability of design parameters such as metacentric height and trim to the coupling between the lateral motions. Results are presented in terms of rudder angle with a qualitative summary at the end of this chapter.

Finally, Chapter VI summarizes the conclusions and presents recommendations for further research and utilization of the mathematical model herein developed.

7

II. MATHEMATICAL MODEL

A. EQUATIONS OF MOTION

For ship motions, the full nonlinear equations of motion in a body fixed axis system are shown in Equations (2.1). These equations reflect an assumption of symmetry along the longitudinal axis (i.e., $y_G=0$). The orthogonal, right-hand axes for the body fixed system is shown in Figure 2.1. The parameters are defined in Table I.

$$\textit{Surge:} \quad m[\dot{u}-x_G(q^2+r^2)+z_G(\dot{q}+pr)-rv+wq] = X \qquad (2.1a)$$

$$\textit{Sway:} \quad m[\dot{v}+x_G(pq+\dot{r})+z_G(qr-\dot{p})+ur-wp] = Y \qquad (2.1b)$$

$$\textit{Heave:} \quad m[\dot{w}+x_G(rp-\dot{q})-z_G(p^2+q^2)+pv-qu] = Z \qquad (2.1c)$$

$$\textit{Roll:} \quad \begin{aligned} I_x\dot{p}+(I_z-I_y)qr-I_{xy}(pq+\dot{r})-mz_G(\dot{v}+ur-wp) \\ = K-\Delta GZ(\phi) \end{aligned} \qquad (2.1d)$$

$$\textit{Pitch:} \quad \begin{aligned} I_y\dot{q}-(I_z-I_x)rp-I_{xz}(r^2-p^2)+m[z_G(\dot{u}+qw-rv)- \\ x_G(\dot{w}+pv-qu)]=M \end{aligned} \qquad (2.1e)$$

$$\textit{Yaw:} \quad I_z\dot{r}+(I_y-I_x)pq+I_{xz}(qr-\dot{p})+mx_G(\dot{v}+ur-wp) = N \qquad (2.1f)$$
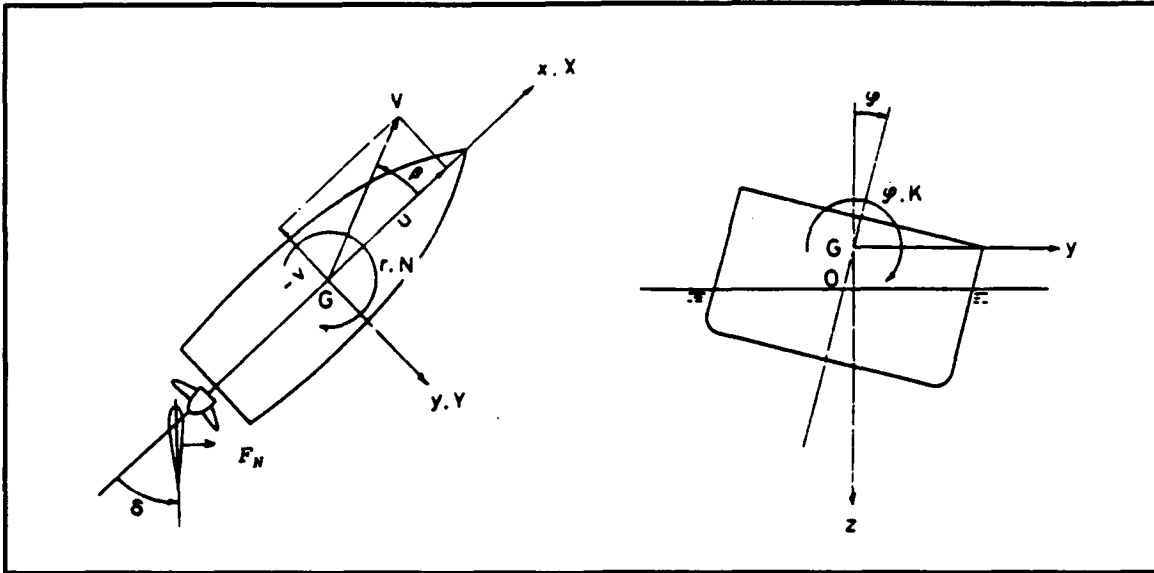
Figure 2.1: Coordinate System [Ref. 11]

B. SIMPLIFYING ASSUMPTIONS

For the purpose of this investigation, a mathematical model having three degrees of freedom vice the six degrees of freedom depicted in Equations (2.1) was used. The following simplifying assumptions were made:

1. The rotational velocity and acceleration about the y-axis are zero. ($q = 0$ and $\dot{q} = 0$)

2. The translational velocity and acceleration in the z direction are zero. ($w = 0$ and $\dot{w} = 0$)

3. The vertical heave and pitch motions are decoupled from the horizontal plane motions.

4. The product of inertia I_{xz} is very small and can be neglected.

5. The surge equation is substituted by an algebraic equation which is a function of u, V, and δ.

6. The longitudinal center of gravity, (LCG) and the longitudinal center of buoyancy, (LCB) are at midship.

9

7. The vertical center of gravity, (VCG) is on the centerline.

8. The only important forces and moments acting on the ship induced by the rudder are those due to rudder deflection. Forces and moments due to $\dot{\delta}$ and $\ddot{\delta}$ are negligible. [Ref. 2]

TABLE I. EQUATIONS OF MOTION PARAMETERS

Parameter	Description
x,y,z	Distance along the principal axes
u,v,w	Translational velocity components of ship relative to fluid along body axes
p,q,r	Rotational velocity components of ship relative to inertial reference system along body axes
X,Y,Z	Hydrodynamic force components along body axes
K,M,N	Hydrodynamic moment components along body axes
ψ,θ,ϕ	ψ yaw angle: bow to starboard positive θ pitch angle: bow up positive ϕ roll angle: starboard down positive
m	Mass of ship
x_G, y_G, z_G	Coordinates of the center of gravity in the body axis system
I_X, I_Y, I_Z	Moments of inertia about the body axis system
I_{XZ}, I_{YZ}, I_{XY}	Products of inertia about the body axis system
∇	Displacement volume of ship
Δ	Displacement weight of ship
$GZ(\phi)$	Righting moment as a function of roll angle
δ	Rudder angle in radians
V	Initial velocity of ship
ρ	Mass density of sea water
L	Ship length between perpendiculars (LBP)

10

Applying these assumptions to Equations (2.1), the three degree of freedom equations of motion for the model used are given in Equations (2.2).

$$\textit{Sway:} \qquad m[\dot{v}+x_G\dot{r}-z_G\dot{p}+ur] = Y \qquad\qquad (2.2a)$$

$$\textit{Roll:} \qquad I_x\dot{p}-mz_G(\dot{v}+ur) = K-\Delta GZ(\phi) \qquad\qquad (2.2b)$$

$$\textit{Yaw:} \qquad I_z\dot{r}+mx_G(\dot{v}+ur) = N \qquad\qquad (2.2c)$$

Equations (2.2) are nondimensionalized for ease of working between model test data and actual ship test data using the relationships shown in Table II.

To demonstrate the use of these nondimensionalizing terms, substitution of the appropriate values from Table II into Equation (2.2a) yields:

$$\left(\frac{1}{2}\rho L^3\right)m'[\left(\frac{V^2}{L}\right)\dot{v}'+(Lx_G')\left(\frac{V^2}{L^2}\dot{r}'\right)-(Lz_G')\left(\frac{V^2}{L^2}\dot{p}'\right)+(Vu')\left(\frac{V}{L}r'\right)] = \left(\frac{1}{2}\rho L^2V^2\right)Y'$$

11

TABLE II. NONDIMENSIONAL PARAMETER RELATIONSHIPS

$v' = \dfrac{v}{V}$	$\dot{v}' = \dot{v}\left(\dfrac{L}{V^2}\right)$	$Y' = Y\left(\dfrac{1}{\frac{1}{2}\rho L^2 V^2}\right)$
$r' = r\left(\dfrac{L}{V}\right)$	$\dot{r}' = \dot{r}\left(\dfrac{L^2}{V^2}\right)$	$N' = N\left(\dfrac{1}{\frac{1}{2}\rho L^3 V^2}\right)$
$\phi' = \phi$	$\dot{\phi}' = \dot{\phi}\left(\dfrac{L}{V}\right)$	$K' = K\left(\dfrac{1}{\frac{1}{2}\rho L^3 V^2}\right)$
$p' = p\left(\dfrac{L}{V}\right)$	$\dot{p}' = \dot{p}\left(\dfrac{L^2}{V^2}\right)$	$u' = \dfrac{u}{V}$
$m' = m\left(\dfrac{1}{\frac{1}{2}\rho L^3}\right)$	$x_G = x_G\left(\dfrac{1}{L}\right)$	$z_G = z_G\left(\dfrac{1}{L}\right)$
$I_x = I_x\left(\dfrac{1}{\frac{1}{2}\rho L^5}\right)$	$I_z = I_z\left(\dfrac{1}{\frac{1}{2}\rho L^5}\right)$	$\Delta GZ(\phi)' =$ $\Delta GZ(\phi)\left(\dfrac{1}{\frac{1}{2}\rho L^3 V^2}\right)$

simplifying by factoring out (V^2/L):

$$\left(\frac{1}{2}\rho L^2 V^2\right) m' [\dot{v}'+x_G'\dot{r}'-z_G'\dot{p}'+u'r'] = \left(\frac{1}{2}\rho L^2 V^2\right) Y'$$

and Equation (2.2a) becomes Equation (2.3) in nondimensional form.

$$m' [\dot{v}' + x_G'\dot{r}' - z_G'\dot{p}' + u'r'] = Y' \qquad (2.3)$$

Since Equation (2.3) and Equation (2.2a) are of the same form, the prime notation will be dropped and all equations will be considered as represented in nondimensional form unless otherwise indicated.

C. FORCE AND MOMENT REPRESENTATION

Using the method of Abkowitz and Strom-Tejsen [Ref. 2], the sway force, roll moment and yaw moment can be expressed as Equations (2.4).

$$\text{Sway Force:} \quad Y = f_1(u,v,r,\dot{u},\dot{v},\dot{r},\phi,\dot{\phi},\delta) \qquad (2.4a)$$

$$\text{Roll Moment:} \quad K = f_2(u,v,r,\dot{u},\dot{v},\dot{r},\phi,\dot{\phi},\ddot{\phi},\delta) \qquad (2.4b)$$

$$\text{Yaw Moment:} \quad N = f_3(u,v,r,\dot{u},\dot{v},\dot{r},\phi,\dot{\phi},\delta) \qquad (2.4c)$$

A third order Taylor expansion of f_1, f_2, and f_3 can be expressed as Equations (2.5).

$$f_1 = Y_v v + Y_{\dot{v}}\dot{v} + Y_{vvv}v^3 + Y_{vrr}vr^2 + Y_r r + Y_{rrr}r^3 + Y_{vvr}v^2 r +$$
$$Y_\phi\phi + Y_{\dot{\phi}}\dot{\phi} + Y_{vv\phi}v^2\phi + Y_{v\phi\phi}v\phi^2 + Y_{r\phi\phi}r\phi^2 + Y_{rr\phi}r^2\phi + Y(\delta) + Y_0 \qquad (2.5a)$$

13

$$f_2 = K_v v + K_{vvv} v^3 + K_{vvr} v^2 r + K_r \dot{r} + K_{rrr} r^3 + K_{vrr} v r^2 + K_\phi \phi + K_{\dot\phi} \dot\phi + K_{\ddot\phi} \ddot\phi +$$

$$K_{vv\phi} v^2 \phi + K_{v\phi\phi} v \phi^2 + K_{r\phi\phi} r \phi^2 + K(\delta) + K_0 - \Delta GZ(\phi) \qquad (2.5b)$$

$$f_3 = N_v v + N_{\dot v} \dot v + N_{vvv} v^3 + N_{vrr} v r^2 + N_r \dot{r} + N_{\dot r} \dot{r} + N_{rrr} r^2 + N_{vvr} v^2 r +$$

$$N_\phi \phi + N_{\dot\phi} \dot\phi + N_{vv\phi} v^2 \phi + N_{v\phi\phi} v \phi^2 + N_{rr\phi} r^2 \phi + N_{r\phi\phi} r \phi^2 + N(\delta) + N_0 \qquad (2.5c)$$

The coefficients in Equations (2.5) are the hydrodynamic coefficients and represent the partial derivative with respect to the subscripted variable. For example, Y_v means $\dfrac{\partial Y}{\partial v}$ and Y_{vrr} means $\dfrac{\partial}{\partial v}\left(\dfrac{\partial^2 Y}{\partial r^2}\right)$. The terms Y_0, K_0, and N_0 are the sway force, roll moment and yaw moment induced by the propeller respectively. In a similar manner $Y(\delta)$, $K(\delta)$ and $N(\delta)$ represent the force and moments induced by the rudder. The righting moment due to the static stability of the ship is represented by the $\Delta GZ(\phi)$ term.

D. RUDDER FORCE AND MOMENT REPRESENTATION

The expressions used to determine the rudder force and moments were taken from Son and Nomoto [Ref. 9] and are presented in Equations (2.6) and (2.7). The parameters are defined in Table III.

$$Y(\delta) = -(1 + a_H) F_N \cos(\delta) \qquad (2.6a)$$

$$K(\delta) = (1 + a_H) z_R F_N \cos(\delta) \qquad (2.6b)$$

$$N(\delta) = -(x_R + a_H x_H) F_N \cos(\delta) \qquad (2.6c)$$

14

TABLE III. RUDDER FORCE AND MOMENT PARAMETERS

Parameter	Description
a_H	Rudder to hull interaction coefficient
F_N	Normal force action on the rudder
z_R	z coordinate of point on which rudder force Y_δ acts
x_R	x coordinate of point on which rudder force Y_δ acts
x_H	x coordinate of point on which normal force F_N acts
Λ	Rudder aspect ratio
A_R	Rudder area
V_R	Effective rudder inflow velocity
α_R	Effective rudder inflow angle
u_R, v_R	Components of rudder effective inflow velocity
ϵ	constant in Equation (2.7c)
u_p	Effective propeller inflow velocity
k	constant in Equation (2.7c)
K_T	Thrust coefficient
J	Advance coefficient
n	Number of propeller revolutions per second
D	Propeller diameter
w_p	Effective propeller wake fraction
τ	constant in Equation (2.7e)
x_p	x coordinate of propeller position
c_{pv}, c_{pr}	propeller flow rectification coefficients
γ	flow rectification coefficients
$c_{\delta r}, c_{\delta rrr}, c_{\delta rrv}$	rudder wake coefficients

15

$$F_N = \left(\frac{6.13\Lambda}{\Lambda+2.25}\right)\left(\frac{A_R}{L^2}\right) V_R^2 \sin(\alpha_R) \qquad (2.7\text{a})$$

$$V_R = \sqrt{u_R^2 + v_R^2} \qquad (2.7\text{b})$$

$$u_R = u_p\epsilon\sqrt{1 + \frac{8kK_T}{\pi J^2}} \qquad (2.7\text{c})$$

$$J = \frac{u_p V}{nD} \qquad (2.7\text{d})$$

$$u_p = u[(1-w_p)+\tau\{(v+x_p r)^2+c_{pv}v+c_{pr}r\}] \qquad (2.7\text{e})$$

$$v_R = \gamma v+c_{\delta r}r+c_{\delta rr}r^3+c_{\delta rrv}r^2 v \qquad (2.7\text{f})$$

$$\alpha_R = \delta + \tan^{-1}\left(\frac{v_R}{u_R}\right) \qquad (2.7\text{g})$$

E. RIGHTING MOMENT REPRESENTATION

For the initial part of the righting arm curve and for wall sided ships, Equation (2.8) gives a good approximation for the function GZ(ϕ). [Ref. 16]

$$GZ(\phi) = \overline{GM}\sin(\phi) + \frac{\overline{BM}}{2}\tan^2(\phi)\sin(\phi) \qquad (2.8)$$

where
$\overline{GM}$ = the transverse metacentric height
$\overline{BM}$ = the transverse metacentric radius
ϕ = the roll angle

Equation (2.8) expresses the fact that for most ships of fairly rectangular midship section, the GZ(ϕ) curve exhibits the typical characteristics of a hardening

16

spring restoring moment. The spring constant is an increasing function of the roll angle ϕ. To see this, we use the Taylor series expansion up to third order for the trigonometric functions:

$$\sin(\phi) = \phi - \frac{1}{6}\phi^3$$

$$\tan(\phi) = \phi + \frac{1}{3}\phi^3$$

Therefore, if terms higher than third order are neglected:

$$\tan^2(\phi)\sin(\phi) = \left(\phi + \frac{1}{3}\phi^3\right)^2\left(\phi - \frac{1}{6}\phi^3\right) = \phi^2\left(\phi - \frac{1}{6}\phi^3\right) = \phi^3 ,$$

and substituting into Equation (2.8) yields:

$$GZ(\phi) = \overline{GM}\left(\phi - \frac{1}{6}\phi^3\right) + \frac{1}{2}\overline{BM}\phi^3 = \overline{GM}\phi + \left(\frac{1}{2}\overline{BM} - \frac{1}{6}\overline{GM}\right)\phi^3 .$$

Now for most ships, $3\overline{BM} > \overline{GM}$, which means that the leading cubic coefficient in the $GZ(\phi)$ curve is positive and the curve concaves up as would a hardening spring.

F.   STATE-SPACE REPRESENTATION

Combining Equations (2.2) and (2.4) and rearranging the terms, the equations of motion can be expressed in vector form:

17

$$\dot{z} = F(z, \delta)$$

(2.9)

where z is the state vector $[v\ r\ p\ \phi]^T$.

Equation (2.9) is more conveniently expressed in matrix notation as is shown in Equations (2.10). The last matrix equation is derived from the kinematic roll rate.

$$\begin{bmatrix} (mx_G-N_{\dot{v}}) & (I_z-N_{\dot{r}}) & 0 & -N_{\dot{\phi}} \\ (m-Y_{\dot{v}}) & (mx_G-Y_{\dot{r}}) & -mz_G & -Y_{\dot{\phi}} \\ -mz_G & 0 & (I_z-K_{\dot{p}}) & -K_{\dot{\phi}} \\ 0 & 0 & 0 & 1 \end{bmatrix} \begin{bmatrix} \dot{v} \\ \dot{r} \\ \dot{p} \\ \dot{\phi} \end{bmatrix} = \begin{bmatrix} f_Y \\ f_S \\ f_R \\ p \end{bmatrix}$$

(2.10a)

$$f_Y = N_v v + N_{vvv} v^3 + N_{vrr} vr^2 + (N_r - mx_G u)r + N_{rrr} r^3 + N_{vvr} v^2 r + N_\phi \phi + N_{vv\phi} v^2\phi + N_{v\phi\phi} v\phi^2 + N_{rr\phi} r^2\phi + N_{r\phi\phi} r\phi^2 + N(\delta) + N_0$$

(2.10b)

$$f_S = Y_v v + Y_{vvv} v^3 + Y_{vrr} vr^2 + (Y_r - mu)r + Y_{rrr} r^3 + Y_{vvr} v^2 r + Y_\phi \phi + Y_{vv\phi} v^2\phi + Y_{v\phi\phi} v\phi^2 + Y_{rr\phi} r^2\phi + Y_{r\phi\phi} r\phi^2 + Y(\delta) + Y_0$$

(2.10c)

$$f_R = K_v v + K_{vvv} v^3 + K_{vvr} v^2 r + (K_r + mz_G u)r + K_{rrr} r^3 + K_{vrr} vr^2 + K_\phi \phi + K_{vv\phi} v^2\phi + K_{v\phi\phi} v\phi^2 + K_{rr\phi} r^2\phi + K_{r\phi\phi} r\phi^2 + K(\delta) + K_0 - \Delta GZ(\phi)$$

(2.10d)

18

III. STEADY STATE REPRESENTATION

A. LINEAR STEADY STATE SOLUTIONS

With the above third order Taylor expansion, the equations of motion represented by Equations (2.10) are highly nonlinear, the solution of which depends upon the initial and equilibrium conditions. The steady state condition requires the acceleration terms $\dot{v}$, $\dot{r}$, $\dot{p}$, $\dot{\phi}$ to be equal to zero. Thus Equation (2.10a) reduces to Equation (3.1) for steady state:

$$\begin{vmatrix} f_Y \\ f_S \\ f_R \\ p \end{vmatrix} = [0] \tag{3.1}$$

where f_Y, f_S, and f_R are defined in Equations (2.10).

The numerical solution to Equation (3.1) is an iterative process which depends upon a fairly accurate initial estimate of the root for convergence. This starting point can be determined by assuming an equilibrium state of $v_0 = r_0 = p_0 = \phi_0 = 0$ and a very small initial rudder deflection ($\delta_0 \leq 1°$). Application of these assumptions to Equation (3.1) yields the linear, steady-state, yaw-sway-roll equations of motion in Equation (3.2).

19

$$\begin{bmatrix} N_v & (N_r - mx_G u) & N_\phi \\ Y_v & (Y_r - mu) & Y_\phi \\ K_v & (K_r + mz_G u) & (K_\phi - \Delta GM) \end{bmatrix} \begin{bmatrix} v \\ r \\ \phi \end{bmatrix} = \begin{bmatrix} -N(\delta) - N_0 \\ -Y(\delta) - Y_0 \\ -K(\delta) - K_0 \end{bmatrix} \qquad (3.2)$$

Equation (3.2) is in the familiar matrix form $Az = B$, where z is the state vector with p=0.

Various computer subroutines are commercially available which solve this simple system of equations for the state vector values, given the other parameters. The values for the state vector obtained in this manner are then used as the initial estimate in solving the nonlinear system of equations.

B. NONLINEAR STEADY STATE SOLUTION

Once the initial estimate for equilibrium is obtained, the system of nonlinear equations in Equation (3.1) can be solved numerically for the state vector nominal points for each rudder angle, δ. Here again, commercial computer subroutines are available. The Levenberg-Marquardt algorithm with analytic Jacobian was chosen as the solution method [Ref. 17]. Since p=0 in Equation (3.1), the system of nonlinear equations is reduced to three and the Jacobian was determined by Equations (3.3).

$$[J] = \begin{vmatrix} \dfrac{\partial f_Y}{\partial v} & \dfrac{\partial f_Y}{\partial r} & \dfrac{\partial f_Y}{\partial \phi} \\[2mm] \dfrac{\partial f_S}{\partial v} & \dfrac{\partial f_S}{\partial r} & \dfrac{\partial f_S}{\partial \phi} \\[2mm] \dfrac{\partial f_R}{\partial v} & \dfrac{\partial f_R}{\partial r} & \dfrac{\partial f_R}{\partial \phi} \end{vmatrix} \qquad (3.3a)$$

$$\frac{\partial f_Y}{\partial v} = N_v + 3N_{vvv}v^2 + N_{vrr}r^2 + 2N_{vvr}vr + 2N_{vv\phi}v\phi + N_{v\phi\phi}\phi^2 + \frac{\partial N(\delta)}{\partial v} \qquad (3.3b)$$

$$\frac{\partial f_Y}{\partial r} = 2N_{vvr}vr + (N_r - mx_G u) + 3N_{rrr}r^2 + N_{vvr}v^2 + 2N_{rr\phi}r\phi + N_{r\phi\phi}\phi^2 + \frac{\partial N(\delta)}{\partial r} \qquad (3.3c)$$

$$\frac{\partial f_Y}{\partial \phi} = N_\phi + N_{vv\phi}v^2 + 2N_{v\phi\phi}v\phi + N_{rr\phi}r^2 + 2N_{r\phi\phi}r\phi + \frac{\partial N(\delta)}{\partial \phi} \qquad (3.3d)$$

$$\frac{\partial f_S}{\partial v} = Y_v + 3Y_{vvv}v^2 + Y_{vrr}r^2 + 2Y_{vvr}vr + 2Y_{vv\phi}v\phi + Y_{v\phi\phi}\phi^2 + \frac{\partial Y(\delta)}{\partial v} \qquad (3.3e)$$

$$\frac{\partial f_S}{\partial r} = 2Y_{vvr}vr + (Y_r - mu) + 3Y_{rrr}r^2 + Y_{vvr}v^2 + 2Y_{rr\phi}r\phi + Y_{r\phi\phi}\phi^2 + \frac{\partial Y(\delta)}{\partial r} \qquad (3.3f)$$

$$\frac{\partial f_S}{\partial \phi} = Y_\phi + Y_{vv\phi}v^2 + 2Y_{v\phi\phi}v\phi + Y_{rr\phi}r^2 + 2Y_{r\phi\phi}r\phi + \frac{\partial Y(\delta)}{\partial \phi} \qquad (3.3g)$$

$$\frac{\partial f_R}{\partial v} = K_v + 3K_{vvv}v^2 + K_{vrr}r^2 + 2K_{vvr}vr + 2K_{vv\phi}v\phi + K_{v\phi\phi}\phi^2 + \frac{\partial K(\delta)}{\partial v} \qquad (3.3h)$$

$$\frac{\partial f_R}{\partial r} = 2K_{vvr}vr + (K_r + mz_G u) + 3K_{rrr}r^2 + K_{vvr}v^2 + 2K_{rr\phi}r\phi + K_{r\phi\phi}\phi^2 + \frac{\partial K(\delta)}{\partial r} \qquad (3.3i)$$

$$\frac{\partial f_R}{\partial \phi} = K_\phi + K_{vv\phi}v^2 + 2K_{v\phi\phi}v\phi + K_{rr\phi}r^2 + 2K_{r\phi\phi}r\phi + \frac{\partial K(\delta)}{\partial \phi} - \frac{\partial(\Delta GZ(\phi))}{\partial \phi} \qquad (3.3j)$$

$$
\text{where} \quad
\begin{aligned}
N(\delta) &= F_1(v,r) \\
Y(\delta) &= F_2(v,r) \\
K(\delta) &= F_3(v,r)
\end{aligned}
\quad \rightarrow \quad
\begin{aligned}
\frac{\partial N(\delta)}{\partial \phi} &= 0 \\
\frac{\partial Y(\delta)}{\partial \phi} &= 0 \quad (3.3k) \\
\frac{\partial K(\delta)}{\partial \phi} &= 0
\end{aligned}
$$

and

$$
\frac{\partial(\Delta GZ(\phi))}{\partial \phi} = \Delta\left[\overline{GM}\cos(\phi)+\overline{BM}\tan^2(\phi)\left(\frac{1}{\cos(\phi)}+\frac{1}{2}\cos(\phi)\right)\right] \quad (3.3l)
$$

Since F_1, F_2, and F_3 are complicated functions of v and r (Equations (2.6) and (2.7)), the following approximation method was used for evaluation:

$$
\frac{\partial F}{\partial x}\bigg|_{equilibrium=x_0} = \frac{F(x_0) - F(0.99x_0)}{x_0 - 0.99x_0} \quad (3.4)
$$

Each term in the Jacobian is determined by evaluation at the previous nominal point with the initial nominal point determined from linear solutions as described in Section A above.

The result of the numerical solution to the nonlinear equations (Equations (3.1)) is the steady state values for v, r, and ϕ for each rudder angle under steady turning conditions and for a given GM and propeller speed.

C.   TYPICAL RESULTS

Utilizing the solution method depicted in Sections A and B above, PROGRAM COUPLED listed in Appendix A, was developed to predict the steady state roll

22

angle, sway velocity and turning rate of a high speed container ship as a function of rudder angle.

The design characteristics of a SR-108 container ship are presented in Table IV. The hydrodynamic derivatives and coefficients used in the computer simulation are listed in Table V.

For a base-line model, the hydrodynamic derivatives and coefficients were held constant in addition to the Froude number (hence the propeller revolutions), the transverse metacentric height, and speed loss ratio. Therefore, for the figures presented in this section:

$$Froude\ number \qquad Fn = 0.3$$
$$Metacentric\ height \qquad \overline{GM} = 0.3\ m$$
$$Speed\ loss\ ratio \qquad \alpha = 0.6$$

Figures 3.1 through 3.3 show the variation of sway velocity, yaw rate, and roll angle as a function of rudder angle during a steady turn. It can be seen that all steady state variables v, r and ϕ are highly nonlinear functions in δ which is attributed to both the effect of the nonlinear terms in our equations of motion and the fact that the ship speed is reduced during the turn. Had a constant speed, linear model been utilized, v, r and ϕ would appear as straight lines versus δ.

TABLE IV. PRINCIPAL DIMENSIONS OF SR-108 CONTAINER SHIP [Ref. 9]

Items			Ship	Model
Hull Length B. P.	L	(m)	175.00	3.000000
Breadth	B	(m)	25.40	0.435000
Draft Fore	T_F	(m)	8.00	0.137100
Aft	T_A	(m)	9.00	0.154300
Mean	T	(m_3)	8.50	0.145700
Displacement Volume		(m^3)	21,222	0.106860
Height from keel to transverse metacenter	KM	(m)	10.3900	0.17810
Height from keel to center of buoyancy	BM	(m)	4.6154	0.07912
Block coefficient	C_B			0.55900
Prismatic coefficient	C_B			0.58000
Waterplane area coefficient	C_W			0.68600
Midship section coefficient	C_M			0.518 L
LCB from forward Perpendicular				0.240 L
Bilge keel				
Length	L_d	(m)	43.75	0.7500
Depth		(cm)	45.00	0.7714
Rudder Area	A_R	(m^2)	33.0376	0.009709
Height	H	(m)	7.7583	0.133000
Aspect Ratio	Λ			1.821900
Area Ratio	A_R/L_d	(m)		1/45.0
Propeller				
Diameter	D	(m)	6.533	0.112
Pitch Ratio	p			1.009
Expanded Area Ratio				0.670
Boss Ratio				0.180
Number of blades				5

TABLE V. HYDRODYNAMIC DERIVATIVES AND COEFFICIENTS [Ref. 9]

A.) Hull Only

Y_v	-0.0116000	N_v	-0.0038545	K_v	0.00030260
Y_r	0.0024200	N_r	-0.0022200	K_r	-0.00006300
Y_ϕ	-0.0000630	N_ϕ	-0.0001424	K_ϕ	-0.00002100
Y_{vv}	-0.1090000	N_{vv}	0.0014920	K_{vv}	0.00284300
Y_{vrr}	-0.0405000	N_{vrr}	0.0015600	K_{vrr}	0.00105650
Y_{rrr}	0.0017700	N_{rrr}	-0.0022900	K_{rrr}	-0.00004620
Y_{vrr}	0.0214000	N_{vrr}	-0.0424000	K_{vrr}	-0.00055800
$Y_{vv\phi}$	0.0460500	$N_{vv\phi}$	-0.0190580	$K_{vv\phi}$	-0.00120120
$Y_{v\phi\phi}$	0.0030400	$N_{v\phi\phi}$	-0.0053766	$K_{v\phi\phi}$	-0.00007930
$Y_{rr\phi}$	0.0093250	$N_{rr\phi}$	-0.0038592	$K_{rr\phi}$	-0.00024300
$Y_{r\phi\phi}$	-0.0013560	$N_{r\phi\phi}$	0.0024195	$K_{r\phi\phi}$	0.00003569

B.) Propeller and Rudder

a_H	0.237	τ	1.090	$(1-w_p)$	0.816
x_H	-0.480	ϵ	0.921	x_R	-0.500
c_{RX}	0.710	k	0.631	x_p	-0.526
z_R	0.033	$c_{\delta r}$	-0.156	K_T	0.527-0.455J
c_{pv}	0.000	$c_{\delta rrr}$	-0.275	γ	0.088 v>0 0.193 v≤0
c_{pr}	0.000	$c_{\delta rrv}$	1.960	N_p	79.10 Fn=0.2 118.64 Fn=0.3 158.19 Fn=0.4
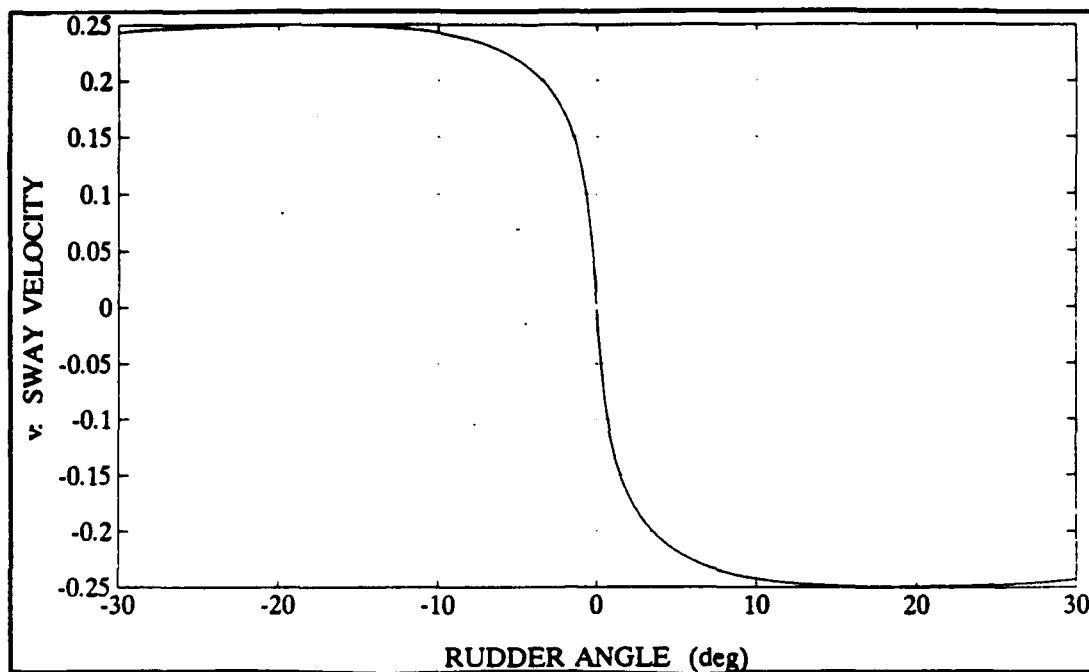
Figure 3.1: Sway Velocity Under Steady Turning
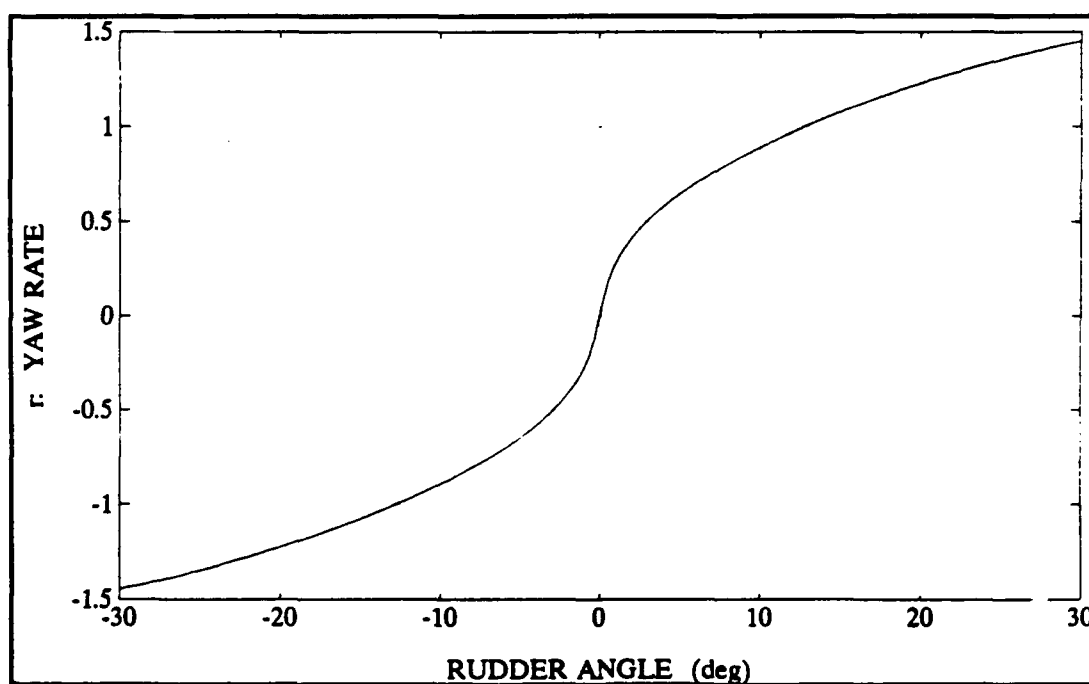
Figure 3.2: Turning Rate Under Steady Turning

26
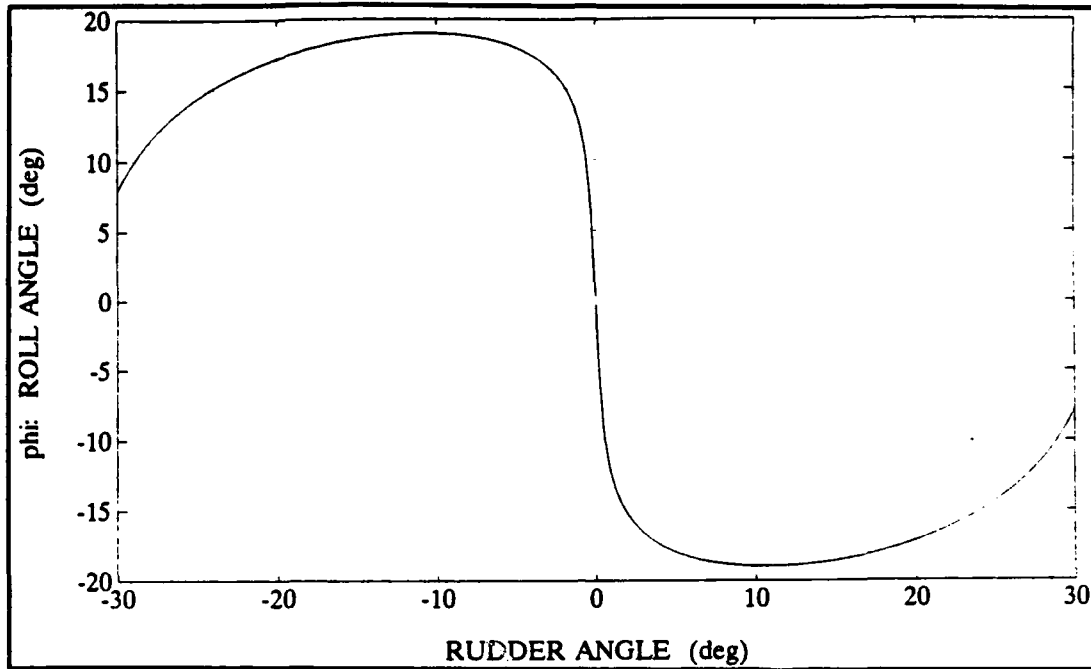
Figure 3.3: Roll Angle Under Steady Turning

IV. STABILITY ANALYSIS

A. COUPLED STEERING AND ROLL EQUATIONS OF MOTION

Once the nominal points are determined for each rudder angle, Equation (2.10a) can be reduced to state-space representation (Equations (3.4)) for stability analysis.

$$B\dot{z} = Az$$

$$\text{where} \quad \dot{z} = \begin{bmatrix} \dot{v} \\ \dot{r} \\ \dot{p} \\ \dot{\phi} \end{bmatrix} \quad ; \quad z = \begin{bmatrix} v \\ r \\ p \\ \phi \end{bmatrix} \tag{4.1a}$$

$$B = \begin{bmatrix} (mx_G - N_{\dot{v}}) & (I_z - N_{\dot{r}}) & 0 & -N_{\dot{\phi}} \\ (m - Y_{\dot{v}}) & (mx_G - Y_{\dot{r}}) & -mz_G & -Y_{\dot{\phi}} \\ -mz_G & 0 & (I_y - K_{\dot{\phi}}) & -K_{\dot{\phi}} \\ 0 & 0 & 0 & 1 \end{bmatrix} \tag{4.1b}$$

$$A = \begin{bmatrix} \dfrac{\partial f_Y}{\partial v} & \dfrac{\partial f_Y}{\partial r} & \dfrac{\partial f_Y}{\partial p} & \dfrac{\partial f_Y}{\partial \phi} \\[2mm] \dfrac{\partial f_S}{\partial v} & \dfrac{\partial f_S}{\partial r} & \dfrac{\partial f_S}{\partial p} & \dfrac{\partial f_S}{\partial \phi} \\[2mm] \dfrac{\partial f_R}{\partial v} & \dfrac{\partial f_R}{\partial r} & \dfrac{\partial f_R}{\partial p} & \dfrac{\partial f_R}{\partial \phi} \\[2mm] \dfrac{\partial p}{\partial v} & \dfrac{\partial p}{\partial r} & \dfrac{\partial p}{\partial p} & \dfrac{\partial p}{\partial \phi} \end{bmatrix} \tag{4.1c}$$

28

Matrix B can be thought of as the generalized mass matrix for the problem while matrix A is the Jacobian matrix of $f(\underline{z},\delta)$ evaluated at each nominal point. For stability analysis purposes, the variables v, r, p, and ϕ are understood to represent small deviations of the actual variables from their respective steady state values as computed in the previous chapter. The rationale behind Equations (4.1) is the introduction of small local perturbations in v, r, p, and ϕ superimposed on their steady turning values. Lyapunov's linearization theorem establishes that stability properties of a nominal point for a nonlinear system can, in general, be deduced from the stability properties of the corresponding linearized system.

The terms in the matrix A are as defined in Equations (3.3) with the following additions:

$$\frac{\partial f_Y}{\partial p} = \frac{\partial f_S}{\partial p} = \frac{\partial f_R}{\partial p} = 0$$

$$\frac{\partial p}{\partial v} = \frac{\partial p}{\partial r} = \frac{\partial p}{\partial \phi} = 0$$

$$\frac{\partial p}{\partial p} = 1$$

Stability can be determined from the solution to the eigenvalue problem:

$$\lambda B z = A z$$
$$or \tag{4.2}$$
$$|A - \lambda B| = 0$$

If all eigenvalues, λ, have negative real parts, the nominal point is asymptotically stable. If at least one eigenvalue is positive, the nominal point is unstable. The degree of stability of the nominal point is therefore related to the real part of the eigenvalues. The more negative they are, the faster the exponential convergence of solutions in time to the nominal point. The imaginary part of the eigenvalues characterizes the frequency content of the oscillatory behavior of the system response.

A subroutine was included in the computer model to solve this eigenvalue problem as a function of rudder angle.

B.   DECOUPLED STEERING EQUATIONS

In order to distinguish the characteristic contributions of the sway and yaw motions from those of roll, the steering equations (Equations (4.3)) were decoupled from the maneuvering equations (Equations (4.1)), resulting in Equations (4.3).

$$\begin{bmatrix} (mx_G - N_{\dot{v}}) & (I_z - N_{\dot{r}}) \\ (m - Y_{\dot{v}}) & (mx_G - Y_{\dot{r}}) \end{bmatrix} \begin{bmatrix} \dot{v} \\ \dot{r} \end{bmatrix} = \begin{bmatrix} f_{YS} \\ f_{SS} \end{bmatrix} \tag{4.3a}$$

$$f_{YS} = Y_v v + Y_{vvv} v^3 + Y_{vrr} vr^2 + (Y_r - mu)r + Y_{rrr} r^3 + Y_{vvr} v^2 r + Y(\delta) \tag{4.3b}$$

$$f_{YS} = N_v v + N_{vvv} v^3 + N_{vrr} vr^2 + (N_r - mx_G u)r + N_{rrr} r^3 + N_{vvr} v^2 r + N(\delta) \tag{4.3c}$$

This decoupling is based on the assumption that all cross coupling coefficients between roll and sway/yaw are zero, which is the usual approximation made for

surface ships where roll is studied independently from sway/yaw. One of the motivations for this study is to evaluate the degree of accuracy of such an approximation.

The additional subscript, S, distinguishes the decoupled steering forces and moments from those of the fully coupled system. Following the same format as before, the state-space formulation for stability analysis is given in Equations (4.4).

$$B_S \underline{\dot{z}}_S = A_S \underline{z}_S$$

$$\text{where} \quad \underline{\dot{z}}_S = \begin{bmatrix} \dot{v} \\ \dot{r} \end{bmatrix} \quad ; \quad \underline{z}_S = \begin{bmatrix} v \\ r \end{bmatrix} \tag{4.4a}$$

$$B_S = \begin{bmatrix} (mx_G - N_{\dot{r}}) & (I_z - N_{\dot{r}}) \\ (m - Y_{\dot{v}}) & (mx_G - Y_{\dot{r}}) \end{bmatrix} \tag{4.4b}$$

$$A_S = \begin{bmatrix} \dfrac{\partial f_{rs}}{\partial v} & \dfrac{\partial f_{rs}}{\partial r} \\[2ex] \dfrac{\partial f_{ss}}{\partial v} & \dfrac{\partial f_{ss}}{\partial r} \end{bmatrix} \tag{4.4c}$$

$$\frac{\partial f_{rs}}{\partial v} = N_v + 3N_{vvv}v^2 + N_{vrr}r^2 + 2N_{vvr}vr + \frac{\partial N(\delta)}{\partial v} \tag{4.4d}$$

$$\frac{\partial f_{rs}}{\partial r} = 2N_{vvr}vr + (N_r - mx_G u) + 3N_{rrr}r^2 + N_{vvr}v^2 + \frac{\partial N(\delta)}{\partial r} \tag{4.4e}$$

$$\frac{\partial f_{ss}}{\partial v} = Y_v + 3Y_{vvv}v^2 + Y_{vrr}r^2 + 2Y_{vvr}vr + \frac{\partial Y(\delta)}{\partial v} \tag{4.4f}$$

$$\frac{\partial f_{ss}}{\partial r} = 2Y_{vvr}vr + (Y_r - mu) + 3Y_{rrr}r^2 + Y_{vvr}v^2 + \frac{\partial Y(\delta)}{\partial r} \tag{4.4g}$$

31

The approximation method of Equation (3.4) was used to determine rudder force and moment contributions in the Jacobian matrix A.

The stability attributable to yaw and sway as a function of rudder angle is thus determined by the solution of the decoupled steering eigenvalue problem in Equations (4.5).

$$\lambda_S B_S \underline{z}_S = A_S \underline{z}_S$$
$$or$$
$$|A_S - \lambda_S B_S| = 0$$

(4.5)

C. DECOUPLED ROLL EQUATIONS

By decoupling the steering equations, the roll equations become uncoupled producing the following relationship:

$$\begin{bmatrix} (I_x - K_{\dot{p}}) & -K_{\phi} \\ 0 & 1 \end{bmatrix} \begin{bmatrix} \dot{p} \\ \dot{\phi} \end{bmatrix} = \begin{bmatrix} f_{RR} \\ p \end{bmatrix}$$

(4.6a)

$$f_{RR} = K_{\phi}\phi + K(\delta) - \Delta GZ(\phi)$$

(4.6b)

The additional subscript, R, refers to the decoupled roll forces and moments and GZ(ϕ) is as given in Equation (2.8). Equations (4.7) are the state-space stability analysis formulations.

$$B_R \underline{\dot{z}}_R = A_R \underline{z}_R \qquad (4.7a)$$

$$\text{where} \quad \underline{\dot{z}}_R = \begin{bmatrix} \dot{\phi} \\ \dot{p} \end{bmatrix} \quad ; \quad \underline{z}_R = \begin{bmatrix} \phi \\ p \end{bmatrix}$$

$$B_R = \begin{bmatrix} (I_x - K_{\dot{p}}) & -K_{\dot{\phi}} \\ 0 & 1 \end{bmatrix} \qquad (4.7b)$$

$$A_R = \begin{bmatrix} \dfrac{\partial f_{RR}}{\partial p} & \dfrac{\partial f_{RR}}{\partial p} \\[2mm] \dfrac{\partial p}{\partial p} & \dfrac{\partial p}{\partial \phi} \end{bmatrix} \qquad (4.7c)$$

$$\frac{\partial f_{RR}}{\partial p} = 0 \quad ; \quad \frac{\partial f_{RR}}{\partial \phi} = K_{\phi} - \frac{\partial(\Delta GZ(\phi))}{\partial \phi} \qquad (4.7d)$$

$$\frac{\partial p}{\partial p} = 1 \quad ; \quad \frac{\partial p}{\partial \phi} = 0$$

$$(4.7e)$$

The expression $\dfrac{\partial(\Delta GZ(\phi))}{\partial \phi}$ is given in Equation (3.3).

Therefore, the stability attributable to roll as a function of rudder angle is attained by solution of the decoupled roll eigenvalue problem of Equations (4.8).

$$\lambda_R B_R \underline{z}_R = A_R \underline{z}_R$$

$$\text{or} \qquad\qquad (4.8)$$

$$|A_R - \lambda_R B_R| = 0$$

33

D. TYPICAL RESULTS

Continuing with the base-line model described in Chapter III Section C, the roots of Equations (4.2), (4.5) and (4.8) were obtained using PROGRAM COUPLED (Appendix A). Figure 4.1 is a plot of the real roots of the fully coupled maneuvering equations as a function of rudder angle. As can be seen, there are three distinct components which were classified as due to roll or due to steering (sway/yaw) by decoupling the steering and roll equations as discussed in Sections B and C above. Figures 4.2 through 4.4 show the three components of the fully coupled system matched with their respective decoupled solutions of Equations (4.5) for steering and Equations (4.8) for roll.

In Figure 4.2, the decoupled roll real roots are constant for each rudder angle, whereas the coupled roots vary with an increasing stability to about five degrees of rudder. The upper steering component shown in Figure 4.3 indicates very little deviation in the coupled and decoupled roots, however, the lower steering component in Figure 4.4 shows a deviation in the two roots as the rudder angle is increased. The steering eigenvalues become increasingly more negative as the rudder angle is increased. This indicates that the steering system is dynamically more stable for a non-zero rudder angle, and as a result, a steering system that is designed to be stable for straight line motions will be even more stable for motions along curved reference paths.

The imaginary roots for the decoupled equations are zero, indicating that all imaginary roots obtained in the solution of the coupled equations are due to roll

34

only. Figure 4.5 shows that for rudder angles less than 15°, the coupled model produces larger values than the decoupled model and for rudder angles greater than 15°, the reverse is true. Comparing Figures 4.2 and 4.5, we can see that the imaginary part of roll response, or the roll frequency of oscillation, can be predicted fairly accurately from the decoupled roll equations. This is not the case for the real part where decoupling the equations results in a severe underestimation.

Figure 4.6 is a root locus plot of the roll eigenvalues for both coupled and uncoupled models. As can be seen, the fully coupled model is more stable than the decoupled model.

The roll damping caused by roll is shown in Figure 4.7. The decoupled roll analysis shows less damping for each rudder angle than does the fully coupled model. Furthermore, the damping increases significantly for large rudder angles. It can be seen that the actual roll damping is significantly larger than what is predicted from the decoupled model, which may underestimate the actual damping ratio by a factor of two to three.
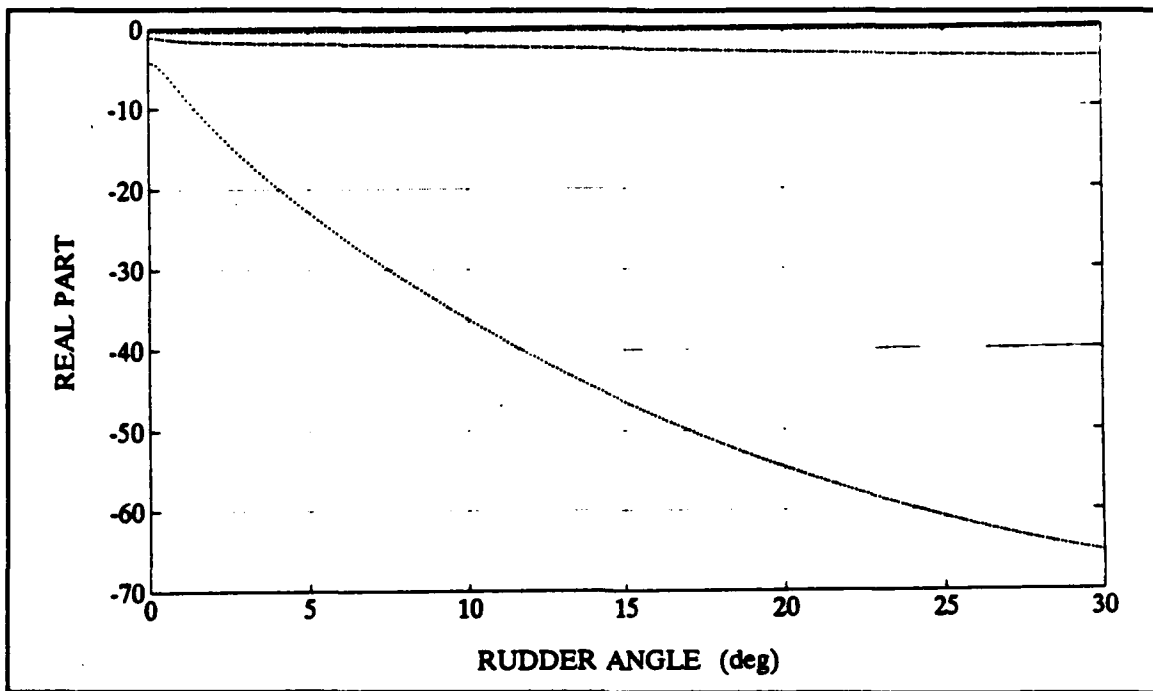
Figure 4.1: Coupled Model Real Eigenvalues
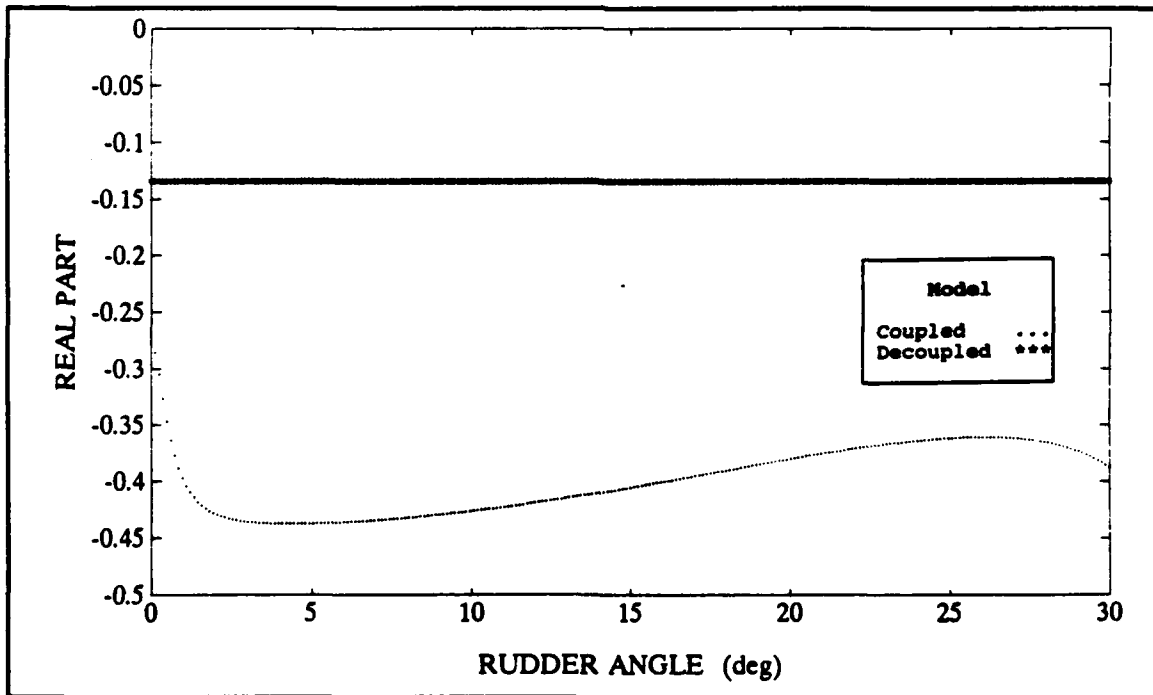
Figure 4.2: Coupled Model and Decoupled Model Roll Eigenvalues
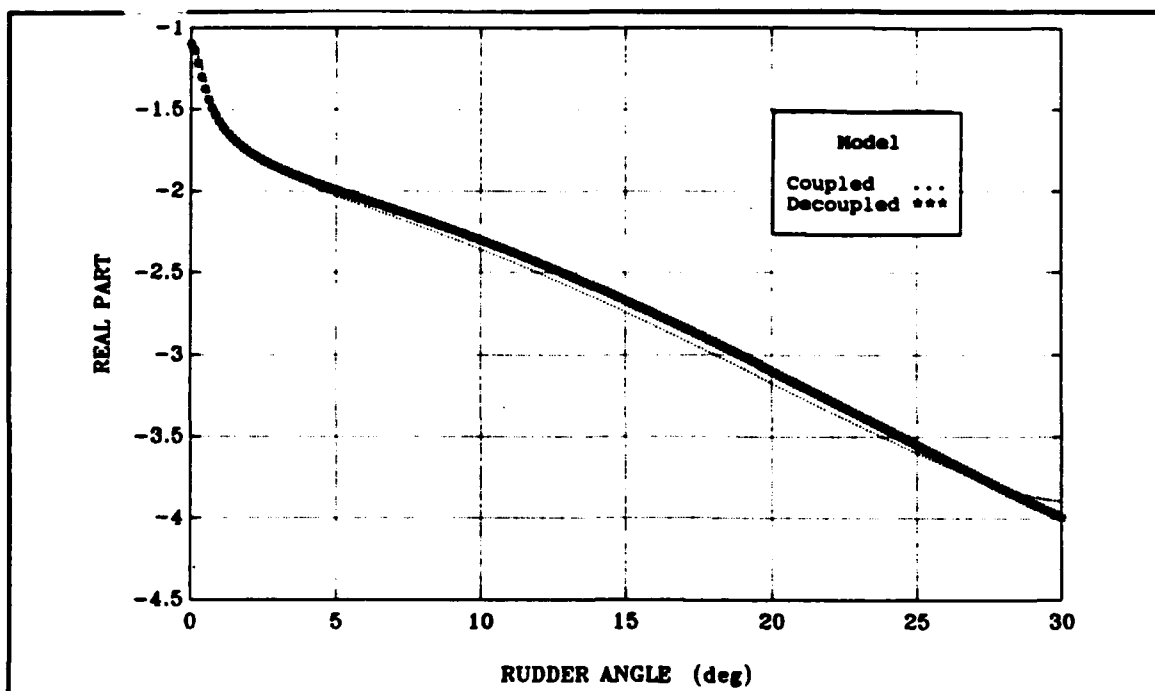
36

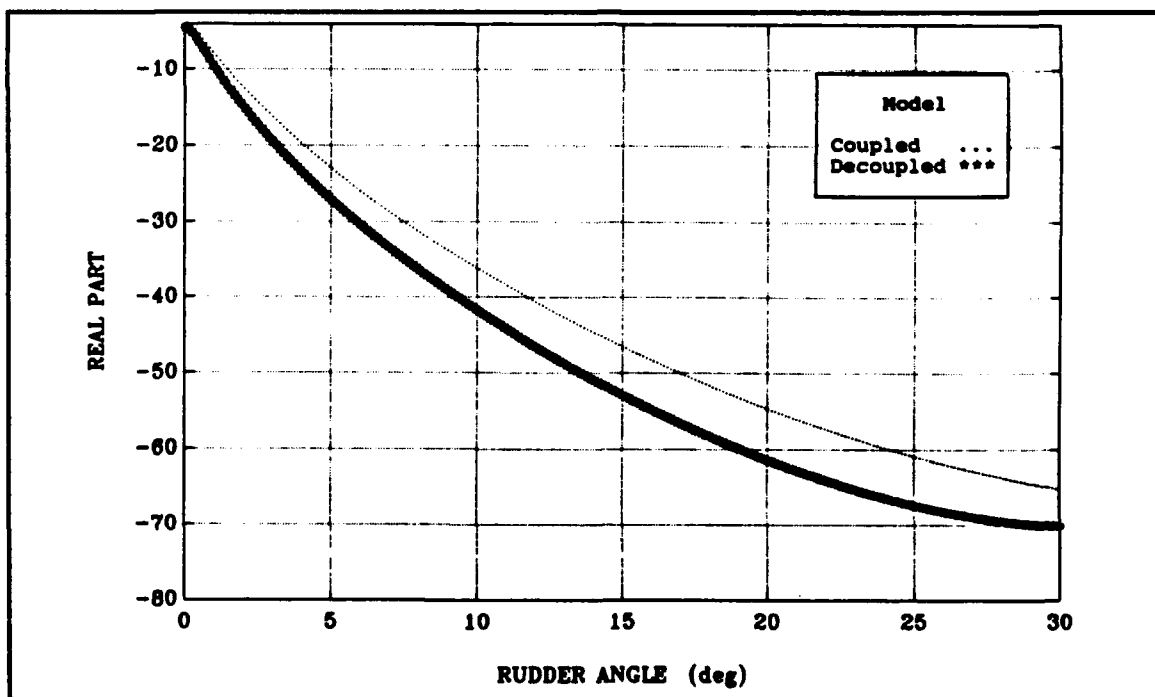**Figure 4.3:** Coupled Model and Decoupled Model Upper Steering Eigenvalues

Figure 4.4: Coupled Model and Decoupled Model Lower Steering Eigenvalues
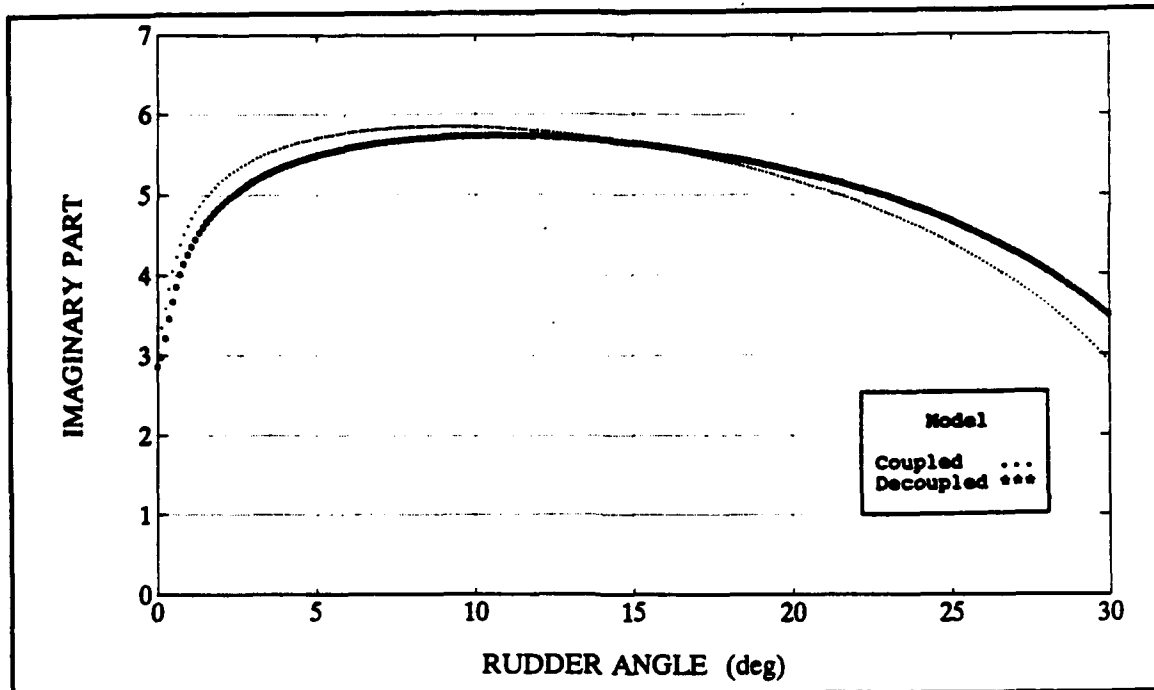
37

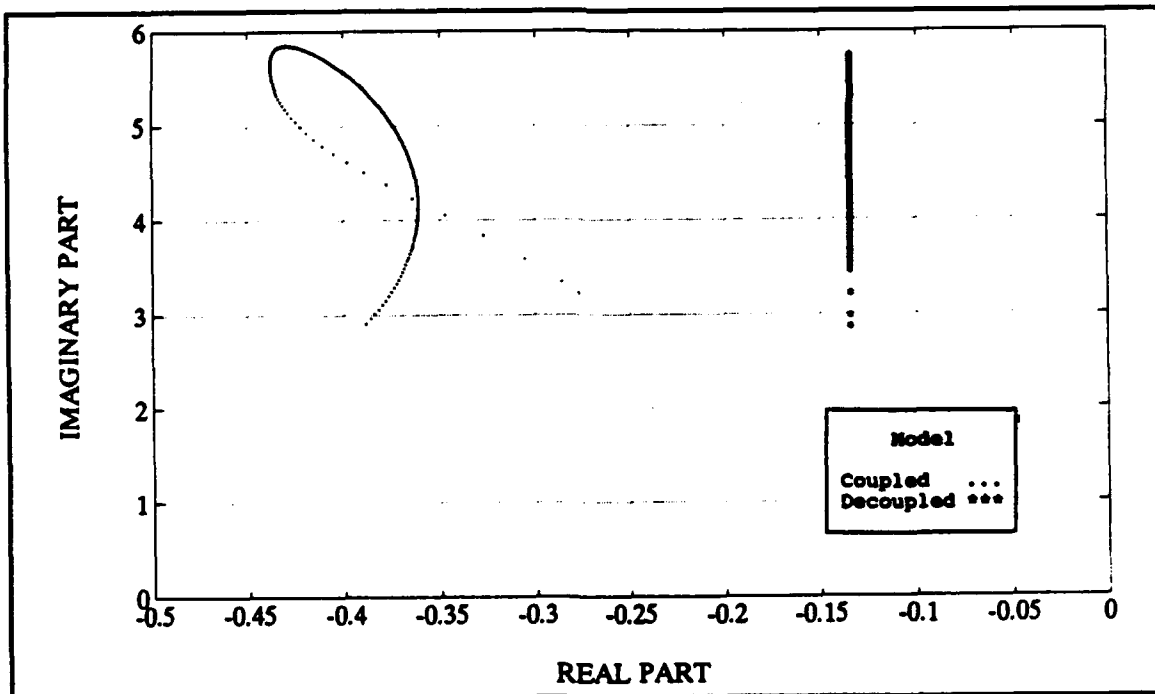**Figure 4.5:** Coupled Model and Decoupled Model Roll Eigenvalues

Figure 4.6: Root Locus of Coupled Model and Decoupled Model Roll Response
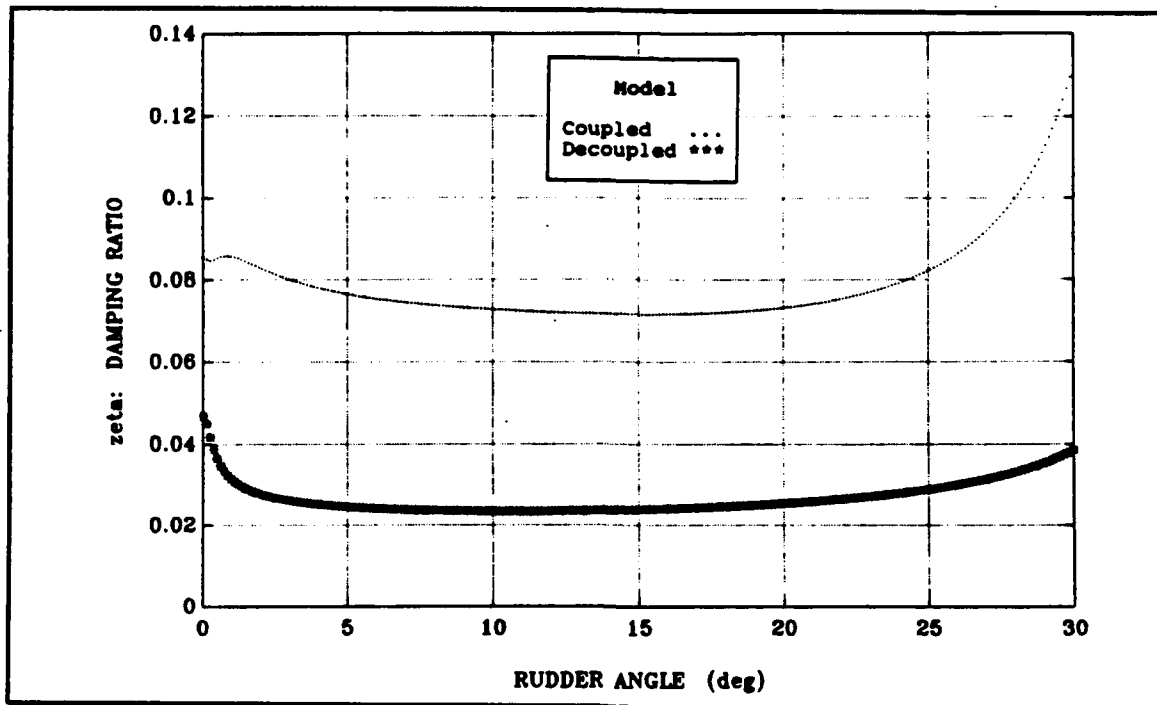
Figure 4.7: Coupled Model and Decoupled Model Damping Ratio

V. SENSITIVITY OF MATHEMATICAL MODEL TO VARIATION IN DESIGN PARAMETERS

A. BACKGROUND

Since actual ships rarely operate under the precise conditions assumed in the development of this mathematical model, changes in certain variables to measure the response sensitivity is prudent, as for any design study. The following sensitivity analysis has this aim in mind as well as to identify any inexplicable response as an area for further study. It must be remembered that certain assumptions were made at the outset which might need refinement as the design spiral continues. For instance, the roll damping term, $K_{\dot{\phi}}$, is assumed to be constant throughout the simulation, although experimental evidence [Ref. 18] suggests that roll damping coefficients are forward speed and motion amplitude dependent. By isolating a parameter, problem areas are enhanced so that a particular parameter can be the focus for analysis of the validity of the assumptions made or the modelling method used.

If, on the other hand, one or more of the dependent variables do not show appreciable sensitivity, further simplifying assumptions could possibly be made when analyzing the more difficult problems of maneuvering in regular and irregular seas.

In the following sections, sensitivity to speed loss during a turn, Froude number of approach spped, metacentric height, operating turn, and righting moment is

evaluated. For brevity, a limited number of plots are presented in each case. Appendix B contains additional plots for metacentric height, Froude number, and speed loss.

B.   SPEED LOSS DURING A TURN AS THE DESIGN PARAMETER

The sensitivity of the model to changes in speed loss during the turn was investigated by holding transverse metacentric height (GM) and Froude number constant:

$$\overline{GM} = 0.3 \ m$$
$$Fn = 0.3$$

In determining the speed loss under steady turning conditions, it was assumed that the water depth was sufficient, i.e. > 110 meters, to neglect this effect [Refs. 2, 3]. However, it has been determined by several sources: Davidson (1944), Shiba (1960), Strom-Tejsen (1965), Eda and Crane (1965), among others [Ref. 2], that speed loss in steady turning is a function of the hull configuration (including rudder) and the turning diameter. Various other sources, [Refs. 3, 9, 10] consider rudder angle as an additional parameter in determining speed loss. In an effort to combine these effects, Figures 25 and 178 and Tables 29(a) and 29(b) from *Principles of Naval Architecture* [Ref. 2], Figure 11 of Eda and Falls [Ref. 3], and Figure 10 of Son and Nomoto [Ref. 9] were used to develop the following simple relationship to represent speed loss:

41

$$\frac{V}{V_0} = 1 - \alpha * \delta_r$$

where

V = steady turning speed
V_0 = approach speed
α = speed loss ratio
δ_r = rudder angle in radians

Variation of the speed loss parameter ranges from no speed loss ($\alpha=0$) to maximum

speed loss ($\alpha=0.73$) during a turn with fixed controls. Results of these effects on

sway velocity, yaw rate and roll angle may be viewed in Figures 5.1 through 5.3. The

influence of speed loss on r is negligible, indicating that in all cases considered, the

ship steady turning rate performance is not affected. On the contrary, v and ϕ show

a relatively significant modification due to speed loss. The sign reversal of the roll

angle plot (Figure 5.3) for large rudder angles is rather uncommon, but it is,

nevertheless, possible as a result of the nonlinearities that are present in the

equations of motion for this model.

The characteristic roots as a function of rudder angle were determined to

establish stability trends. The real roots indicate three distinct components as

previously discussed in Chapter IV, Section C. Both the upper and lower steering

components demonstrate a significant increase in stability with rudder angle but little

variance in stability due to speed loss. The roll component, however, indicates

greater stability as speed loss decreases. We discovered earlier, that the non-zero

values in the root locus were due solely to the roll contribution owing to the

imaginary parts of the steering elements. The damping ratio of the roll contribution

42
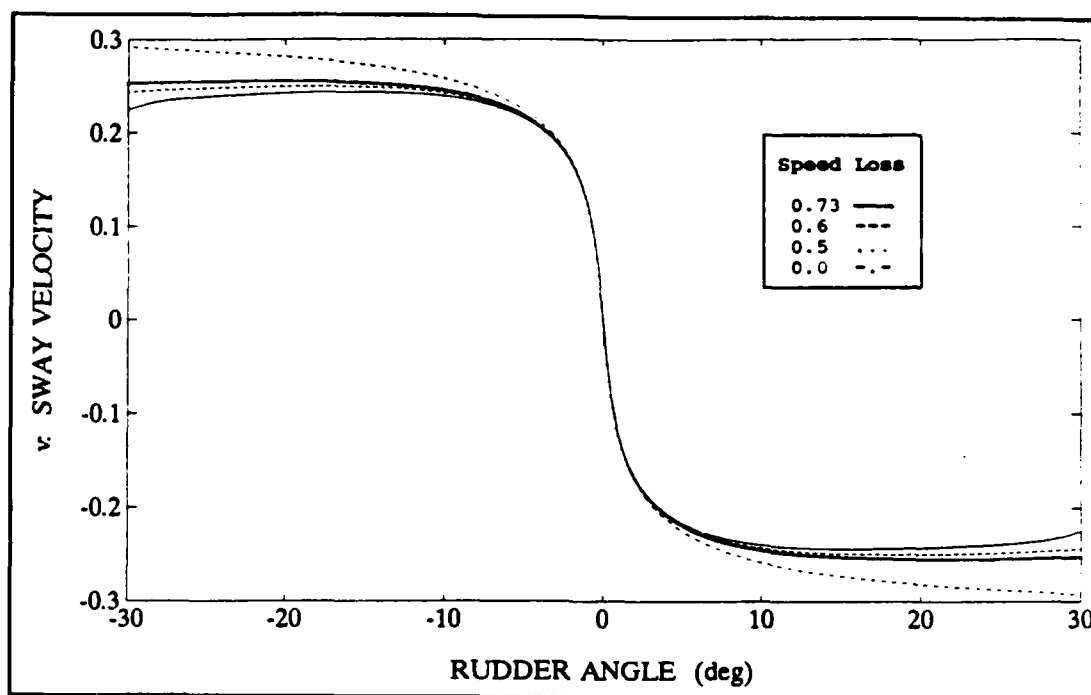
Figure 5.1:   Effect of Speed Loss on Sway Velocity
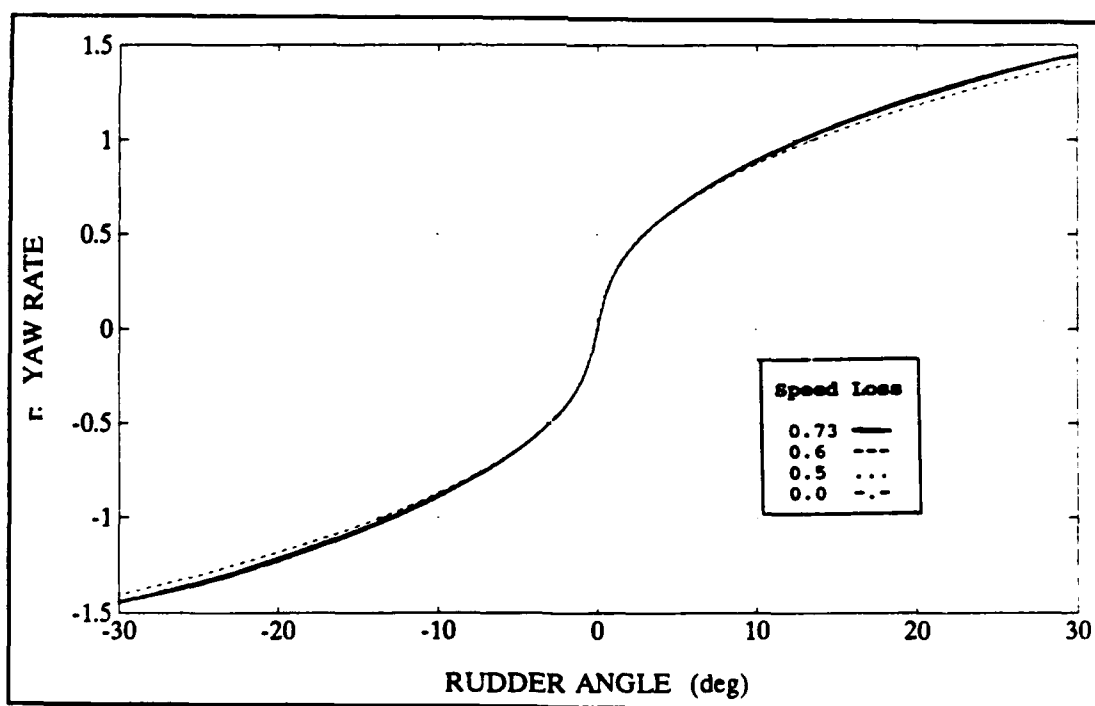
Figure 5.2:   Effect of Speed Loss on Yaw Rate

43
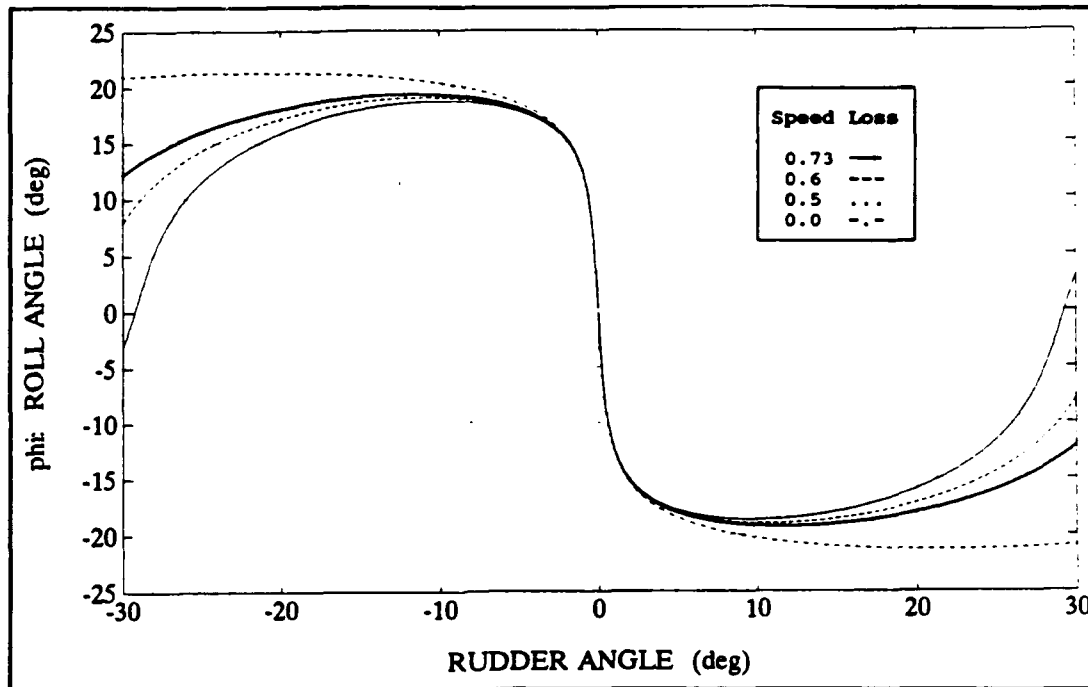
Figure 5.3: Effect of Speed Loss on Roll Angle

imaginary parts of the steering elements. The damping ratio of the roll contribution
is related to both real and imaginary parts of the eigenvalues. Figures 5.4 and 5.5,
for the fully coupled and uncoupled models respectively, show this as a function of
rudder angle. Both models exhibit qualitatively the same trend, with the uncoupled
model showing a significant underestimation of the true damping ratio value.

C.   FROUDE NUMBER AS THE DESIGN PARAMETER

In testing the model sensitivity to Froude number changes, the transverse
metacentric height and speed loss ratio were kept constant:

$$\overline{GM} = 0.3 \, m$$
$$\alpha = 0.6$$
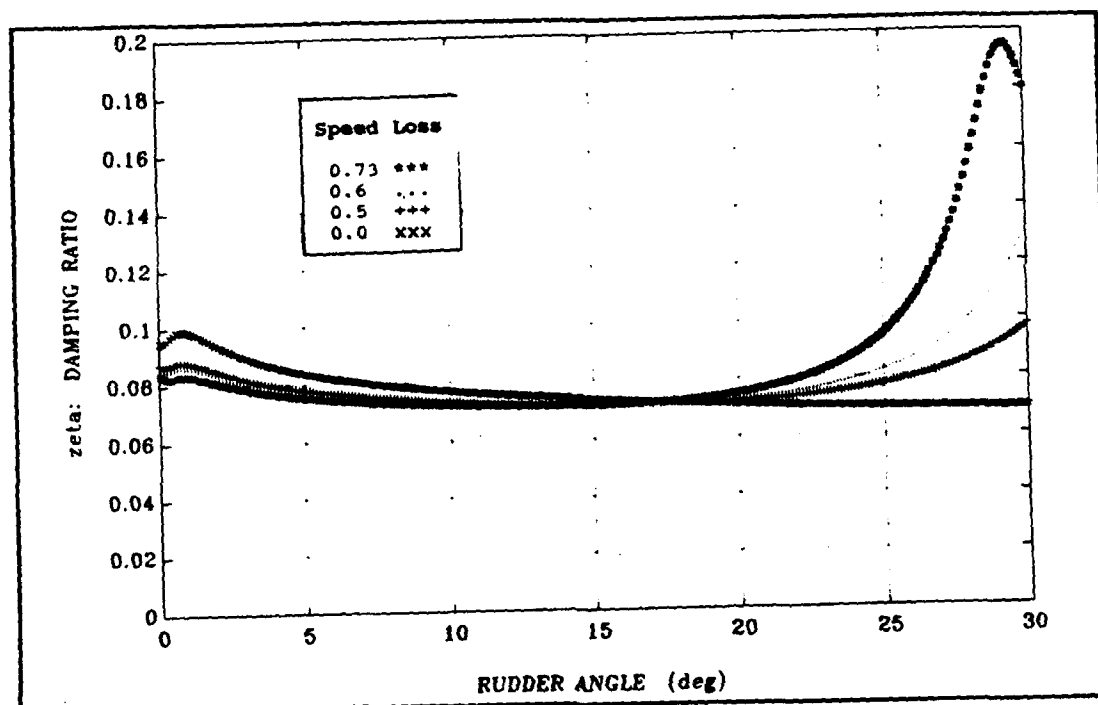
Figure 5.4: Effect of Speed Loss on Coupled Model Damping Ratio
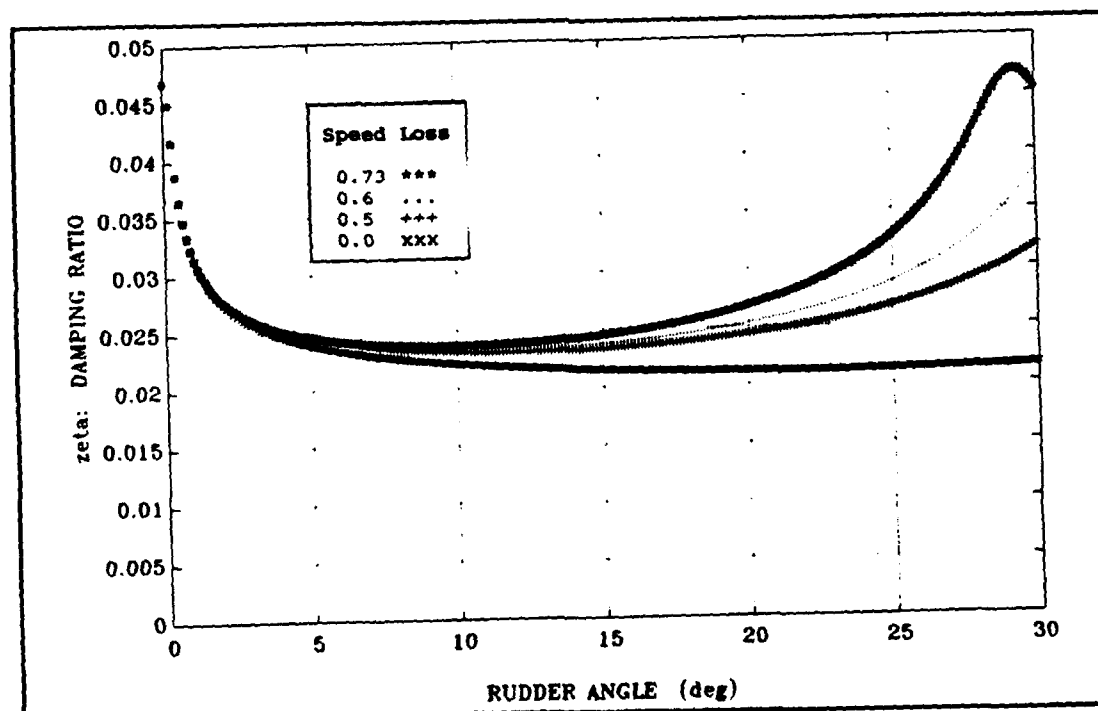
Figure 5.5: Effect of Speed Loss on Decoupled Model Damping Ratio

45

Froude numbers used to calculate the forward velocity prior to initiating the turn aswell as propeller revolutions were assumed to remain constant during the turn. For each Froude number and rudder angle, the sway velocity, yaw rate and roll angle were determined using the model program. Figures 5.6 through 5.8 at the end of this section depict graphic results. Note that v and r are not readily affected by change in Froude number, whereas ϕ is greatly changed, increasing dramatically with Froude number.

Using these values, the stability of the coupled response was determined. The real roots of the coupled maneuvering equations for the three Froude numbers are indistinguishable when plotted as in Figure 4.1, as are the roots for the lower steering components (Figure 4.2). The upper steering component exhibits nonlinear behavior through five degrees of rudder for all Froude numbers with increasing stability as both Froude number and rudder angle increase. The roll component was nonlinear throughout the range of rudder angles tried. Furthermore, as the Froude number increased, so did the range of rudder angles for which stability increased.

The coupled model roll damping ratio remains relatively insensitive to Froude number (Figure 5.9), while the uncoupled model suggests a wide variation (Figure 5.10). This demonstrates the incorrect conclusions which can be reached when using linear/uncoupled models that neglect the actual coupling of the lateral sway/yaw motions back into roll.
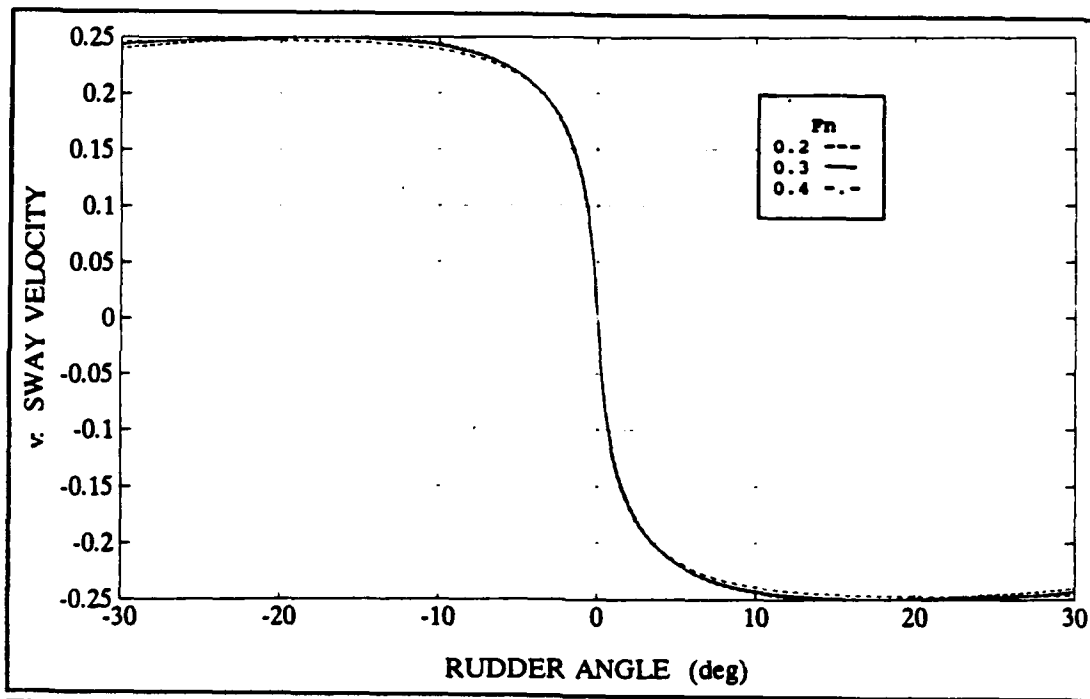
Figure 5.6: Effect of Fn on Sway Velocity
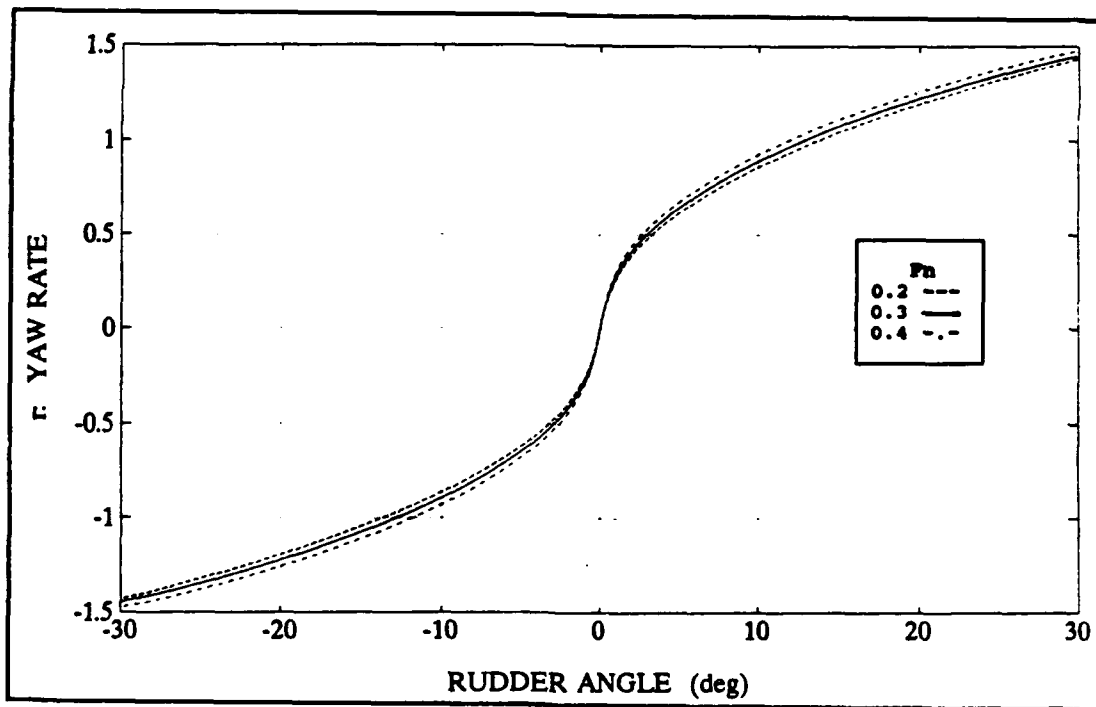
Figure 5.7: Effect of Fn on Yaw Rate

47
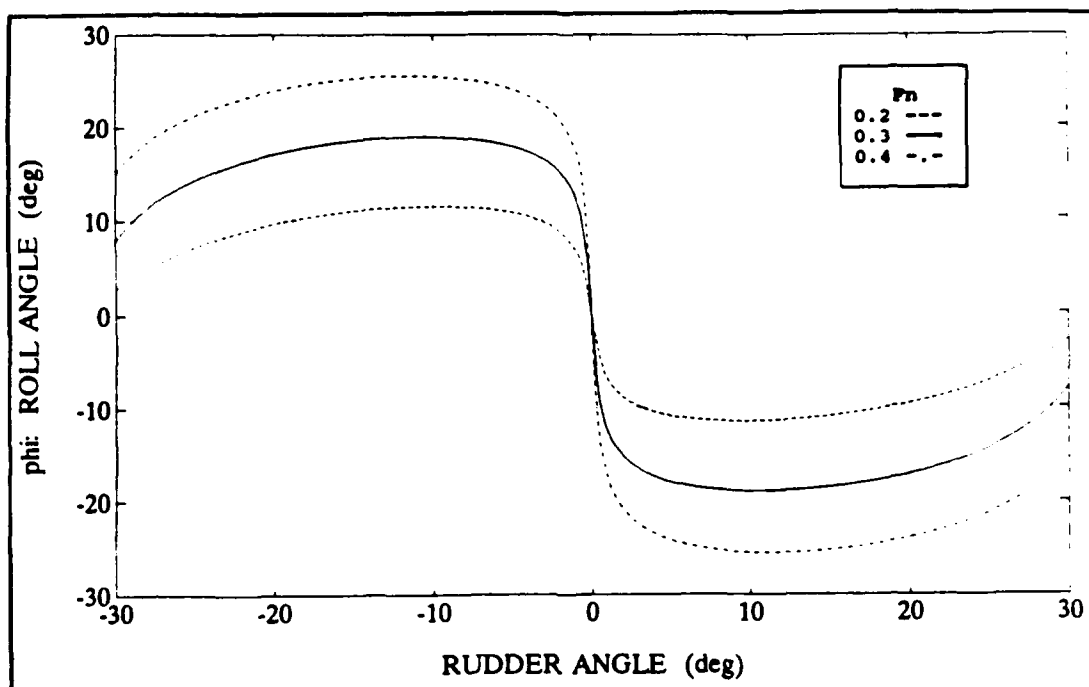
Figure 5.8: Effect of Fn on Roll Angle
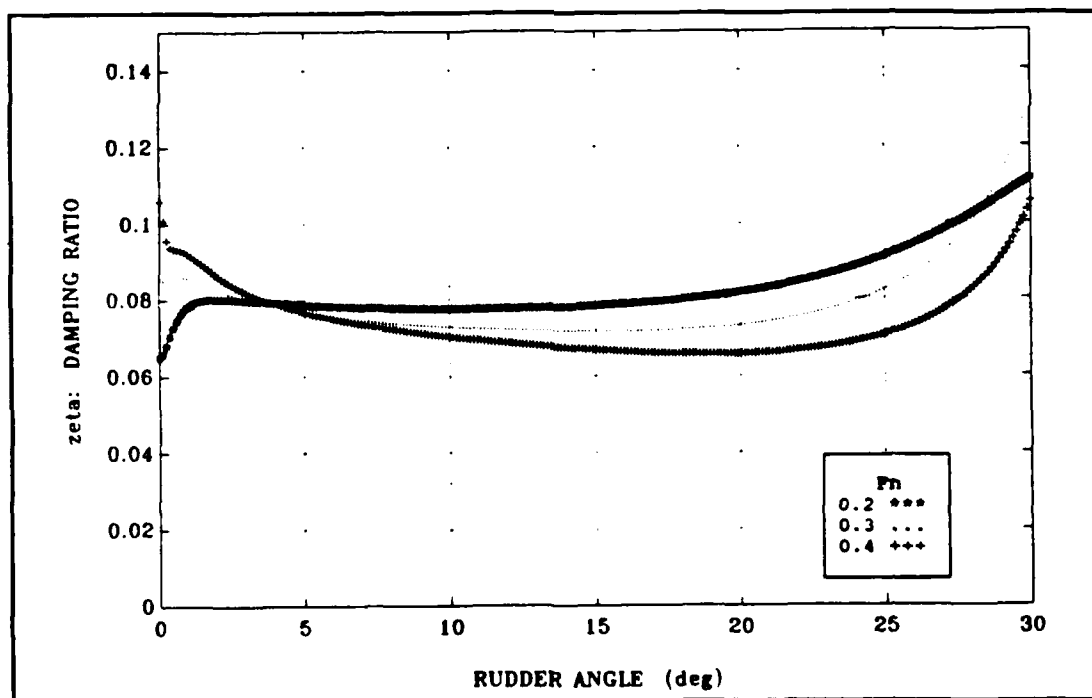
Figure 5.9: Effect of Fn on Coupled Model Damping Ratio

48
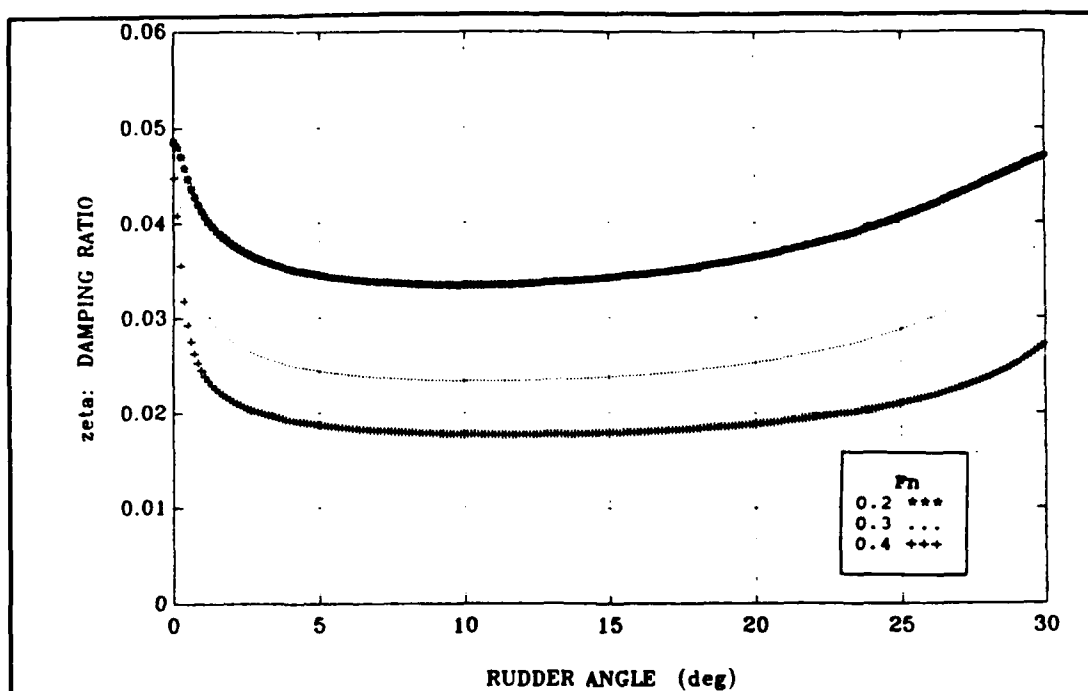
Figure 5.10:   Effect of Fn on Decoupled Model Damping Ratio

D.   TRANSVERSE METACENTRIC HEIGHT AS THE DESIGN PARAMETER

For transverse metacentric height as the design parameter in the model, Froude

number and speed loss ratio were held constant:

$$Fn = 0.3$$
$$\alpha = 0.6$$

Here again, the sway velocity, yaw rate and roll angle for each GM and rudder

angle were computed using the model program. The results are represented in

Figures 5.11 through 5.13. As indicated for the case of Froude number being the

design parameter, v and r are affected very little by even an order of magnitude

49

change in GM. On the other hand, the increase in GM not only causes a large decrease in the magnitude of the roll angle, but in the range as well.

In determining the influence of GM on the stability characteristics, it was found that the real roots plotted as a function of rudder angle showed no distinction between GM's. When the components were separated out, only the upper steering and roll constituents exhibited significant variation. The upper steering response reflected a somewhat incongruous reaction, that is, as the GM increases, the stability due to steering decreases slightly. The roll component demonstrated a marked increase in stability with increase in GM. This result is evident in the root locus diagram of Figure 5.14.

Conversely, the damping ratio did not change significantly, as shown in Figure 5.15. Computation of the damping ratio from the decoupled model showed a much wider deviation among different GM's.

E.   TRIM AS THE DESIGN PARAMETER

For the investigation of a vessel in the trimmed condition, the transverse metacentric height, Froude number and speed loss ratio were held constant:

$$\overline{GM} = 0.3 \ m$$
$$Fn = 0.3$$
$$\alpha = 0.6$$
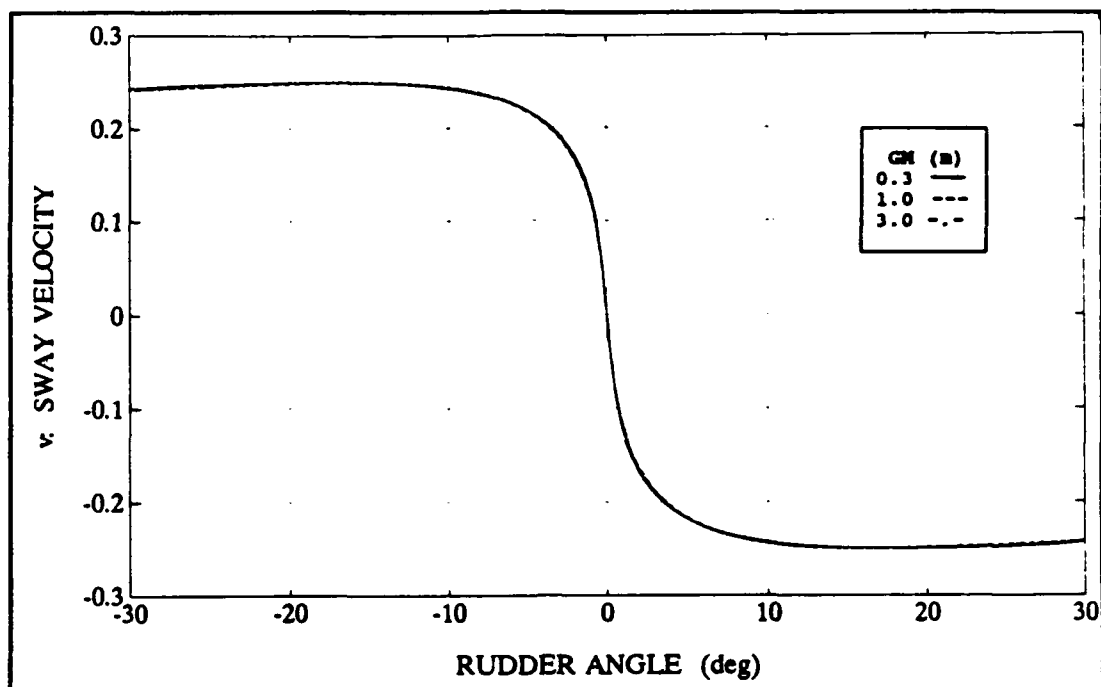
Figure 5.11: Effect of GM on Sway Velocity
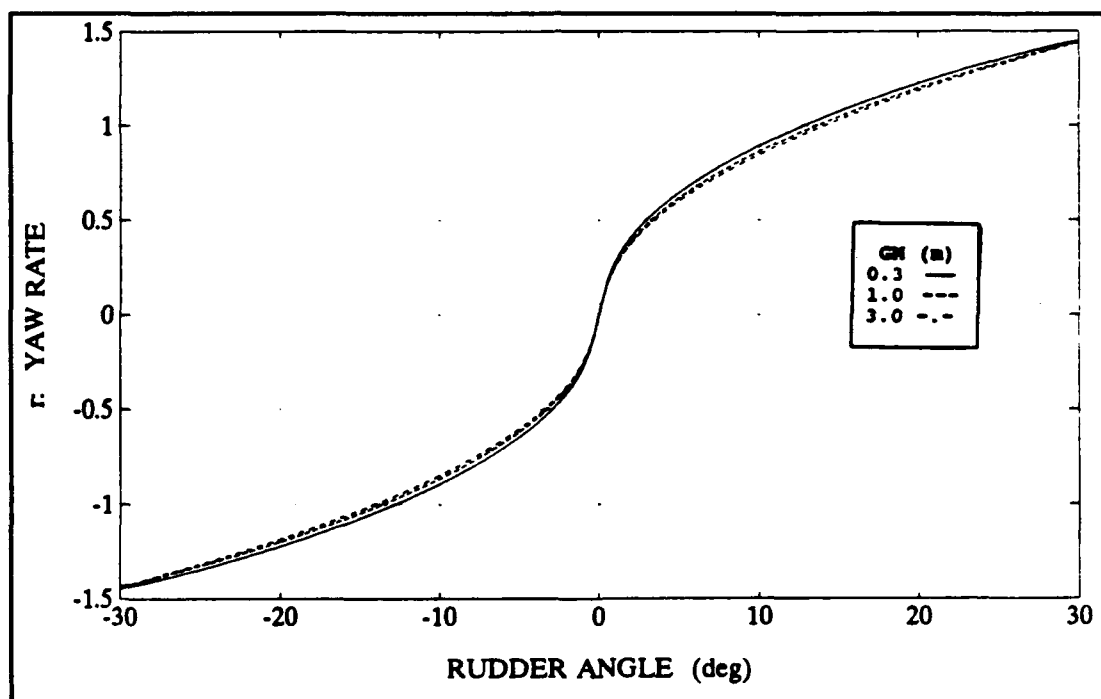
Figure 5.12: Effect of GM on Yaw Rate

51
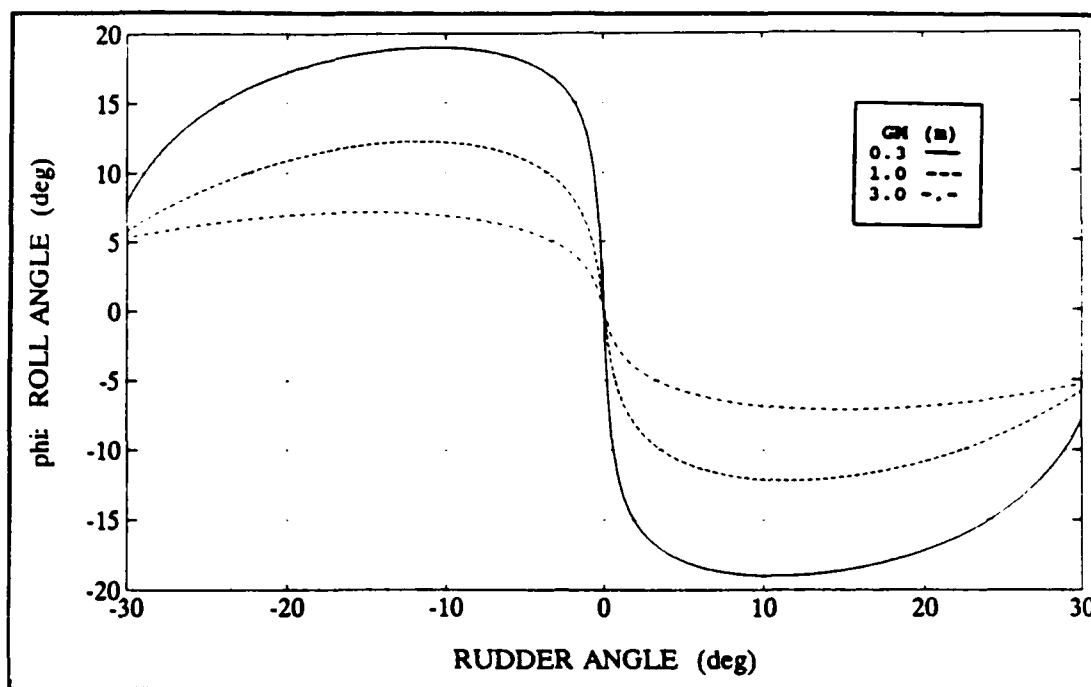
Figure 5.13:   Effect of GM on Roll Angle
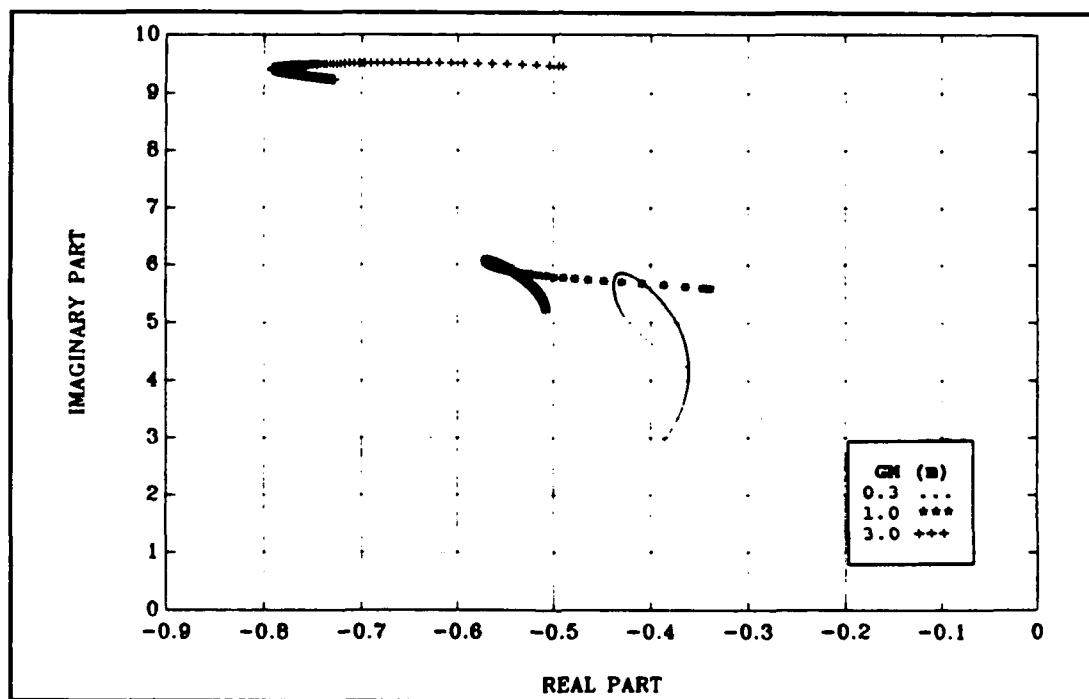
Figure 5.14:   Effect of GM on Coupled Model Root Locus
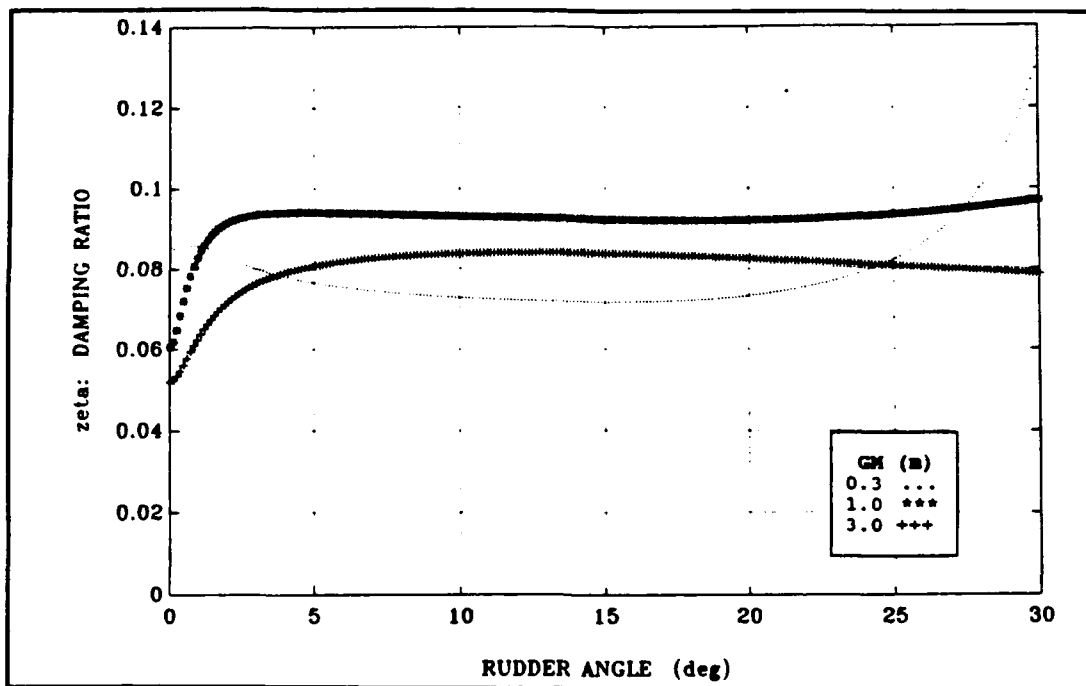
Figure 5.15: Effect of GM on Coupled Model Damping Ratio
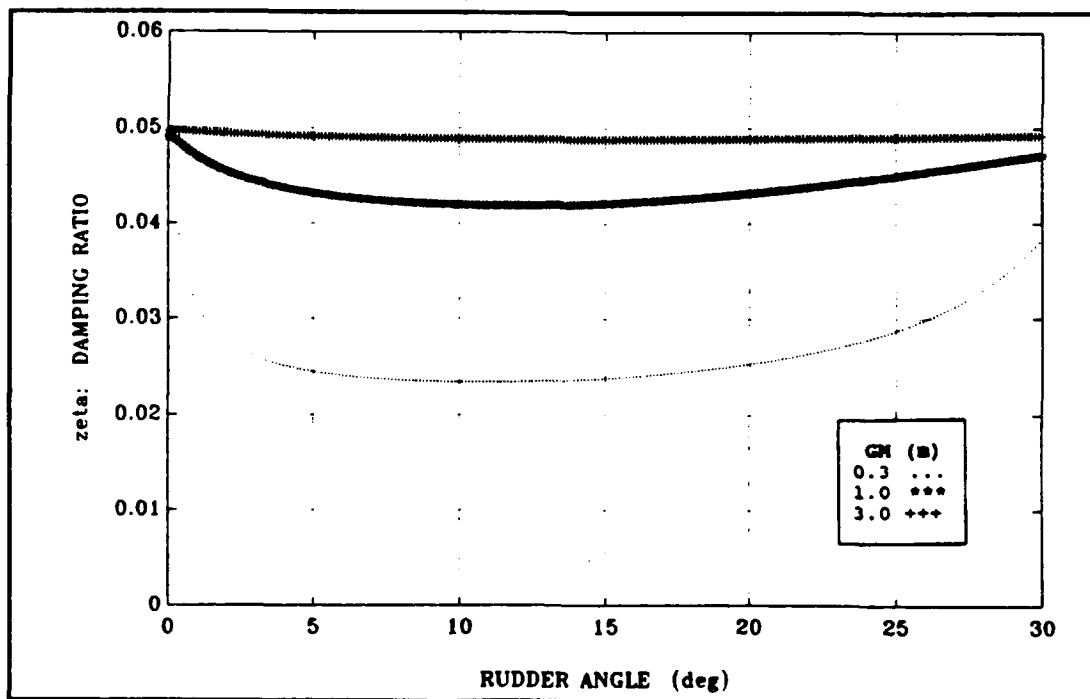
Figure 5.16: Effect of GM on Decoupled Model Damping Ratio

The base-line model chosen for this study, and therefore the hydrodynamic derivatives and coefficients derived from model tests, were for a design trim of 0.5 meters by the stern and a mean draft of 8.5 meters for the actual ship (refer to Table IV for model parameters). It has been shown [Ref. 11] through linear theory that these derivatives and coefficients change for the trimmed condition by the following semi-empirical relations: [Ref. 15]

$$Y_v(\tau) = Y_v(0)\left[1 + \frac{2\tau}{3d_m}\right]$$

$$N_v(\tau) = N_v(0)\left[1 - \frac{0.27\tau}{l_v d_m}\right]$$

$$Y_r(\tau) = Y_r(0)\left[1 + \frac{0.8\tau}{d_m}\right]$$

$$N_r(\tau) = N_r(0)\left[1 + \frac{0.3\tau}{d_m}\right]$$

$$l_v = \frac{N_v(0)}{Y_v(0)}$$

where $\tau = $ + *for trim by stern*
           − *for trim by bow*

d_m = *design mean draft*

$Y_v(0)$ = Y_v *at design condition*

The application of these relationships are somewhat questionable, but in the absence of model tests, they will suffice to indicate trends for further study.

A further modification in the model was made to the z_R parameter (Table III) or the z coordinate of the point on which the rudder force acts:

54

$$z_R(\tau) = z_R(0) + \frac{1}{2}\left(\frac{\tau}{d_m}\right)\left(\frac{d_m}{L}\right)$$

Figures 5.17 through 5.19 depict the effects of $\frac{\tau}{d_m}$ = ±0.2 which equates to a significant change in operating condition. The sensitivity of v and r to the previous parameters was practically negligible with the exception of the speed loss ratio. This is not the case for trim where turning rate is improved for trim by the bow and decreased for trim by the stern. It should be noted that this is contrary to linear theory results. For sway velocity at small angles of rudder the variation is small, but for large rudder angles the trim by stern curve deviates considerably from the other two conditions. The difference is more pronounced in the roll angle curves (Figure 5.19) where trim by the bow generates higher angles during the turn. On the other hand, trim by the stern results in smaller roll angles with a roll angle sign reversal beyond a certain rudder angle. This is due to the fact that for large rudder angles, the hydrodynamic moment exerted by the rudder force dominates over the fluid forces on the hull.

The root locus diagram (Figure 5.20) for the roll stability analysis is revealing in that very different trends can be observed. Trim by the stern is considerably more stable than by the bow for the entire range of heel angle, although at larger rudder angles, the stability is less than at the design condition. This is possibly qualitatively explained by noticing in Figures 5.21 and 5.22, that the damping ratio for trim by the stern increases sharply precisely at the inflection point of the roll angle as shown in

55

Figure 5.19. Here again, it must be pointed out that the damping ratio's variance between the coupled model and the decoupled model is at least a factor of two. It can be seen from both coupled and decoupled models that at the inflection point of the roll angle, the damping ratio reaches its peak value. This maximum value of the damping ratio exists for the other trim conditions as well, but its actual location is shifted outside the range of rudder angle variations considered here.

F.   RIGHTING ARM CURVE AS THE DESIGN PARAMETER

The sensitivity of the model to changes in the righting arm as a function of the roll angle was tested by holding the transverse metacentric height, Froude number and speed loss constant:

$$\overline{GM} = 1.0 \ m$$
$$Fn = 0.3$$
$$\alpha = 0.6$$

In general, the righting arm curve, $GZ(\phi)$, is taken to be a very simplified version of Equation (2.8), namely $GZ(\phi)=GM^*\phi$. This linear righting arm gives good approximations for small angles of heel and is derived much the same as was done for Equation (2.8) in Chapter II, Section E. For the purpose of this investigation, the simplified $GZ(\phi)$ was left in its nonlinear form, $GZ(\phi)=GM^*\sin(\phi)$. Figure 5.23 illustrates the two $GZ(\phi)$ curves used. Note that GZ1 (representing Equation (2.8)) develops a much larger righting arm at increased angles of heel than does GZ2 (representing $GM^*\sin(\phi)$).

56
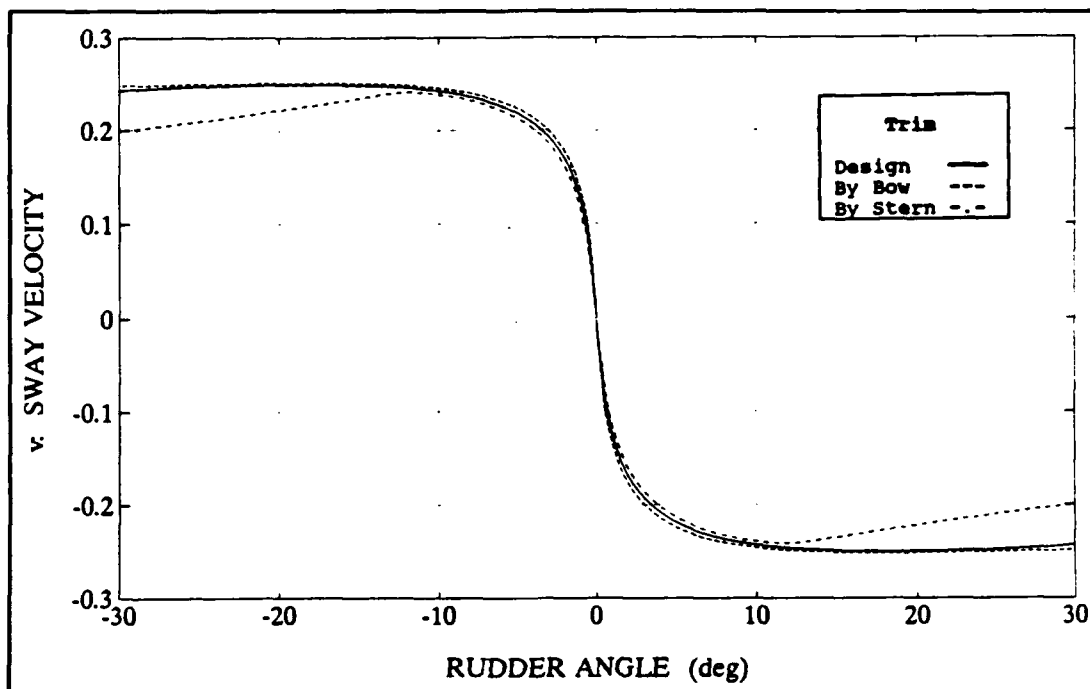
Figure 5.17: Effect of Trim on Sway Velocity
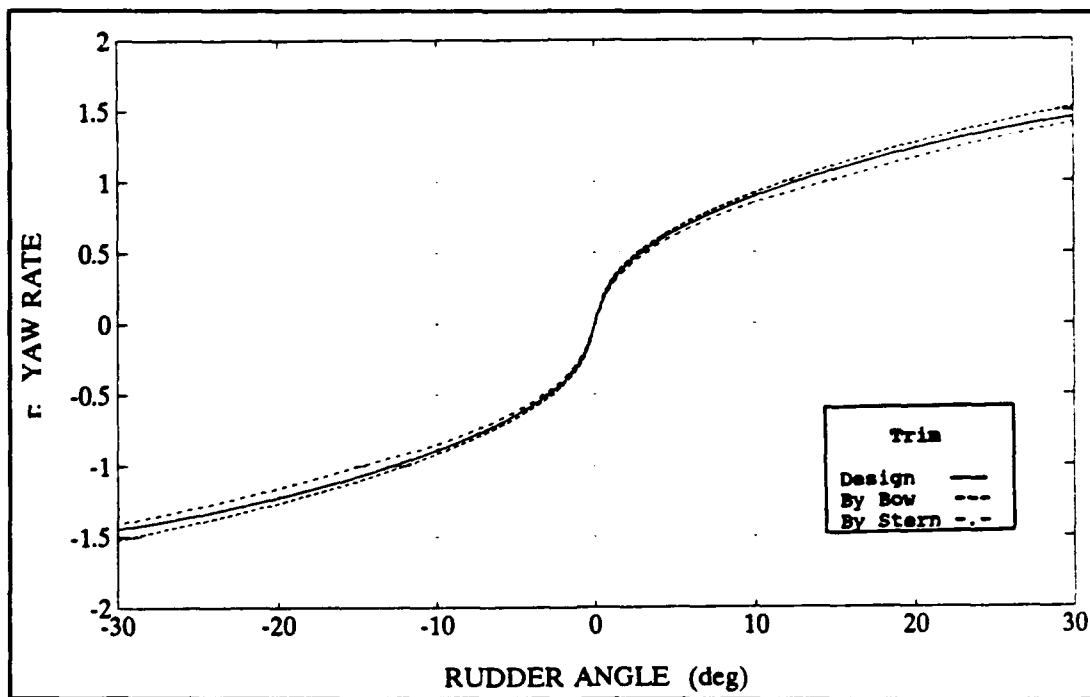
Figure 5.18: Effect of Trim on Yaw Rate
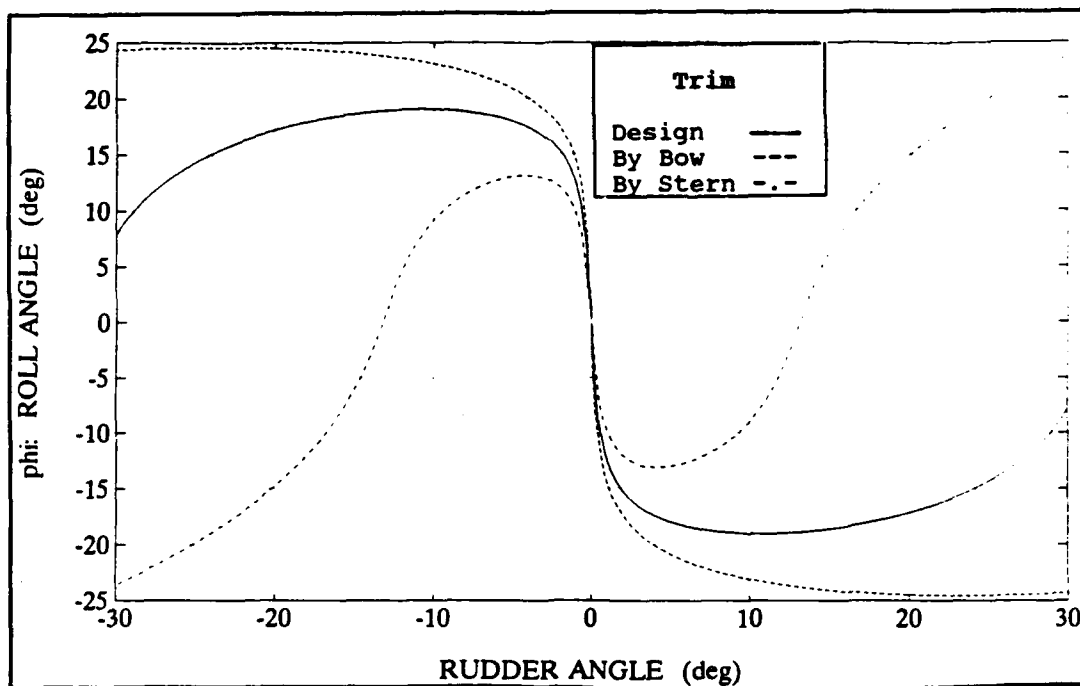
**Figure 5.19:** Effect of Trim on Roll Angle
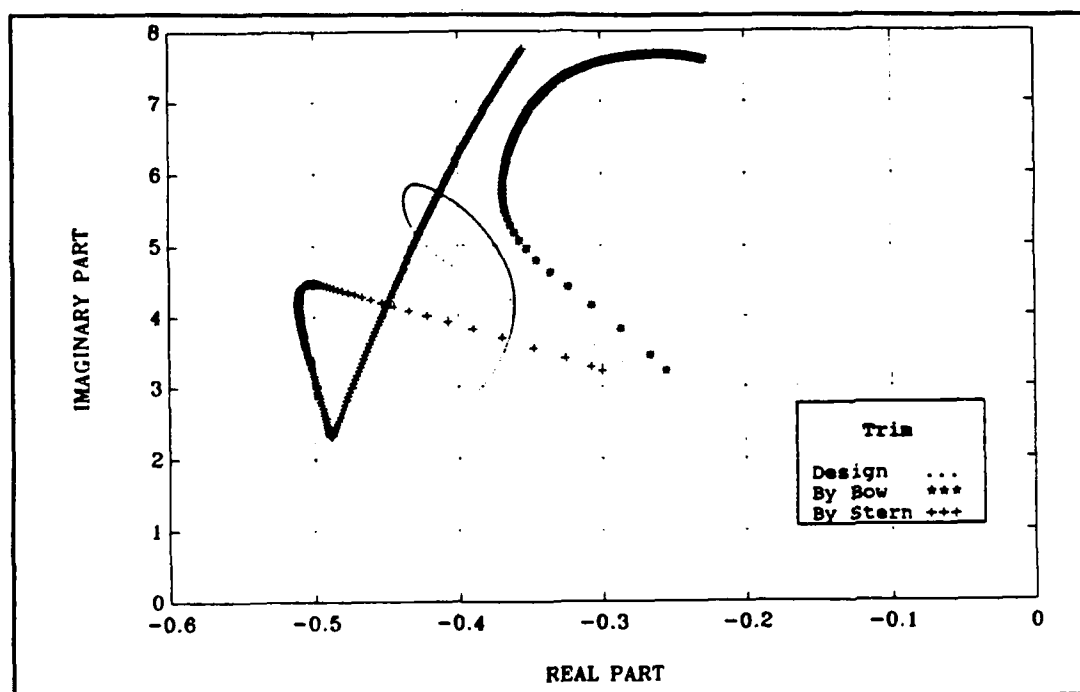
Figure 5.20: Effect of Trim on Coupled Model Root Locus

58
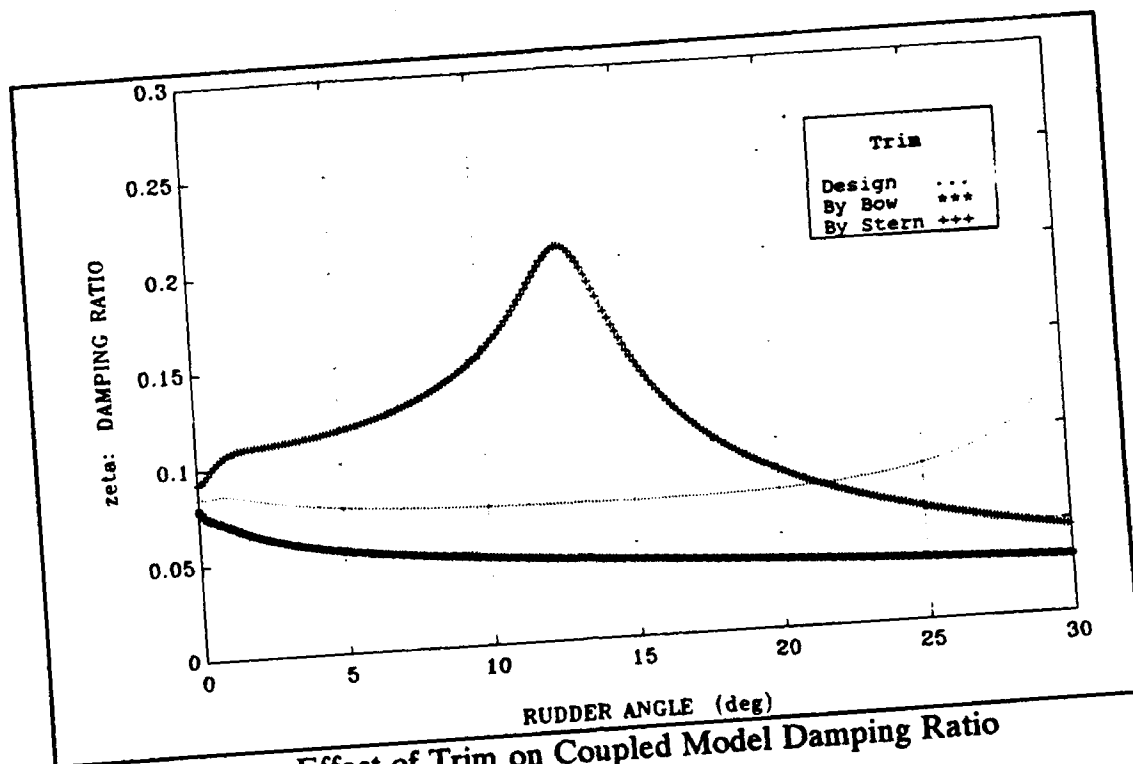
Figure 5.21: Effect of Trim on Coupled Model Damping Ratio
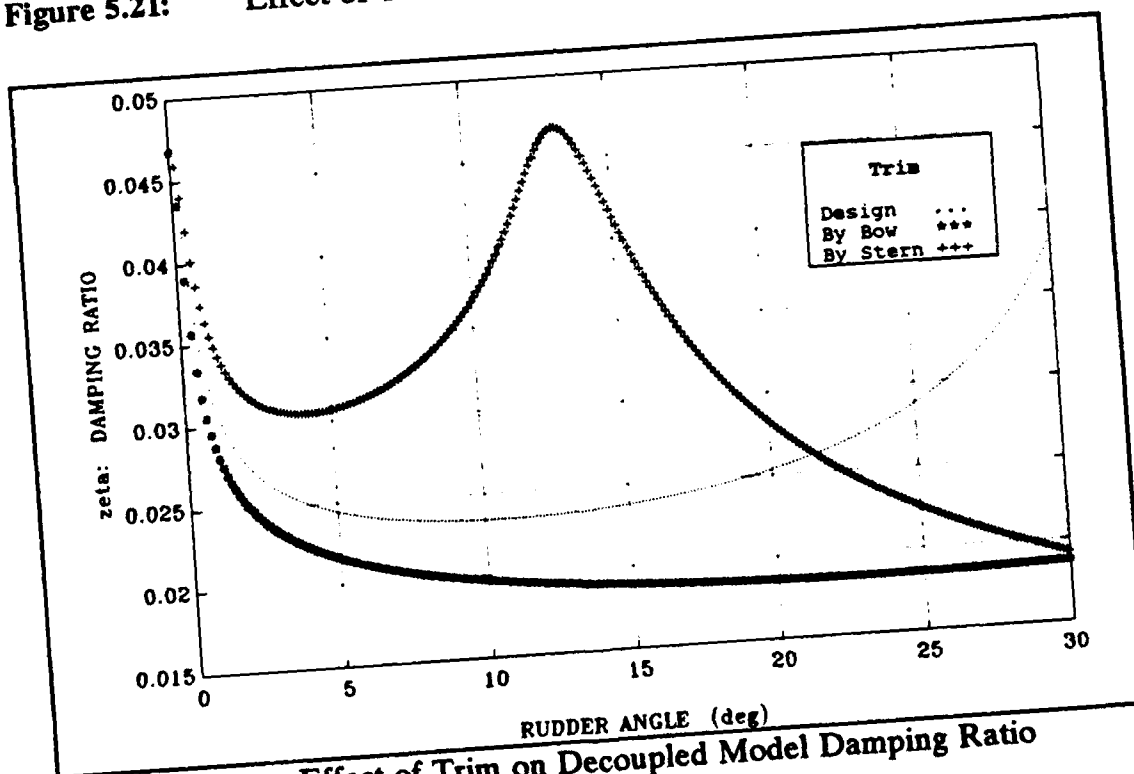
Figure 5.22: Effect of Trim on Decoupled Model Damping Ratio

59

The effects of these different righting arm curves on the model for v, r, and ϕ, are shown in Figures 5.24 through 5.26. Sway velocity and yaw rate appear to be unaffected by this parameter change in contrast to roll angle, which shows relatively high sensitivity, as expected.

Figures 5.27 (coupled model) and 5.28 (decoupled model) indicate the same trend in damping ratio sensitivity as the previous parameters, specifically, the decoupled model underestimates ς by a factor of two.

G. SUMMARY OF RESULTS

A qualitative summary of results is presented in Table VI below. All comparisons are to the base-line configuration of:[1]

$$\overline{GM} = 0.3 \ m$$
$$Fn = 0.3$$
$$\alpha = 0.6$$

---

[1] For GZ sensitivity GM = 1.0 m.
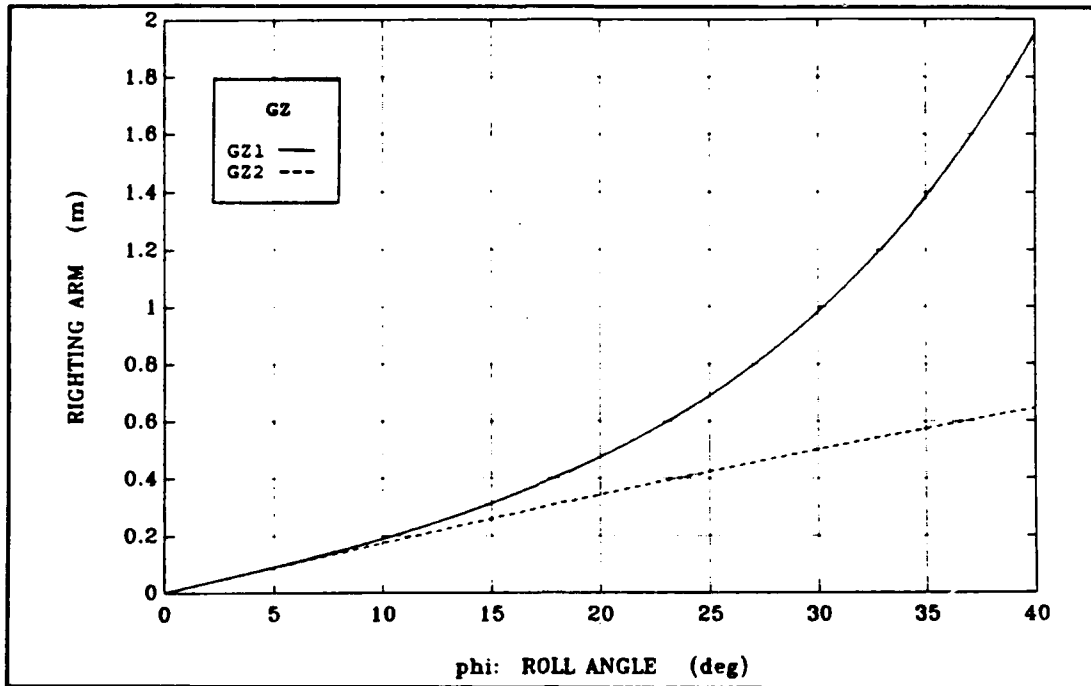
Figure 5.23: The Two Righting Arm Curves
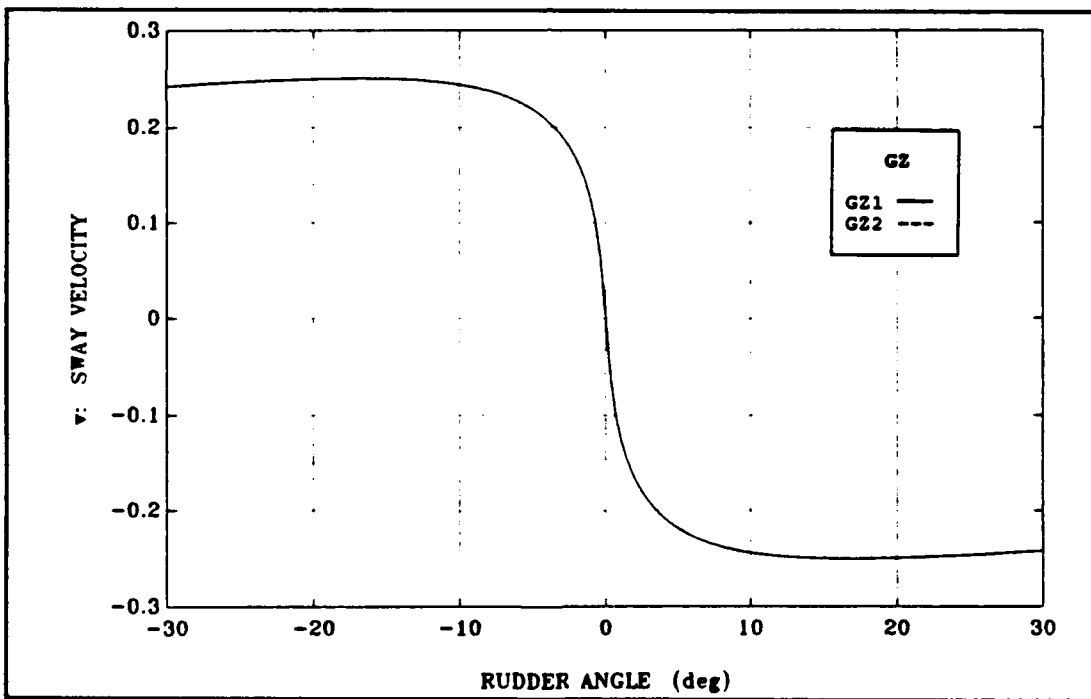
Figure 5.24: Effect of GZ(ϕ) on Sway Velocity

61
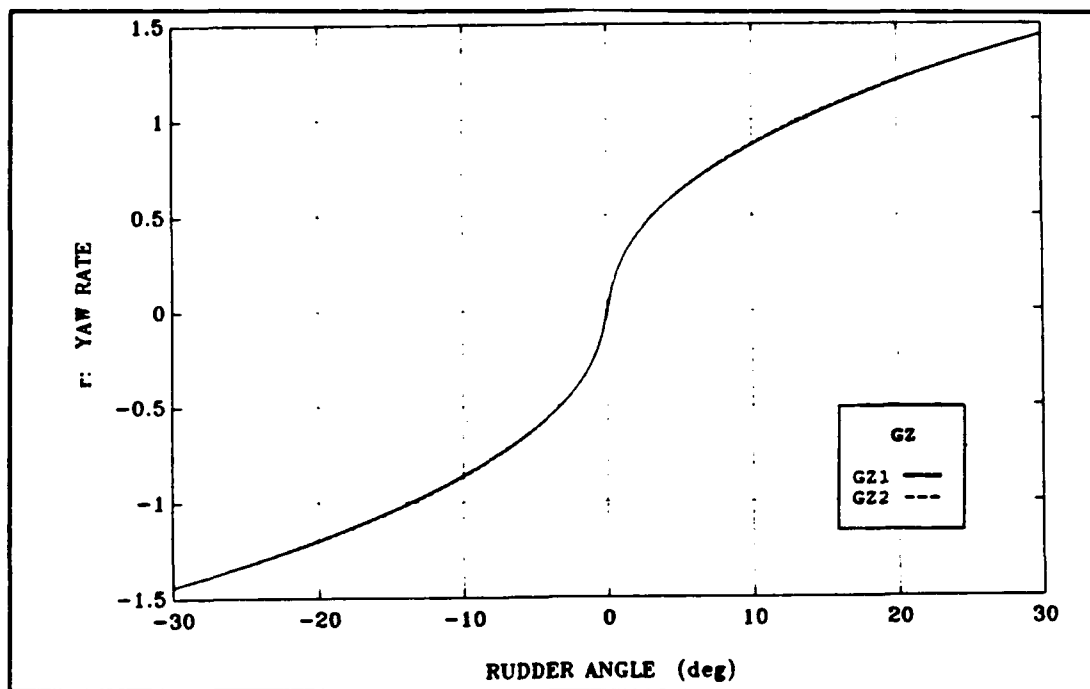
Figure 5.25:   Effect of GZ(ϕ) on Yaw Rate
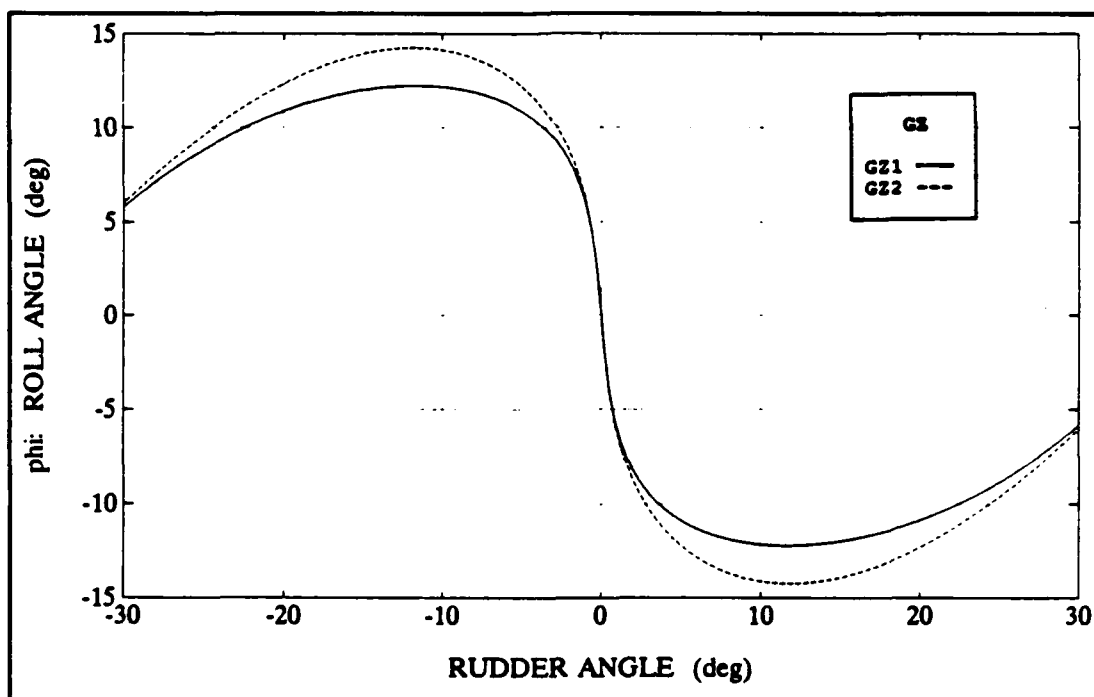
Figure 5.26:   Effect of GZ(ϕ) on Roll Angle

62
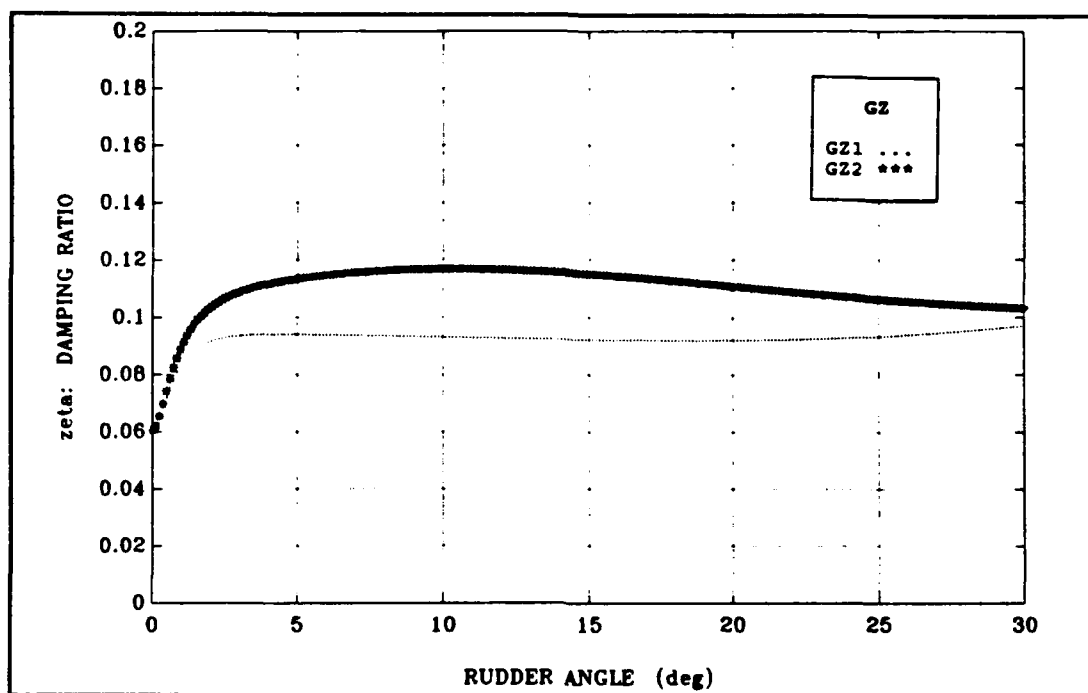
Figure 5.27: Effect of GZ(ϕ) on Coupled Model Damping Ratio
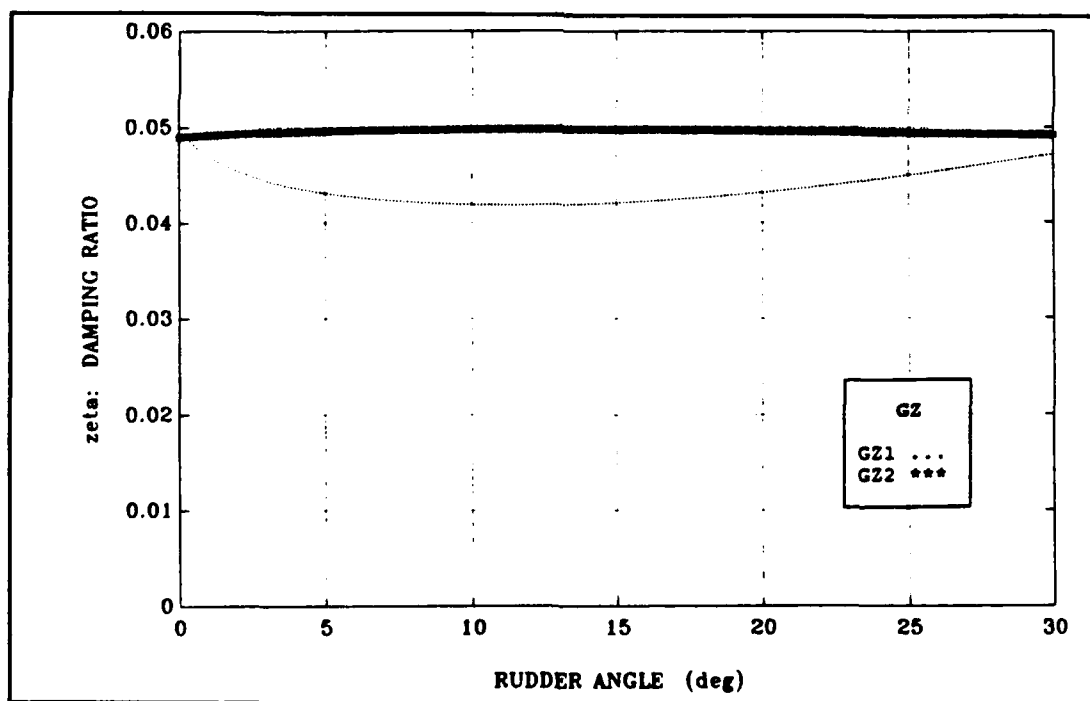
Figure 5.28: Effect of GZ(ϕ) on Decoupled Model Damping Ratio

63

Notation in the table refers to the largest noted deviations from the model according to the following subjective scale:

Sensitivity	Symbol	Standard
Negligible	N	< 1%
Low	L	1% - 5%
Moderate	M	5% - 20%
High	H	> 20%
Mixed	X	⇒ large change over the range

Additionally, A, B and C refer to rudder angle range for the noted deviations such that:

$$0° < A \leq 10°$$
$$10° < B \leq 20°$$
$$20° < C \leq 30°$$

TABLE VI. QUALITATIVE SENSITIVITY SUMMARY

Parameter	δ	α	Fn	GM	Trim	GZ(ϕ)
v	A	M	N	N	L	N
	B	M	N	N	M	N
	C	H	N	N	H	N
r	A	N	L	N	L	N
	B	N	L	N	L	N
	C	L	L	N	L	N
ϕ	A	M	H	H	X	H
	B	M	H	H	H	H
	C	H	H	M	H	M
coupled damping	A	M	M	X	X	X
	B	L	M	H	X	H
	C	X	X	X	X	H
uncoupled damping	A	L	H	X	X	X
	B	M	H	H	X	H
	C	H	H	H	X	H

This reference table shows clearly that the sway velocity and turning rate are relatively insensitive to Froude number, metacentric height and righting moment, while being quite sensitive to the speed loss and trim parameters. Roll and damping ratio show the greatest response for all the parameters considered.

VI. CONCLUSIONS AND RECOMMENDATIONS

A. CONCLUSIONS

This thesis developed a mathematical model for the coupled sway, yaw and roll equations of motion with rudder deflection as the independent variable. Additionally, various components of the hydrodynamic forces and moments, e.g., rudder to hull interaction, were modelled using existing research formulation. Deviation of this study from current solution methods was in the manner of evaluating the Taylor expansion for the steady state Jacobian matrix. The equilibrium position for each rudder angle was found to deviate significantly from the commonly used zero state, even for rudder angles of less than 10°. In fact, the roll angle and sway velocity nominal points are nearly maximum at 10° of rudder.

Comparison of stability results for the coupled lateral motion model to those of models representing the steering equations of motion decoupled from the roll equations of motion showed:

1. The directional stability characteristics signified by the real part of the complex eigenvalues are not affected significantly by the coupling of roll *into* sway and yaw. This indicates that sway and yaw can be treated separately from roll when studying directional stability.

2. Roll stability represented by the magnitude of the damping ratio is considerably affected by the coupling of sway and yaw *into* roll. The fact that the damping ratio is underestimated by a factor of two by the uncoupled treatment of sway and yaw, indicates ship design by this means is a significant

66

over-design that bears more attention, especially with the economic constraints of today's Navy.

3. The natural frequency is not significantly affected by coupling. This indicates that while maneuvering in a seaway studies require the coupling of the lateral motions, the induced roll from the static righting moment can be studied from decoupled systems.

4. Steering stability increases with increasing rudder deflection. This may indicate that if a ship is directionally unstable for straight line motion, it becomes directionally stable during a turn through the coupling of the lateral motions.

The sensitivity of certain design parameters to the coupled system was investigated with the following determinations:

1. The parameters tested were speed loss during a turn, transverse metacentric height, Froude number of initial forward speed, trim and righting moment. Of these parameters, trim proved to be the most affected. This indicates that during all phases of design, operating trim must be considered in addition to the design trim.

2. Sway velocity and turning rate were relatively insensitive for all parameters except for trim and speed loss.

3. Roll angle and damping ratio of all the parameters were significantly affected.

4. The coupled model damping ratio showed significantly lower sensitivity than the decoupled model for small rudder angles in all parameters.

B. RECOMMENDATIONS

The results produced in this thesis were as a consequence of experimentally reported nonlinear hydrodynamic coefficients and design parameters of a SR-108 container ship [Ref. 10]. Additional studies using similar data are required.

Utilizing the method of determining equilibrium points for each rudder position, design a control law for an autopilot and determine the effects of the coupled lateral motions on antopilot dynamics.

The sharp change in roll angle (ϕ) for small values of rudder angle (δ) suggests that this ship would be an excellent candidate for rudder roll stabilizing techniques.

Finally, as indicated in Chapter I, Section B, use the coupled sway, yaw and roll equations of motion and build a mathematical model which treats wave effects in regular and irregular seas. Once this model is developed, analyze maneuvering in waves from the standpoint of biased roll oscillations. Biased roll oscillations are meant as roll about non-zero heel angle.

APPENDIX A

```
**********************************************************************
*                                                                    *
*     PROGRAM COUPLED                                                 *
*                                                                    *
*     This program solves the coupled yaw-sway-roll ship maneuvering *
*     equations.  In addition, the yaw-sway steering equations are de-*
*     coupled from the roll equations and solved in order to compare  *
*     results with the fully coupled results.  The program is broken  *
*     into several subroutines, both original and standard commercial *
*     programs.                                                       *
*                                                                    *
**********************************************************************
**********************************************************************
*                                                                    *
*     The INCLUDE statement is used to pass all the variables between *
*     the many subroutines.                                          *
*                                                                    *
      INCLUDE 'HYDCOMN.for'
      COMMON/WORKSP/RWKSP
      REAL RWKSP(5000)
      REAL*8 VDEL(300),V(300),R(300),RPHI(300)
      EXTERNAL FCN,LSJAC,DNEQNJ
*
*     Open the input and output files
*
      OPEN(10, FILE ='COEF.INP',status='old')
      OPEN(15, FILE ='VAR.OUT',status='new')
      OPEN(20, FILE ='NLIN.DAT',status='new')
      OPEN(25, FILE ='EIGVAL1.DAT',status='new')
      OPEN(30, FILE ='EIGVAL2.DAT',status='new')
      OPEN(26, FILE ='EIGVALL.DAT',status='new')
      OPEN(27, FILE ='EIGVALp.DAT',status='new')
      OPEN(35, FILE ='ZETA.DAT',status='new')
      OPEN(36, FILE ='OMEGA.DAT',status='new')
      OPEN(37, FILE ='ZROLL.DAT',status='new')
      OPEN(38, FILE ='RUDDER.DAT',status='new')
      PI=4.0D0*DATAN(1.0D0)
      ERRREL=0.0001
      ITMAX=200
*
*     This subroutine reads the hydrodynamic derivative and coefficient
*     values from COEF.INP and writes pertinent values in VAR.OUT.

      CALL INPUT
      DEL=DEL*(PI/180.0D0)
*
*     This subroutine sets up the linear EOM's in matrix form:
*                         A x = B
*
      CALL LINEAR
*
*     This is an IMSL MATH/LIBRARY Subroutine [Ref. 19]
*
```

```
*
*      Purpose:  Solve a real general system of linear equations with
*                iterative refinement
*
*      Arguments:
*
*         N      -Number of equations.  (Input)
*         A      -N by N matrix containing the coefficients of the linear
*                 system.  (Input)
*         LDA    -Leading dimension of A.  (Input)
*         B      -Vector of length N containing the right-hand side of the
*                 linear system.  (Input)
*         IPATH  -Path indicator, if = 1 the system A*x=B is solved
*         X      -Vector of length N containing the solution to the linear
*                 system.  (Output)
*
          CALL DLSARG(N,A,3,B,1,XGUESS)
          WRITE(15,*)'THE SOLUTION TO THE LINEAR SYSTEM OF EQUATIONS IS'
          WRITE(15,*)' '
          WRITE(15,*)'VO=',XGUESS(1)
          WRITE(15,*)'RO=',XGUESS(2)
          WRITE(15,*)'PHIO=',XGUESS(3)
          WRITE(15,*)' '
          PHIO=XGUESS(3)*(180.0D0/PI)
          WRITE(15,*)'PHIO IN DEGREES =',PHIO
          WRITE(15,*)' '
*
*      Set the rudder limits for steady turning
*
          DELMIN=0.01D0
          DELMAX=30.0D0
*
*      This Do-Loop calculates the values of sway velocity, yaw rate and
*      roll angle for each rudder angle.
*
          DO 100 IDEL=1,IMAX
          WRITE (*,*) IDEL,IMAX
          RDEL=DELMIN+(DELMAX-DELMIN)*REAL((IDEL-1)/(IMAX-1))
          DEL=RDEL*(PI/180.0D0)
          UND=1.0D0-SLR*(DABS(DEL))
*
*      This is an IMSL MATH/LIBRARY Subroutine [Ref. 17]
*
*      Purpose:  Solve a system of nonlinear equations using the
*                Levenberg-Marquardt algorithm with a user-supplied
*                Jacobian.
*      Arguments:
*
*         FCN    - User-supplied SUBROUTINE to evaluate the system of
*                  equations to be solved.  The usage is
*                  CALL FCN (X, F, N), where
*                  X       - The point at which the functions are
*                            evaluated.  (Input)
*                            X should not be changed by FCN.
*                  F       - The computed function values at the point X.
*                            (Output)
*                  N       - Length of X, F.  (Input)
*                  FCN must be declared EXTERNAL in the calling program.
*         LSJAC  - User-supplied SUBROUTINE to evaluate the Jacobian at a
*                  point X.  The usage is
*                  CALL LSJAC (N, X, FJAC), where
```

70

```
*                N       - Length of X.  (Input)
*                X       - The point at which the function is evaluated.
*                          (Input)
*                          X should not be changed by LSJAC.
*                FJAC    - The computed N by N Jacobian at the point X.
*                          (Output)
*                LSJAC must be declared EXTERNAL in the calling program.
*        ERRREL - Stopping criterion.  (Input)
*                 The root is accepted if the relative error between two
*                 successive approximations to this root is less than
*                 ERRREL.
*        N      - The number of equations to be solved and the number
*                 of unknowns.  (Input)
*        ITMAX  - The maximum allowable number of iterations.  (Input)
*                 The maximum number of calls to FCN is ITMAX*(N+1).
*                 Suggested value = 200.
*        XGUESS - A vector of length N.  (Input)
*                 XGUESS contains the initial estimate of the root.
*        X      - A vector of length N.  (Output)
*                 X contains the best estimate of the root found by
*                 DNEQNJ.
*        FNORM  - A scalar which has the following value,
*                 F(1)**2+...+F(N)**2 at the point X.  (Output)
*
*
         CALL DNEQNJ(FCN,LSJAC,ERRREL,N,ITMAX,XGUESS,X,FNORM)
         PHI=X(3)*180.0D0/PI
         WRITE(20,50)RDEL,X(1),X(2),PHI
  50     FORMAT(4E15.5)
*
*    Calculate the rudder forces and moments:  Equations 2.6 and 2.7
*
         UP=UND*(WP+TAU*((X(1)+XP*X(2))**2+CPV*X(1)+CPR*X(2)))
         JP=(U*UP)/(NP*D)
         KT=KTA+(KTB*JP)
         UR=UP*EPSILON*((1.0D0+8.0D0*K*KT)/(PI*(JP**2)))**0.5
         VR=GAMMA*X(1)+CDR*X(2)+CDRRR*(X(2)**3)+CDRRV*X(1)*(X(2)**2)
         VD=(UR**2+VR**2)**0.5
         ALPHAR=DEL+DATAN(VR/UR)
         FLAM=(6.13D0*LAMBDA)/(LAMBDA+2.25D0)
         FNN=FLAM*(AR/(L**2))*((VD)**2)*DSIN(ALPHAR)
*
         YD=-(1.0D0+AH)*FNN*DCOS(DEL)
         ND=-(XR+AH*XH)*FNN*DCOS(DEL)
         KD=(1.0D0+AH)*ZR*FNN*DCOS(DEL)
         WRITE(38,*)ND,YD,KD
*
*    Rudder angle in degrees
*
         VDEL(IDEL)=DEL
         V(IDEL)=X(1)
         R(IDEL)=X(2)
*
*    Rudder angle in radians
*
         RPHI(IDEL)=X(3)
         XGUESS(1)=X(1)
         XGUESS(2)=X(2)
         XGUESS(3)=X(3)
 100     CONTINUE
*
```

```
*     This subroutine solves the eigenvalue problem |A - lambda*B|= 0
*     for the fully coupled yaw-sway-roll equations, using the values
*     for v, r, and phi obtained above.

      CALL EIGTH1(VDEL,V,R,RPHI)
*
*     This subroutine solves the eigenvalue problem |As - lambda*Bs|= 0
*     for the steering yaw-sway equations.
*
      CALL EIGTH2(VDEL,V,R)
*
*     This subroutine solves the eigenvalue problem |Ar - lambda*Br|= 0
*     for the roll equations.
*
      CALL EIGTH3(VDEL,Rphi)
      STOP
      END
*
*
      SUBROUTINE INPUT
      INCLUDE 'HYDCOMN.for'
*
*     The numbers in the variables such as N122 stand for:
*                         1 implies v
*                         2 implies r
*                         3 implies phi
*                         4 implies delta
*
      READ(10,*)NO,N1,N2,N3,N111,N122,N222,N112,N113,N133,N223,
     & N233,K0,K1,K2,K3,K111,K122,K222,K112,K113,K133,K223,K233,
     & Y0,Y1,Y2,Y3,Y111,Y122,Y222,Y112,Y113,Y133,Y223,Y233,L,W,XG,
     & AH,AR,LAMBDA,XR,XH,ZR,BM,WP,TAU,XP,CPV,CPR,EPSILON,K,KTA,KTB,
     & D,CDR,CDRRR,CDRRV,GAMMA
*
*     Calculate the nondimensional mass
*
      M=W/(0.5D0*(L**3))
      WRITE(*,*)'ENTER THE GM  AND THE SPEED LOSS RATIO'
      READ(*,*)GM,SLR
      WRITE(15,*)'GM=',GM
      WRITE(15,*)' '
      WRITE(15,*)'THE SPEED LOSS RATIO IS=',SLR
*
*     Adjusts the z coordinate of CG based on the GM
*
      ZGM=DABS(0.3D0-GM)/L
      ZG=0.00078-ZGM
      WRITE(15,*)'THE SHIP DISPLACEMENT (IN CUBIC METERS) IS W=',W
      WRITE(15,*)' '
      WRITE(15,*)'THE SHIP NONDIMENSIONAL MASS IS M=',M
      WRITE(15,*)' '
      XG=XG/L
      WRITE(15,*)'L=',L
      WRITE(15,*)'XG=',XG
      WRITE(15,*)'ZG=',ZG
      WRITE(15,*)' '
      WRITE(*,*)'ENTER THE INITIAL RUDDER ANGLE IN DEGREES'
      READ(*,*)DEL
      WRITE(15,*)'THE INITIAL RUDDER ANGLE DEL=',DEL
      WRITE(*,*)'ENTER THE FROUDE NUMBER AND THE IMAX'
      READ(*,*)FN,IMAX
```

```fortran
      WRITE(15,*)'THE FROUDE NUMBER IS FN=',FN
*
*   Calculate the initial forward speed
*
      U=FN*((9.8D0*L)**0.5D0)
      WRITE(15,*)'THE FORWARD VELOCITY IS U=',U
      WRITE(15,*)' '
      WRITE(*,*)'ENTER THE PROPELLER SPEED IN RPMS FOR THE FN'
      READ(*,*)NP
      WRITE(15,*)'THE PROPELLER SPEED IN RPMS IS NP=',NP
*
*   Change rpm's to radians per sec
*
      NP=NP*(PI/30.0D0)
*
*   The weight component is nondimensionalized such that WG*GM is
*   dimensionless
*
      WG=(W*9.81D0)/(0.5D0*(L**3)*(U**2))
      WRITE(15,*)'THE NONDIM COMPONENT OF DISPLACEMENT IS WG=',WG
      RETURN
      END
*
      SUBROUTINE LINEAR
*
      INCLUDE 'HYDCOMN.for'
      INTEGER IROW, ICOL
      DO 100 IROW=1,N
       B(IROW)=0.0D0
      DO 90 ICOL=1,N
       A(IROW,ICOL)=0.0D0
   90 CONTINUE
  100 CONTINUE
*
*   Equation 3.2
*
      A(1,1)=N1
      A(1,2)=N2-(M*XG*UND)
      A(1,3)=N3
      A(2,1)=Y1
      A(2,2)=Y2-(M*UND)
      A(2,3)=Y3
      A(3,1)=K1
      A(3,2)=K2+(M*ZG*UND)
      A(3,3)=K3-(WG*GM)
*
      FNL=((6.13D0*LAMBDA)/(LAMBDA+2.25D0))*(AR/L**2)
      N4=-(XR+(AH*XH))*FNL
      Y4=-(1.0D0+AH)*FNL
      K4=(1.0D0+AH)*ZR*FNL
*
      B(1)=-(N4*DEL)-NO
      B(2)=-(Y4*DEL)-YO
      B(3)=-(K4*DEL)-KO
      RETURN
      END
*
      SUBROUTINE FCN(Z,Q,NDIM)
      INCLUDE 'HYDCOMN.for'
      INTEGER NDIM
      DIMENSION Z(NDIM),Q(NDIM)
```

73

```
*
*    Equation 2.7
*
      UP=UND*(WP+TAU*((Z(1)+XP*Z(2))**2+CPV*Z(1)+CPR*Z(2)))
      JP=(U*UP)/(NP*D)
      KT=KTA+(KTB*JP)
      UR=UP*EPSILON*((1.0D0+8.0D0*K*KT)/(PI*(JP**2)))**0.5
      VR=GAMMA*Z(1)+CDR*Z(2)+CDRRR*(Z(2)**3)+CDRRV*Z(1)*(Z(2)**2)
      VD=(UR**2+VR**2)**0.5
      ALPHAR=DEL+DATAN(VR/UR)
      FLAM=(6.13D0*LAMBDA)/(LAMBDA+2.25D0)
      FNN=FLAM*(AR/(L**2))*((VD)**2)*DSIN(ALPHAR)
*
*    Equation 2.6
*
      Y4=-(1.0D0+AH)*FNN*DCOS(DEL)
      N4=-(XR+AH*XH)*FNN*DCOS(DEL)
      K4=(1.0D0+AH)*ZR*FNN*DCOS(DEL)
*
*    Equation 2.10b
*
      C1=N1*Z(1)+N111*(Z(1)**3)+N122*Z(1)*(Z(2)**2)
      C2=N222*(Z(2)**3)+N112*(Z(1)**2)*Z(2)+N3*Z(3)
      C3=N113*(Z(1)**2)*Z(3)+N133*Z(1)*(Z(3)**2)+(N2-(M*XG*UND))*Z(2)
      C4=N233*Z(2)*(Z(3)**2)+N4+NO+N223*(Z(2)**2)*Z(3)
*
      Q(1)=C1+C2+C3+C4
*
*    Equation 2.10c
*
      D1=Y1*Z(1)+Y111*(Z(1)**3)+Y122*Z(1)*(Z(2)**2)+(Y2-(M*UND))*Z(2)
      D2=Y222*(Z(2)**3)+Y112*(Z(1)**2)*Z(2)+Y3*Z(3)
      D3=Y113*(Z(1)**2)*Z(3)+Y133*Z(1)*(Z(3)**2)+Y223*(Z(2)**2)*Z(3)
      D4=Y233*Z(2)*(Z(3)**2)+Y4+YO
*
      Q(2)=D1+D2+D3+D4
*
*    Equation 2.9
*
c       GZ=GM*DSIN(Z(3))+0.5*BM*(DTAN(Z(3)))**2*DSIN(Z(3))
        GZ=GM*DSIN(Z(3))
*
*    Equation 2.10d
*
      E1=K1*Z(1)+K111*(Z(1)**3)+K122*Z(1)*(Z(2)**2)+(K2+M*ZG*UND)*Z(2)
      E2=K222*(Z(2)**3)+K112*(Z(1)**2)*Z(2)+K3*Z(3)
      E3=K113*(Z(1)**2)*Z(3)+K133*Z(1)*(Z(3)**2)+K223*(Z(2)**2)*Z(3)
      E4=K233*Z(2)*(Z(3)**2)+K4+KO-(WG*GZ)
*
      Q(3)=E1+E2+E3+E4
*
      RETURN
      END
*
      SUBROUTINE LSJAC(NDIM,Z,QJAC)
      INCLUDE 'HYDCOMN.for'
      INTEGER NDIM
      DIMENSION Z(NDIM),QJAC(NDIM,NDIM)
*
*    Equation 2.7
*
```

```
       UP=UND*(WP+TAU*((Z(1)+XP*Z(2))**2+CPV*Z(1)+CPR*Z(2)))
       V9=Z(1)*0.99D0
       R9=Z(2)*0.99D0
       UPV9=UND*(WP+TAU*((V9+XP*Z(2))**2+CPV*V9+CPR*Z(2)))
       UPR9=UND*(WP+TAU*((Z(1)+XP*R9)**2+CPV*Z(1)+CPR*R9))
       JP=(U*UP)/(NP*D)
       JPV9=(U*UPV9)/(NP*D)
       JPR9=(U*UPR9)/(NP*D)
       KT=KTA+(KTB*JP)
       KTV9=KTA+(KTB*JPV9)
       KTR9=KTA+(KTB*JPR9)
       UR=UP*EPSILON*((1.0D0+8.0D0*K*KT)/(PI*(JP**2)))**0.5
       URV9=UPV9*EPSILON*((1.0D0+8.0D0*K*KTV9)/(PI*(JPV9**2)))**0.5
       URR9=UPR9*EPSILON*((1.0D0+8.0D0*K*KTR9)/(PI*(JPR9**2)))**0.5
       VR=GAMMA*Z(1)+CDR*Z(2)+CDRRR*(Z(2)**3)+CDRRV*Z(1)*(Z(2)**2)
       VRV9=GAMMA*V9+CDR*Z(2)+CDRRR*(Z(2)**3)+CDRRV*V9*(Z(2)**2)
       VRR9=GAMMA*Z(1)+CDR*R9+CDRRR*(R9**3)+CDRRV*Z(1)*(R9**2)
       VD=(UR**2+VR**2)**0.5
       VDV9=(URV9**2+VRV9**2)**0.5
       VDR9=(URR9**2+VRR9**2)**0.5
       ALPHAR=DEL+DATAN(VR/UR)
       ALPHARV=DEL+DATAN(VRV9/URV9)
       ALPHARR=DEL+DATAN(VRR9/URR9)
       FLAM=(6.13D0*LAMBDA)/(LAMBDA+2.25D0)
       FNN=FLAM*(AR/(L**2))*((VD)**2)*DSIN(ALPHAR)
       FNNV9=FLAM*(AR/(L**2))*((VDV9)**2)*DSIN(ALPHARV)
       FNNR9=FLAM*(AR/(L**2))*((VDR9)**2)*DSIN(ALPHARR)
*
       Y4=-(1.0D0+AH)*FNN*DCOS(DEL)
       Y4V9=-(1.0D0+AH)*FNNV9*DCOS(DEL)
       Y4R9=-(1.0D0+AH)*FNNR9*DCOS(DEL)
*
*  Equation 3.4
*
       PY4V=(Y4-Y4V9)/(Z(1)-V9)
       PY4R=(Y4-Y4R9)/(Z(2)-R9)
       N4=-(XR+AH*XH)*FNN*DCOS(DEL)
       N4V9=-(XR+AH*XH)*FNNV9*DCOS(DEL)
       N4R9=-(XR+AH*XH)*FNNR9*DCOS(DEL)
       PN4V=(N4-N4V9)/(Z(1)-V9)
       PY4R=(Y4-Y4R9)/(Z(2)-R9)
       N4=-(XR+AH*XH)*FNN*DCOS(DEL)
*
*  Equation 3.4
*
       N4V9=-(XR+AH*XH)*FNNV9*DCOS(DEL)
       N4R9=-(XR+AH*XH)*FNNR9*DCOS(DEL)
       PN4V=(N4-N4V9)/(Z(1)-V9)
       PN4R=(N4-N4R9)/(Z(2)-R9)
       K4=(1.0D0+AH)*ZR*FNN*DCOS(DEL)
       K4V9=(1.0D0+AH)*ZR*FNNV9*DCOS(DEL)
       K4R9=(1.0D0+AH)*ZR*FNNR9*DCOS(DEL)
*
*  Equation 3.4
*
       PK4V=(K4-K4V9)/(Z(1)-V9)
PK4R=(K4-K4R9)/(Z(2)-R9)
*
*  Equation 3.3b
*
       C11=N1+3*N111*(Z(1)**2)+N122*(Z(2)**2)+2.0D0*N112*Z(1)*Z(2)
```

```
        C12=2.0D0*N113*Z(1)*Z(3)+N133*(Z(3)**2)
*
        QJAC(1,1)=C11+C12+PN4V
*
*  Equation 3.3c
*
        C21=2.0D0*N122*Z(1)*Z(2)+(N2-M*XG*UND)+3.0D0*N222*(Z(2)**2)
        C22=N112*(Z(1)**2)+2.0D0*N223*Z(2)*Z(3)+N233*(Z(3)**2)
*
        QJAC(1,2)=C21+C22+PN4R
*
*  Equation 3.3d
*
        C31=N3+N113*(Z(1)**2)+2.0D0*N133*Z(1)*Z(3)+N223*(Z(2)**2)
        C32=2.0D0*N233*Z(2)*Z(3)
*
        QJAC(1,3)=C31+C32
*
*  Equation 3.3e
*
        D11=Y1+3.0D0*Y111*(Z(1)**2)+Y122*(Z(2)**2)+2.0D0*Y112*Z(1)*Z(2)
        D12=2.0D0*Y113*Z(1)*Z(3)+Y133*(Z(3)**2)
*
        QJAC(2,1)=D11+D12+PY4V
*
*  Equation 3.3f
*
        D21=2.0D0*Y122*Z(1)*Z(2)+(Y2-M*UND)+3.0D0*Y222*(Z(2)**2)
        D22=2.0D0*Y223*Z(2)*Z(3)+Y233*(Z(3)**2)+Y112*(Z(1)**2)
*
        QJAC(2,2)=D21+D22+PY4R
*
*  Equation 3.3g
*
        D31=Y3+Y113*(Z(1)**2)+2.0D0*Y133*Z(1)*Z(3)+Y223*(Z(2)**2)
        D32=2.0D0*Y233*Z(2)*Z(3)
*
        QJAC(2,3)=D31+D32
*
*  Equation 3.3h
*
        E11=K1+3.0D0*K111*(Z(1)**2)+K122*(Z(2)**2)+2.0D0*K112*Z(1)*Z(2)
        E12=2.0D0*K113*Z(1)*Z(3)+K133*(Z(3)**2)
*
        QJAC(3,1)=E11+E12+PK4V
*
*  Equation 3.3i
*
        E21=2.0D0*K122*Z(1)*Z(2)+(K2+M*ZG*UND)+3.0D0*K222*(Z(2)**2)
        E22=2.0D0*K223*Z(2)*Z(3)+K233*(Z(3)**2)+K112*(Z(1)**2)
*
        QJAC(3,2)=E21+E22+PK4R
*
*  Equation 3.3k
*
c       DGZ1=GM*DCOS(Z(3))+0.5D0*BM*(DTAN(Z(3)))**2*DCOS(Z(3))
c       DGZ2=BM*(DTAN(Z(3))*((1.0D0/DCOS(Z(3)))**2)*DSIN(Z(3)))
c       DGZ=DGZ1+DGZ2
        DGZ=GM*DCOS(Z(3))
*
*  Equation 3.3j
```

```
*
          E31=K3+K113*(Z(1)**2)+2.0D0*K133*Z(1)*Z(3)+K223*(Z(2)**2)
          E32=2.0D0*K233*Z(2)*Z(3)-WG*DGZ
*
          QJAC(3,3)=E31+E32
*
          RETURN
          END
*
          SUBROUTINE EIGTH1(VDEL,V,R,RPHI)
*
          INCLUDE 'HYDCOMN.for'
          INTEGER I,J,IERR
          REAL*8 AE(4,4),BE(4,4),BETA(4),VDEL(300),V(300),R(300),RPHI(300)
          REAL*8 P(300),EVALR(4),EVALI(4),EVAL(4),ALFR(4),ALFI(4),Z(4,4)
          EXTERNAL DMACH,RGG
          DO 500 I=1,IMAX
          P(I)=0.0D0
*   SET UP THE B MATRIX AND RESET EACH I
          UP=UND*(WP+TAU*((V(I)+XP*R(I))**2+CPV*V(I)+CPR*R(I)))
          V9=V(I)*0.99D0
          R9=R(I)*0.99D0
          UPV9=UND*(WP+TAU*((V9+XP*R(I))**2+CPV*V9+CPR*R(I)))
          UPR9=UND*(WP+TAU*((V(I)+XP*R9)**2+CPV*V(I)+CPR*R9))
          JP=(U*UP)/(NP*D)
          JPV9=(U*UPV9)/(NP*D)
          JPR9=(U*UPR9)/(NP*D)
          KT=KTA+(KTB*JP)
          KTV9=KTA+(KTB*JPV9)
          KTR9=KTA+(KTB*JPR9)
          UR=UP*EPSILON*((1.0D0+8.0D0*K*KT)/(PI*(JP**2)))**0.5
          URV9=UPV9*EPSILON*((1.0D0+8.0D0*K*KTV9)/(PI*(JPV9**2)))**0.5
          URR9=UPR9*EPSILON*((1.0D0+8.0D0*K*KTR9)/(PI*(JPR9**2)))**0.5
          VR=GAMMA*V(I)+CDR*R(I)+CDRRR*(R(I)**3)+CDRRV*V(I)*(R(I)**2)
          VRV9=GAMMA*V9+CDR*R(I)+CDRRR*(R(I)**3)+CDRRV*V9*(R(I)**2)
          VRR9=GAMMA*V(I)+CDR*R9+CDRRR*(R9**3)+CDRRV*V(I)*(R9**2)
          VD=(UR**2+VR**2)**0.5
          VDV9=(URV9**2+VRV9**2)**0.5
          VDR9=(URR9**2+VRR9**2)**0.5
          ALPHAR=VDEL(I)+DATAN(VR/UR)
          ALPHARV=VDEL(I)+DATAN(VRV9/URV9)
          ALPHARR=VDEL(I)+DATAN(VRR9/URR9)
          FLAM=(6.13D0*LAMBDA)/(LAMBDA+2.25D0)
          FNN=FLAM*(AR/(L**2))*((VD)**2)*DSIN(ALPHAR)
          FNNV9=FLAM*(AR/(L**2))*((VDV9)**2)*DSIN(ALPHARV)
          FNNR9=FLAM*(AR/(L**2))*((VDR9)**2)*DSIN(ALPHARR)
*
          Y4=-(1.0D0+AH)*FNN*DCOS(VDEL(I))
          Y4V9=-(1.0D0+AH)*FNNV9*DCOS(VDEL(I))
          Y4R9=-(1.0D0+AH)*FNNR9*DCOS(VDEL(I))
          PY4V=(Y4-Y4V9)/(V(I)-V9)
          PY4R=(Y4-Y4R9)/(R(I)-R9)
          N4=-(XR+AH*XH)*FNN*DCOS(VDEL(I))
          N4V9=-(XR+AH*XH)*FNNV9*DCOS(VDEL(I))
          ''4R9=-(XR+AH*XH)*FNNR9*DCOS(VDEL(I))
           .4V=(N4-N4V9)/(V(I)-V9)
          PN4R=(N4-N4R9)/(R(I)-R9)
          K4=(1.0D0+AH)*ZR*FNN*DCOS(VDEL(I))
          K4V9=(1.0D0+AH)*ZR*FNNV9*DCOS(VDEL(I))
          K4R9=(1.0D0+AH)*ZR*FNNR9*DCOS(VDEL(I))
          PK4V=(K4-K4V9)/(V(I)-V9)
```

77

```
        PK4R=(K4-K4R9)/(R(I)-R9)
*
*    Calculate the fundamental circular frequency
*
        WN=((WG*GM)/(0.000021D0))**0.5
        IF(FN.LE.0.1)THEN
        KAPPA=0.1D0
        ELSE IF(FN.GE.0.2)THEN
        KAPPA=0.2D0
        ELSE
        KAPPA=FN
        ENDIF
        KPHIDOT=-0.000021D0*KAPPA*WN
*
*    Equation 4.1b
*
        BE(1,1)=0.00035245D0
        BE(1,2)=0.000875D0
        BE(1,3)=0.0D0
        BE(1,4)=-0.000213D0
        BE(2,1)=0.014969D0
        BE(2,2)=0.00035245D0
        BE(2,3)=-0.000221D0
        BE(2,4)=0.0D0
        BE(3,1)=-0.000221D0
        BE(3,2)=0.0D0
        BE(3,3)=0.000021D0
        BE(3,4)=-KPHIDOT
        BE(4,1)=0.0D0
        BE(4,2)=0.0D0
        BE(4,3)=0.0D0
        BE(4,4)=1.0D0
*
*    Equation 4.1c              SET UP THE A MATRIX
*
        C11=N1+3*N111*(V(I)**2)+N122*(R(I)**2)+2.0D0*N112*V(I)*R(I)
        C12=2.0D0*N113*V(I)*RPHI(I)+N133*(RPHI(I)**2)
*
        AE(1,1)=C11+C12+PN4V
*
        C21=2.0D0*N122*V(I)*R(I)+(N2-M*XG*UND)+3.0D0*N222*(R(I)**2)
        C22=N112*(V(I)**2)+2.0D0*N223*R(I)*RPHI(I)+N233*(RPHI(I)**2)
*
        AE(1,2)=C21+C22+PN4R
        AE(1,3)=0.0D0
*
        C41=N3+N113*(V(I)**2)+2.0D0*N133*V(I)*RPHI(I)+N223*(R(I)**2)
        C42=2.0D0*N233*R(I)*RPHI(I)
*
        AE(1,4)=C41+C42
*
        D11=Y1+3.0D0*Y111*(V(I)**2)+Y122*(R(I)**2)+2.0D0*Y112*V(I)*R(I)
        D12=2.0D0*Y113*V(I)*RPHI(I)+Y133*(RPHI(I)**2)
*
        AE(2,1)=D11+D12+PY4V
*
        D21=2.0D0*Y122*V(I)*R(I)+(Y2-M*UND)+3.0D0*Y222*(R(I)**2)
        D22=2.0D0*Y223*R(I)*RPHI(I)+Y233*(RPHI(I)**2)+Y112*(V(I)**2)
*
        AE(2,2)=D21+D22+PY4R
        AE(2,3)=0.0D0
```

```
*
       D41=Y3+Y113*(V(I)**2)+2.0D0*Y133*V(I)*RPHI(I)+Y223*(R(I)**2)
       D42=2.0D0*Y233*R(I)*RPHI(I)
*
       AE(2,4)=D41+D42
*
       E11=K1+3.0D0*K111*(V(I)**2)+K122*(R(I)**2)+2.0D0*K112*V(I)*R(I)
       E12=2.0D0*K113*V(I)*RPHI(I)+K133*(RPHI(I)**2)
*
       AE(3,1)=E11+E12+PK4V
*
       E21=2.0D0*K122*V(I)*R(I)+(K2+M*ZG*UND)+3.0D0*K222*(R(I)**2)
       E22=2.0D0*K223*R(I)*RPHI(I)+K233*(RPHI(I)**2)+K112*(V(I)**2)
*
       AE(3,2)=E21+E22+PK4R
       AE(3,3)=0.0D0
*
c      DGZ1=GM*DCOS(RPHI(I))+0.5D0*BM*(DTAN(RPHI(I)))**2*DCOS(RPHI(I))
c      DGZ2=BM*(DTAN(RPHI(I))*((1.0D0/DCOS(RPHI(I)))**2)*DSIN(RPHI(I)))
c      DGZ=DGZ1+DGZ2
       DGZ=GM*DCOS(RPHI(I))
       E41=K3+K113*(V(I)**2)+2.0D0*K133*V(I)*RPHI(I)+K223*(R(I)**2)
       E42=2.0D0*K233*R(I)*RPHI(I)-WG*DGZ
*
       AE(3,4)=E41+E42
       AE(4,1)=0.0D0
       AE(4,2)=0.0D0
       AE(4,3)=1.0D0
       AE(4,4)=0.0D0
*
*    This is a subroutine that utilizes the EISPACK LIBRARY [Ref. 20]
*
*
*    Purpose:  Calls the recommended sequence of subroutines from the
*              Eigensystem subroutine package (EISPACK) to find the
*              eigenvalues of the real generalized eigenproblem:
*                       AX = (LAMBDA)*BX
*
*    Arguments:
*
*      NM    -Row dimension of the two-dimensional array parameters as
*             declared in the calling program Dimension statement
*             (Input)
*      N     -The order of the matrices A and B.    (Input)
*      A     -Contains a real general matrix   (Input)
*      B     -Contains a real general matrix   (Input)
*      MATZ  -Path indicator.  If= 0, eigenvalues are found.  (Input)
*      ALFR  -Real parts of the numerators of the eigenvalues. (Output)
*      ALFI  -Imaginary parts of the numerators of the eigenvalues.
*             (Output)
*      BETA  -Contains the denominators of the eigenvalues, which are
*             given by the ratios: (ALFR+I*ALFI)/BETA.  (Output)
*      Z     -For eigenvector usage if MATZ not equal to zero. (Output)
*      IERR  -Error completion code.  (Output)
*
*
       CALL RGG(4,4,AE,BE,ALFR,ALFI,BETA,O,Z,IERR)
       DO 600 J=1,4
        IF(BETA(J).NE.0.0D0)THEN
          EVALR(J)=ALFR(J)/BETA(J)
          EVALI(J)=ALFI(J)/BETA(J)
```

```fortran
      ELSE
         EVALR(J)=DMACH(2)
         EVALI(J)=DMACH(2)
      ENDIF
  600 CONTINUE
      WRITE(25,25)EVALR(1),EVALI(1),EVALR(2),EVALI(2)
      WRITE(30,25)EVALR(3),EVALI(3),EVALR(4),EVALI(4)
*
*  Calculate the damping ratio and the natural frequency
*
      Z1=-EVALR(1)/(DSQRT(EVALI(1)**2+EVALR(1)**2))
      Z2=-EVALR(2)/(DSQRT(EVALI(2)**2+EVALR(2)**2))
      Z3=-EVALR(3)/(DSQRT(EVALI(3)**2+EVALR(3)**2))
      Z4=-EVALR(4)/(DSQRT(EVALI(4)**2+EVALR(4)**2))
      WN1=DSQRT(EVALI(1)**2+EVALR(1)**2)
      WN2=DSQRT(EVALI(2)**2+EVALR(2)**2)
      WN3=DSQRT(EVALI(3)**2+EVALR(3)**2)
      WN4=DSQRT(EVALI(4)**2+EVALR(4)**2)
      WRITE(35,25)Z1,Z2,Z3,Z4
      WRITE(36,25)WN1,WN2,WN3,WN4
   25 FORMAT(4E15.5)
  500 CONTINUE
      RETURN
      END
*
      SUBROUTINE EIGTH2(VDEL,V,R)
*
      INCLUDE 'HYDCOMN.for'
      INTEGER I,J,IERR
      REAL*8 AE(2,2),BE(2,2),BETA(2),VDEL(300),V(300),R(300)
      REAL*8 EVALR(2),EVALI(2),EVAL(2),ALFR(2),ALFI(2),Z(2,2)
      EXTERNAL DMACH,RGG
      DO 500 I=1,imax
*  SET UP THE B MATRIX AND RESET EACH I
      UP=UND*(WP+TAU*((V(I)+XP*R(I))**2+CPV*V(I)+CPR*R(I)))
      V9=V(I)*0.99D0
      R9=R(I)*0.99D0
      UPV9=UND*(WP+TAU*((V9+XP*R(I))**2+CPV*V9+CPR*R(I)))
      UPR9=UND*(WP+TAU*((V(I)+XP*R9)**2+CPV*V(I)+CPR*R9))
      JP=(U*UP)/(NP*D)
      JPV9=(U*UPV9)/(NP*D)
      JPR9=(U*UPR9)/(NP*D)
      KT=KTA+(KTB*JP)
      KTV9=KTA+(KTB*JPV9)
      KTR9=KTA+(KTB*JPR9)
      UR=UP*EPSILON*((1.0D0+8.0D0*K*KT)/(PI*(JP**2)))**0.5
      URV9=UPV9*EPSILON*((1.0D0+8.0D0*K*KTV9)/(PI*(JPV9**2)))**0.5
      URR9=UPR9*EPSILON*((1.0D0+8.0D0*K*KTR9)/(PI*(JPR9**2)))**0.5
      VR=GAMMA*V(I)+CDR*R(I)+CDRRR*(R(I)**3)+CDRRV*V(I)*(R(I)**2)
      VRV9=GAMMA*V9+CDR*R(I)+CDRRR*(R(I)**3)+CDRRV*V9*(R(I)**2)
      VRR9=GAMMA*V(I)+CDR*R9+CDRRR*(R9**3)+CDRRV*V(I)*(R9**2)
      VD=(UR**2+VR**2)**0.5
      VDV9=(URV9**2+VRV9**2)**0.5
      VDR9=(URR9**2+VRR9**2)**0.5
      ALPHAR=VDEL(I)+DATAN(VR/UR)
      ALPHARV=VDEL(I)+DATAN(VRV9/URV9)
      ALPHARR=VDEL(I)+DATAN(VRR9/URR9)
      FLAM=(6.13D0*LAMBDA)/(LAMBDA+2.25D0)
      FNN=FLAM*(AR/(L**2))*((VD)**2)*DSIN(ALPHAR)
      FNNV9=FLAM*(AR/(L**2))*((VDV9)**2)*DSIN(ALPHARV)
      FNNR9=FLAM*(AR/(L**2))*((VDR9)**2)*DSIN(ALPHARR)
```

```fortran
*
      Y4=-(1.0D0+AH)*FNN*DCOS(VDEL(I))
      Y4V9=-(1.0D0+AH)*FNNV9*DCOS(VDEL(I))
      Y4R9=-(1.0D0+AH)*FNNR9*DCOS(VDEL(I))
      PY4V=(Y4-Y4V9)/(V(I)-V9)
      PY4R=(Y4-Y4R9)/(R(I)-R9)
      N4=-(XR+AH*XH)*FNN*DCOS(VDEL(I))
      N4V9=-(XR+AH*XH)*FNNV9*DCOS(VDEL(I))
      N4R9=-(XR+AH*XH)*FNNR9*DCOS(VDEL(I))
      PN4V=(N4-N4V9)/(V(I)-V9)
      PN4R=(N4-N4R9)/(R(I)-R9)
*
      WN=((WG*GM)/(0.000021D0))**0.5
*
*     Equation 4.4b
*
      BE(1,1)=0.00035245D0
      BE(1,2)=0.000875D0
      BE(2,1)=0.014969D0
      BE(2,2)=0.00035245D0
*
*     Equation 4.4c-g
*
      C11=N1+3*N111*(V(I)**2)+N122*(R(I)**2)+2.0D0*N112*V(I)*R(I)
*
      AE(1,1)=C11+PN4V
*
      C21=2.0D0*N122*V(I)*R(I)+(N2-M*XG*UND)+3.0D0*N222*(R(I)**2)
      C22=N112*(V(I)**2)+PN4R
*
      AE(1,2)=C21+C22
*
      D11=Y1+3.0D0*Y111*(V(I)**2)+Y122*(R(I)**2)+2.0D0*Y112*V(I)*R(I)
*
      AE(2,1)=D11+PY4V
*
      D21=2.0D0*Y122*V(I)*R(I)+(Y2-M*UND)+3.0D0*Y222*(R(I)**2)
      D22=Y112*(V(I)**2)+PY4R
*
      AE(2,2)=D21+D22
*
      CALL RGG(2,2,AE,BE,ALFR,ALFI,BETA,0,Z,IERR)
      DO 600 J=1,2
        IF(BETA(J).NE.0.0D0)THEN
          EVALR(J)=ALFR(J)/BETA(J)
          EVALI(J)=ALFI(J)/BETA(J)
        ELSE
          EVALR(J)=DMACH(2)
          EVALI(J)=DMACH(2)
        ENDIF
 600  CONTINUE
      WRITE(26,25)EVALR(1),EVALI(1),EVALR(2),EVALI(2)
  25  FORMAT(4E15.5)
 500  CONTINUE
      RETURN
      END
*
      SUBROUTINE EIGTH3(VDEL,RPHI)
*
      INCLUDE 'HYDCOMN.for'
      INTEGER I,J,IERR
```

81

```fortran
      REAL*8 AE(2,2),BE(2,2),BETA(2),VDEL(300),RPHI(300)
      REAL*8 P(300),EVALR(2),EVALI(2),EVAL(2),ALFR(2),ALFI(2),Z(2,2)
      EXTERNAL DMACH,RGG
      DO 500 I=1,imax
      P(I)=0.0D0
*   SET UP THE B MATRIX AND RESET EACH I
      WN=((WG*GM)/(0.000021D0))**0.5
      IF(FN.LE.0.1)THEN
      KAPPA=0.1D0
      ELSE IF(FN.GE.0.2)THEN
      KAPPA=0.2D0
      ELSE
      KAPPA=FN
      ENDIF
      KPHIDOT=-0.000021D0*KAPPA*WN
*
*     Equation 4.7b
*
      BE(1,1)=0.000021D0
      BE(1,2)=-KPHIDOT
      BE(2,1)=0.0d0
      BE(2,2)=1.0D0
*
*     Equation 4.7c-e
*
      AE(1,1)=0.0d0
c     DGZ1=GM*DCOS(RPHI(I))+0.5D0*BM*(DTAN(RPHI(I)))**2*DCOS(RPHI(I))
c     DGZ2=BM*(DTAN(RPHI(I))*((1.0D0/DCOS(RPHI(I)))**2)*DSIN(RPHI(I)))
c     DGZ=DGZ1+DGZ2
      DGZ=GM*DCOS(RPHI(I))
      AE(1,2)=K3-WG*DGZ
      AE(2,1)=1.0D0
      AE(2,2)=0.0D0
      CALL RGG(2,2,AE,BE,ALFR,ALFI,BETA,0,Z,IERR)
      DO 600 J=1,2
        IF(BETA(J).NE.0.0D0)THEN
          EVALR(J)=ALFR(J)/BETA(J)
          EVALI(J)=ALFI(J)/BETA(J)
        ELSE
          EVALR(J)=DMACH(2)
          EVALI(J)=DMACH(2)
        ENDIF
 600  CONTINUE
      WRITE(27,25)EVALR(1),EVALI(1),EVALR(2),EVALI(2)
       Z1=-EVALR(1)/(DSQRT(EVALI(1)**2+EVALR(1)**2))
       Z2=-EVALR(2)/(DSQRT(EVALI(2)**2+EVALR(2)**2))
       WN1=DSQRT(EVALI(1)**2+EVALR(1)**2)
       WN2=DSQRT(EVALI(2)**2+EVALR(2)**2)
      WRITE(37,25)Z1,Z2,WN1,WN2
  25  FORMAT(4E15.5)
 500  CONTINUE
      RETURN
      END
```

APPENDIX B

Fn = 0.3 and α = 0.6
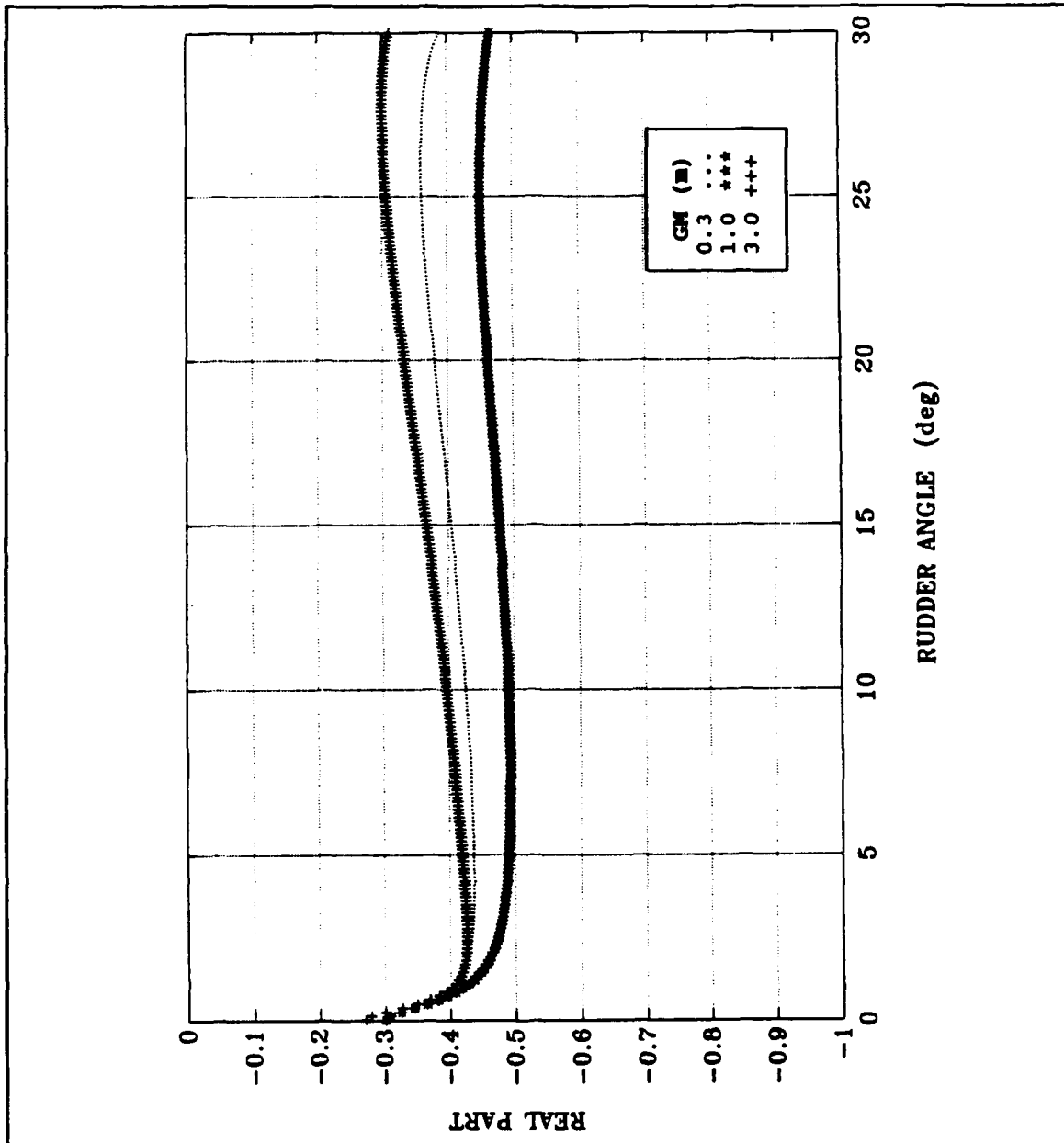
B.1: Effect of GM on Coupled Model Roll Eigenvalues; Real Part

Fn = 0.3 m and α = 0.6
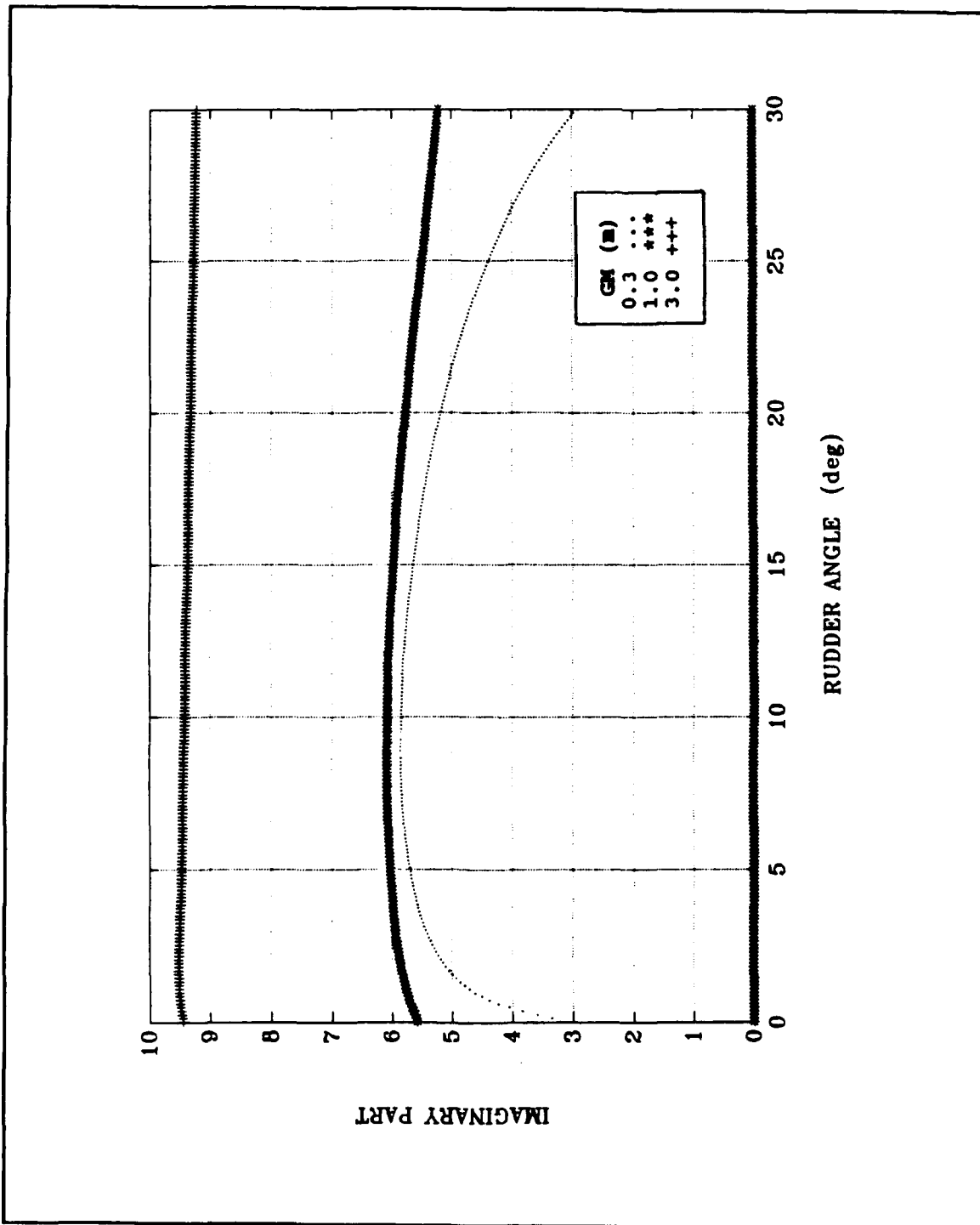
B.2: Effect of GM on Coupled Model Roll Eigenvalues; Imaginary Part

GM = 0.3 m and α = 0.6
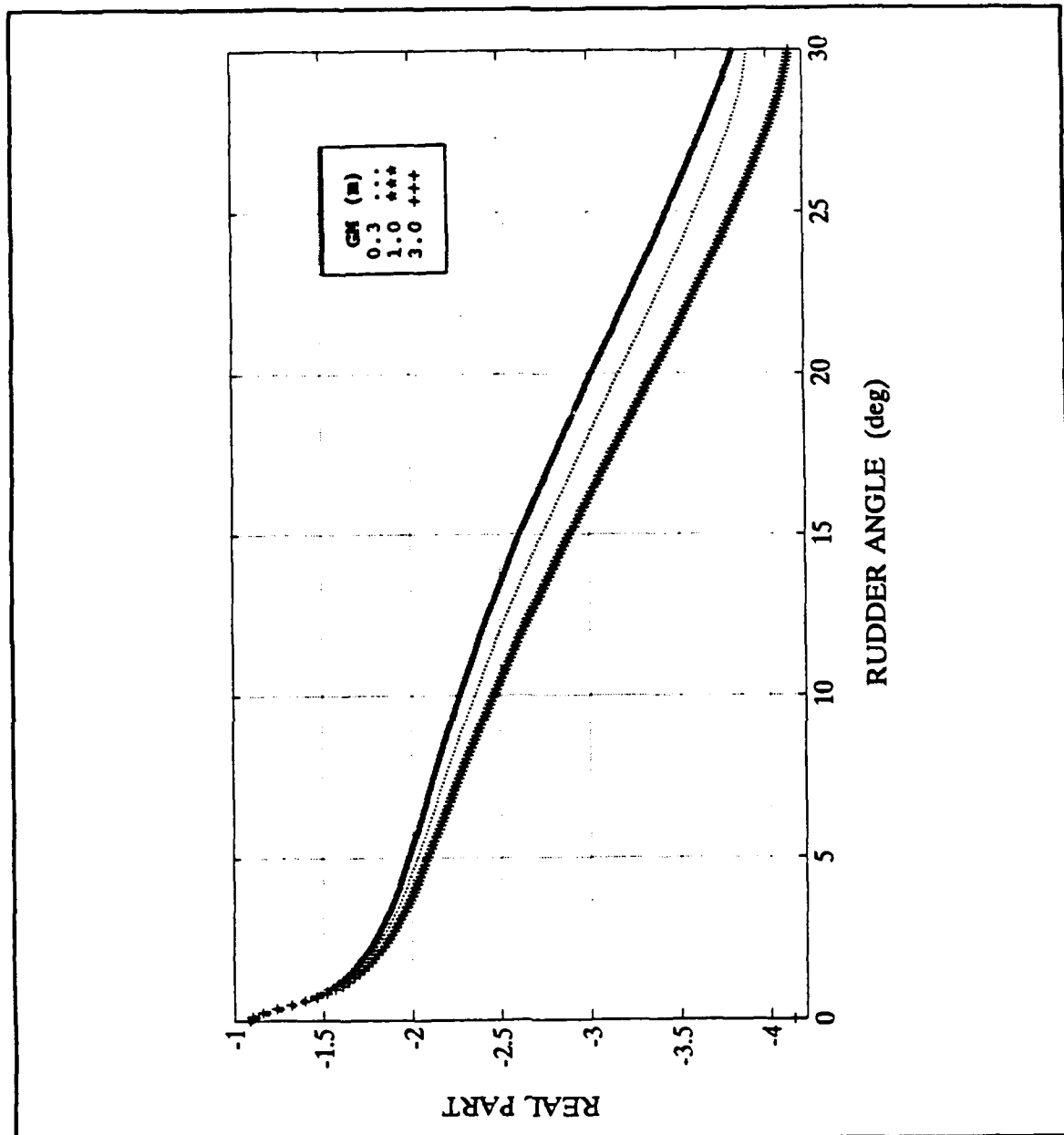
B.3: Effect of GM on Coupled Model Upper Steering Eigenvalues
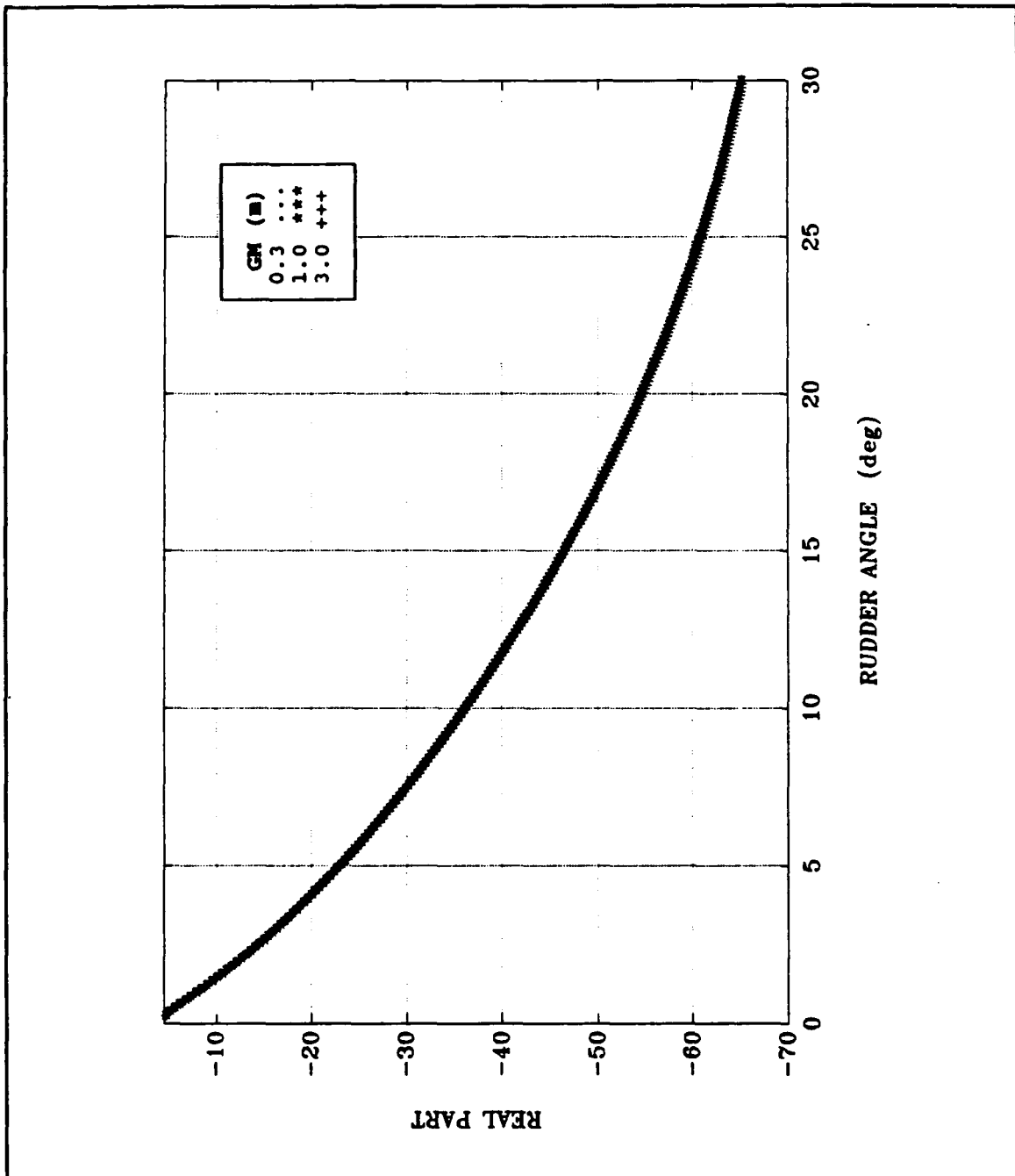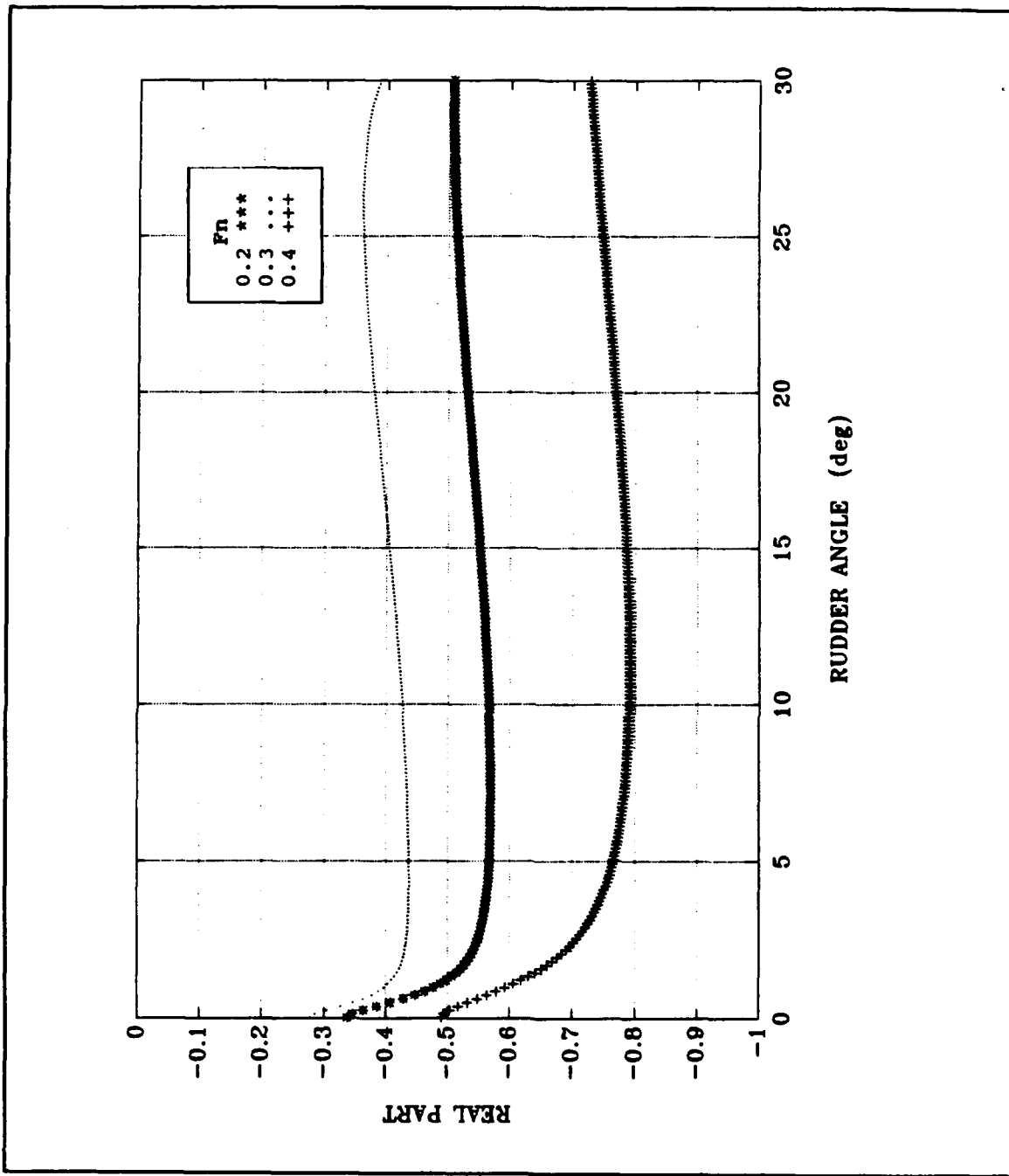
GM = 0.3 m and α = 0.6

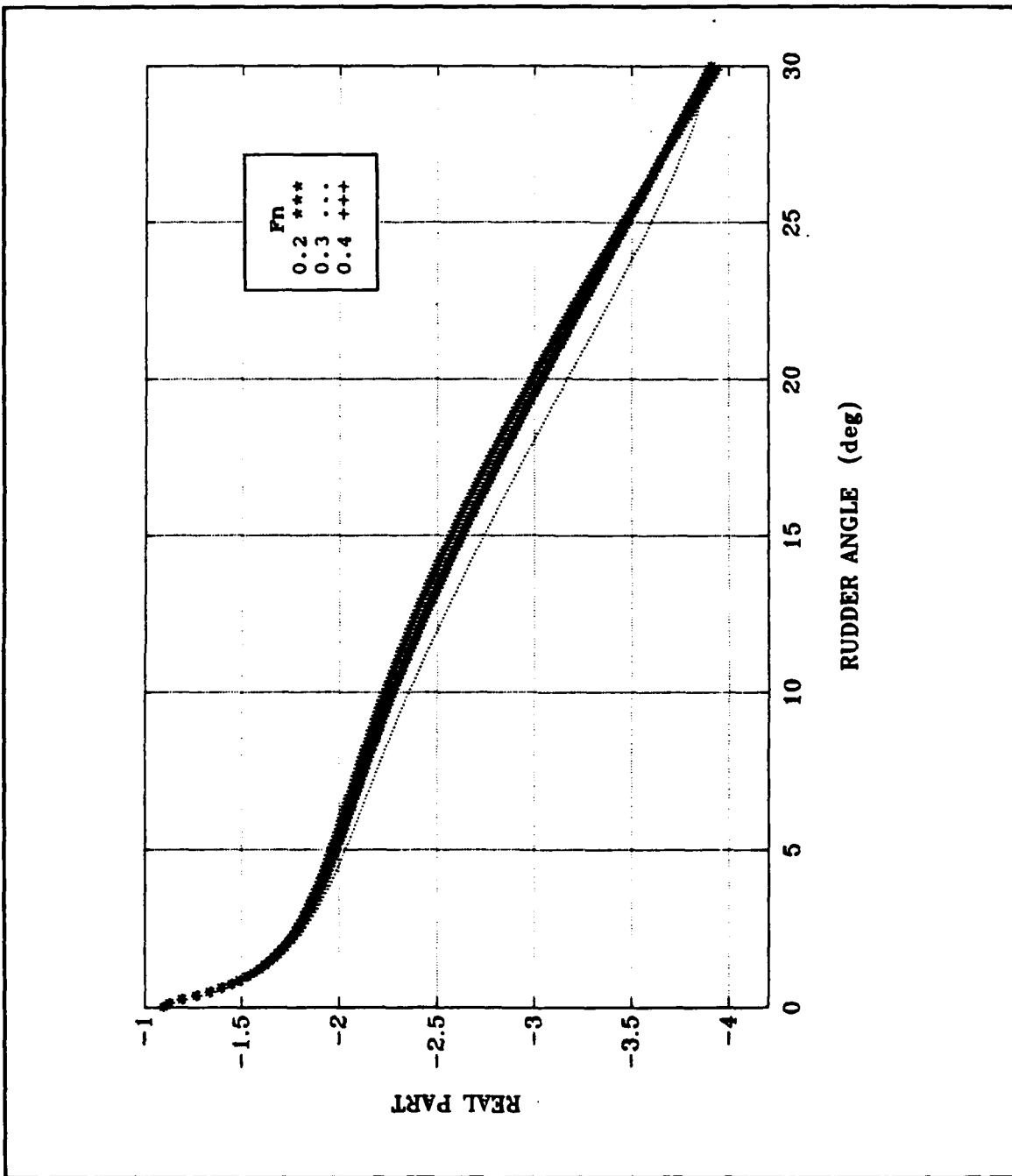B.4: Effect of GM on Coupled Model Lower Steering Eigenvalues
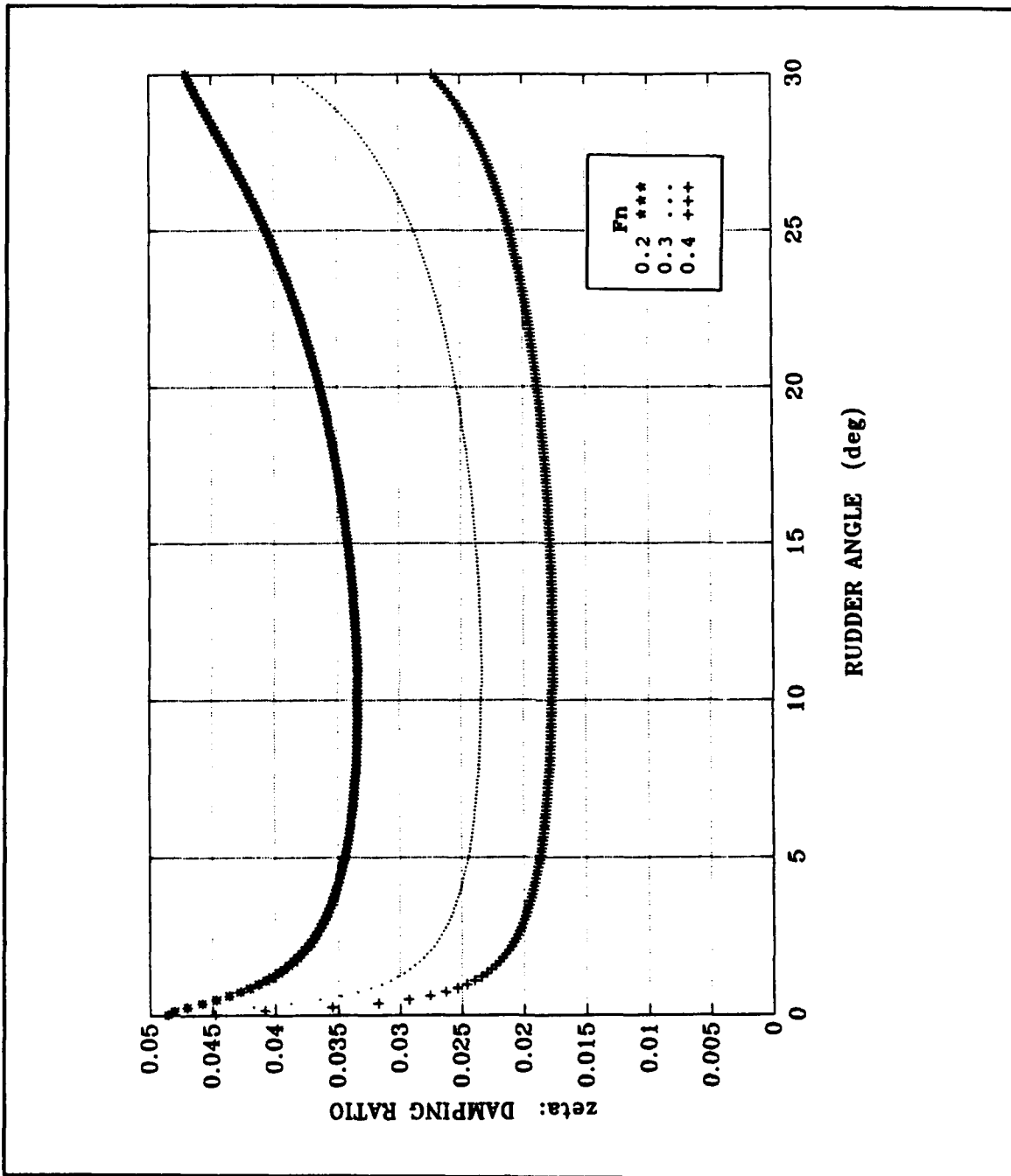
GM = 0.3 m and α = 0.6

B.5: Effect of Fn on Decoupled Model Damping Ratio

GM = 0.3 m and Fn = 0.6

B.6: Effect of Fn on Coupled Model Roll Eigenvalues

GM = 0.3 m and Fn = 0.6

B.7: Effect of Fn on Coupled Model Upper Steering Eigenvalues

89
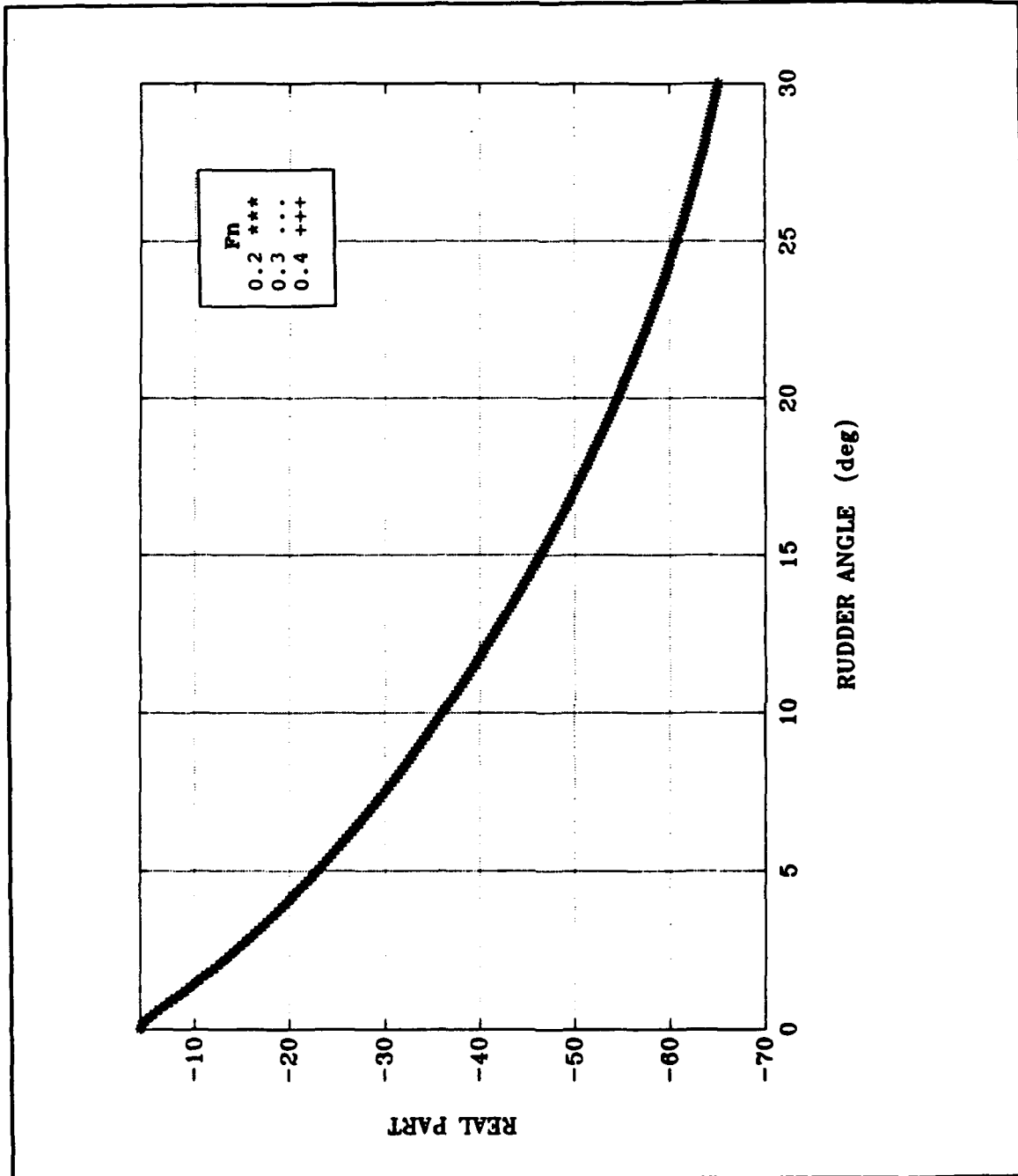
GM = 0.3 m and α = 0.6

B.8: Effect of Fn on Coupled Model Lower Steering Eigenvalues
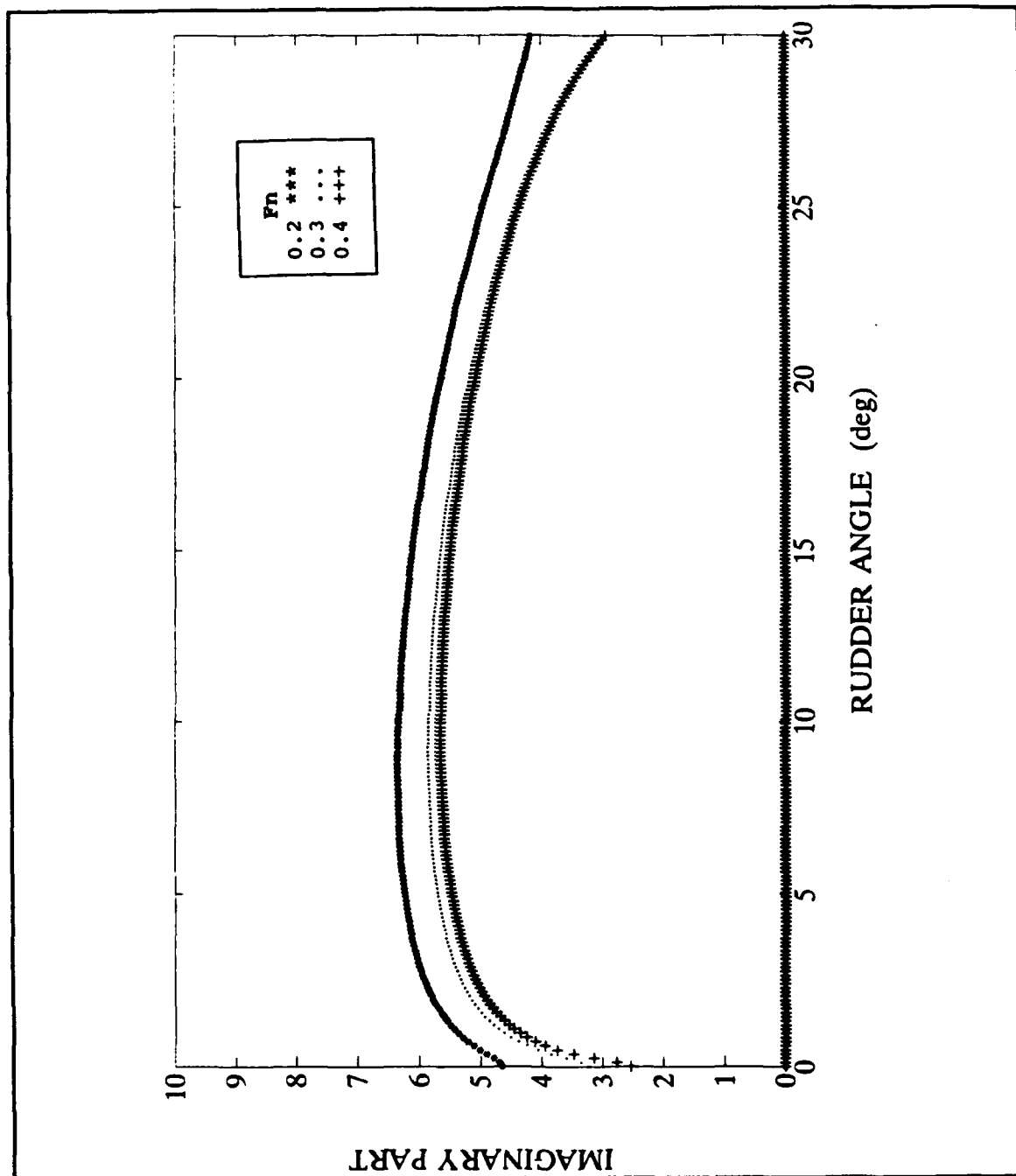
GM = 0.3 m and α = 0.6

B.9:   Effect of Fn on Coupled Model Roll Eigenvalues

91
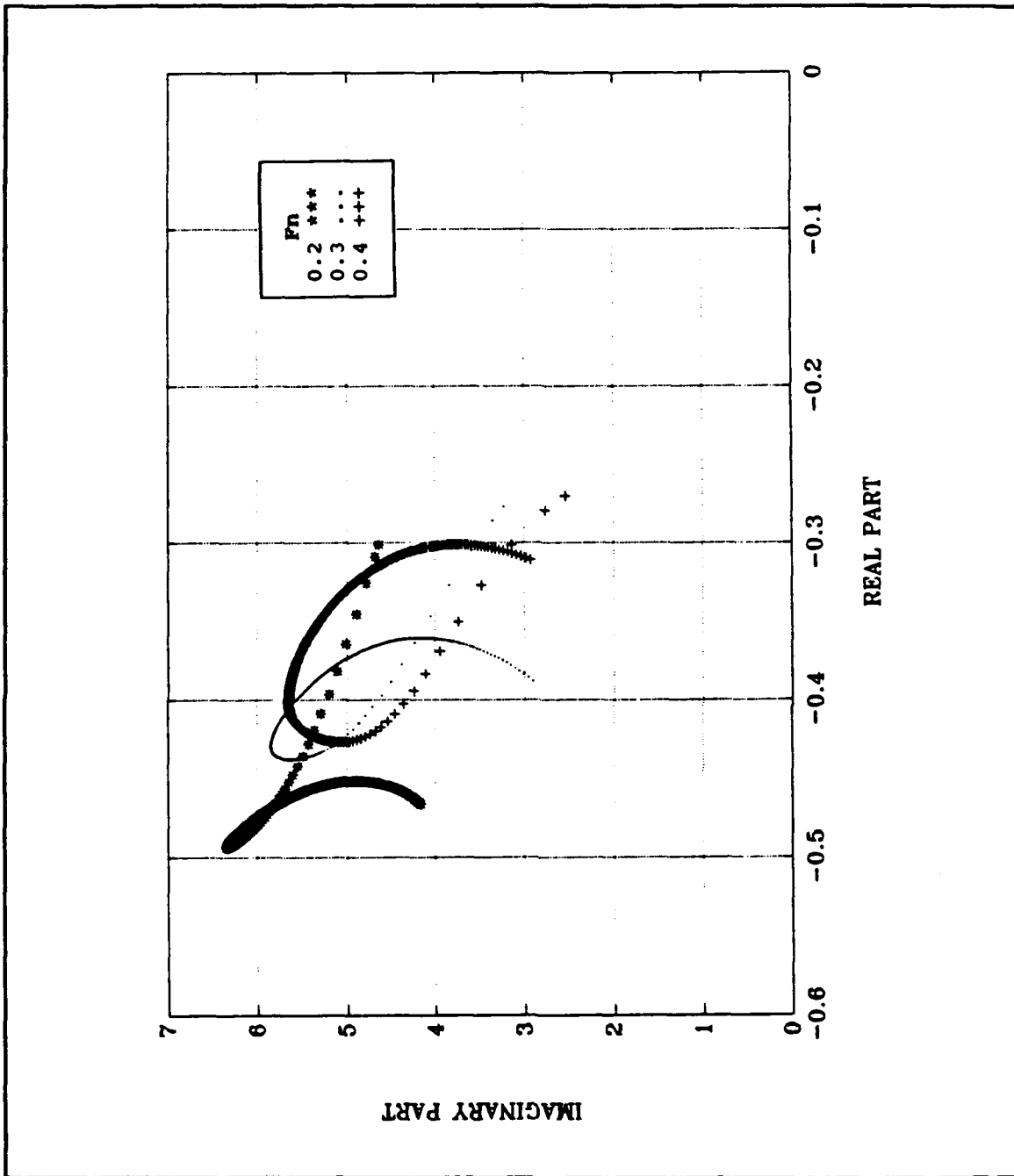
GM = 0.3 m and α = 0.6

B.10: Effect of Fn on Coupled Model Root Locus

GM = 0.3 m and Fn = 0.3
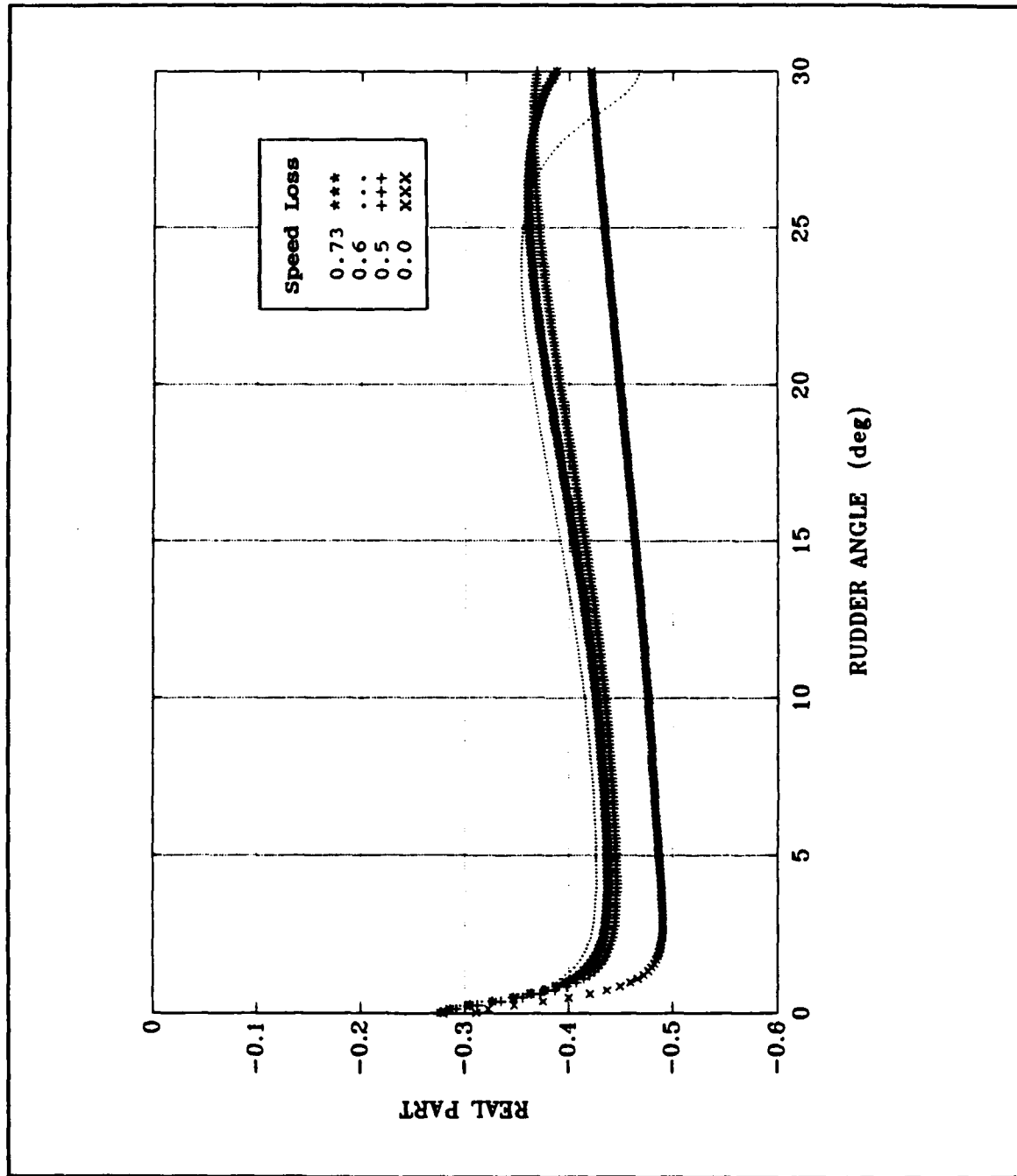
B.11: Effect of Speed Loss on Coupled Model Roll Eigenvalues
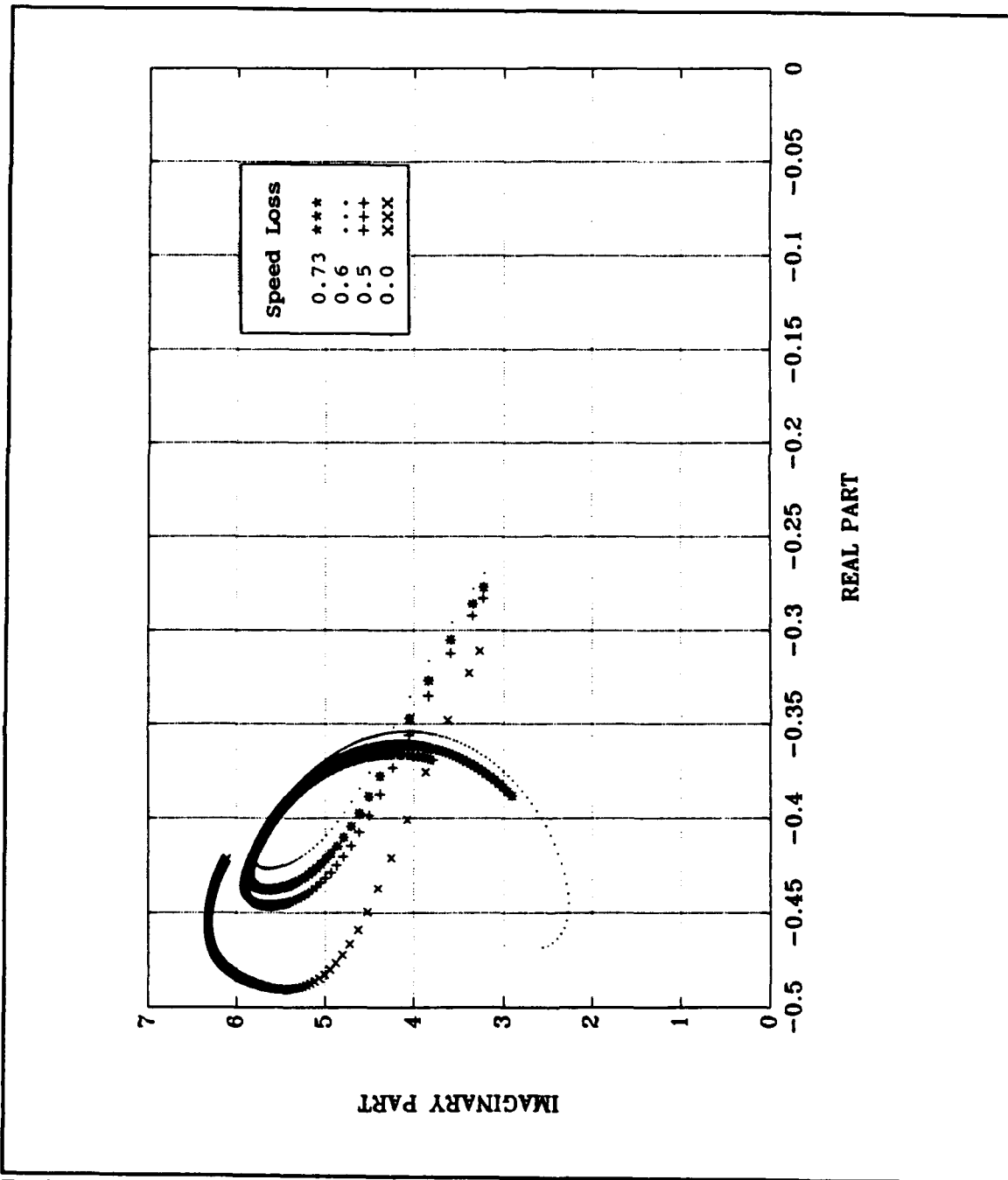
GM = 0.3 m and Fn = 0.3
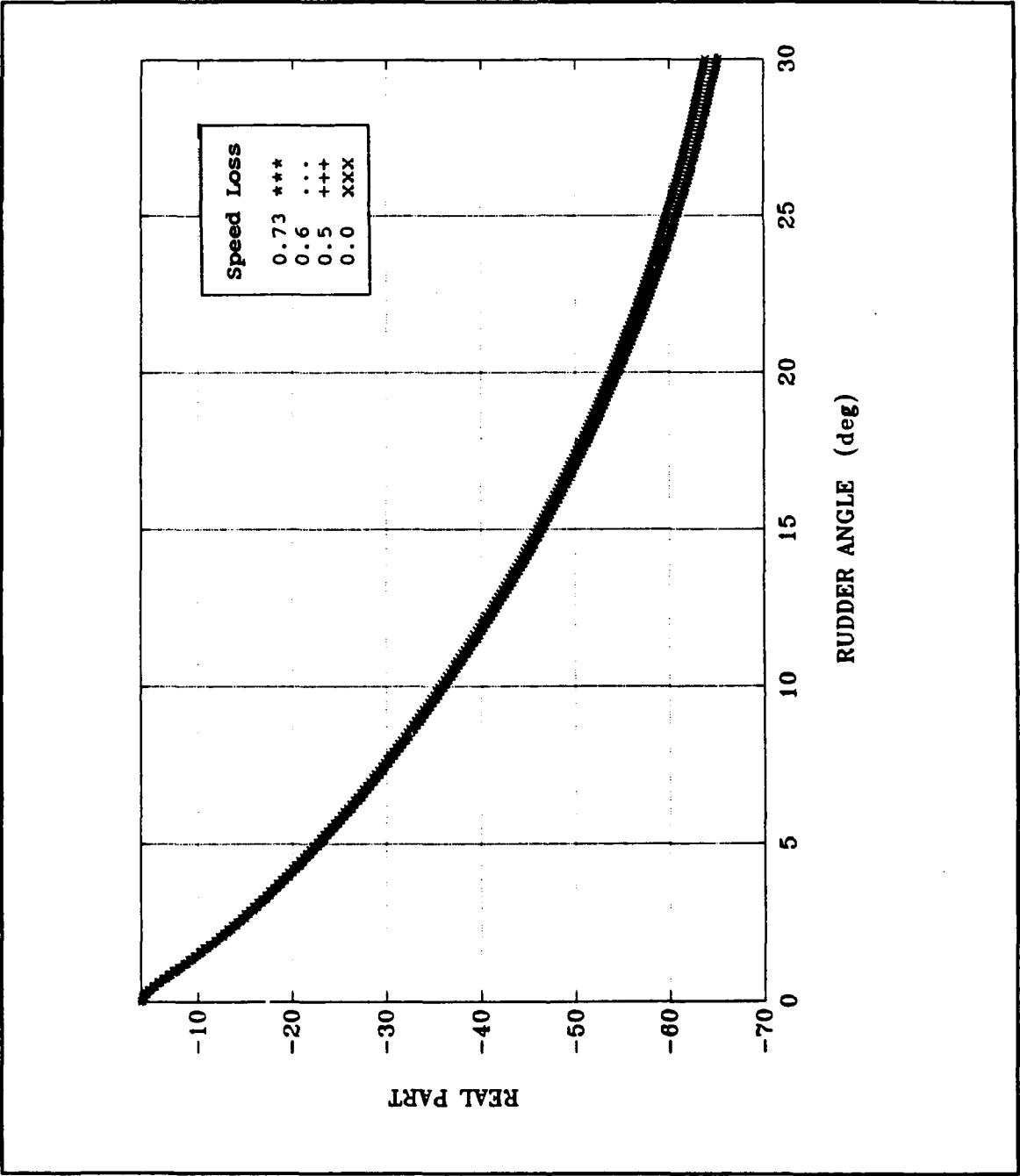

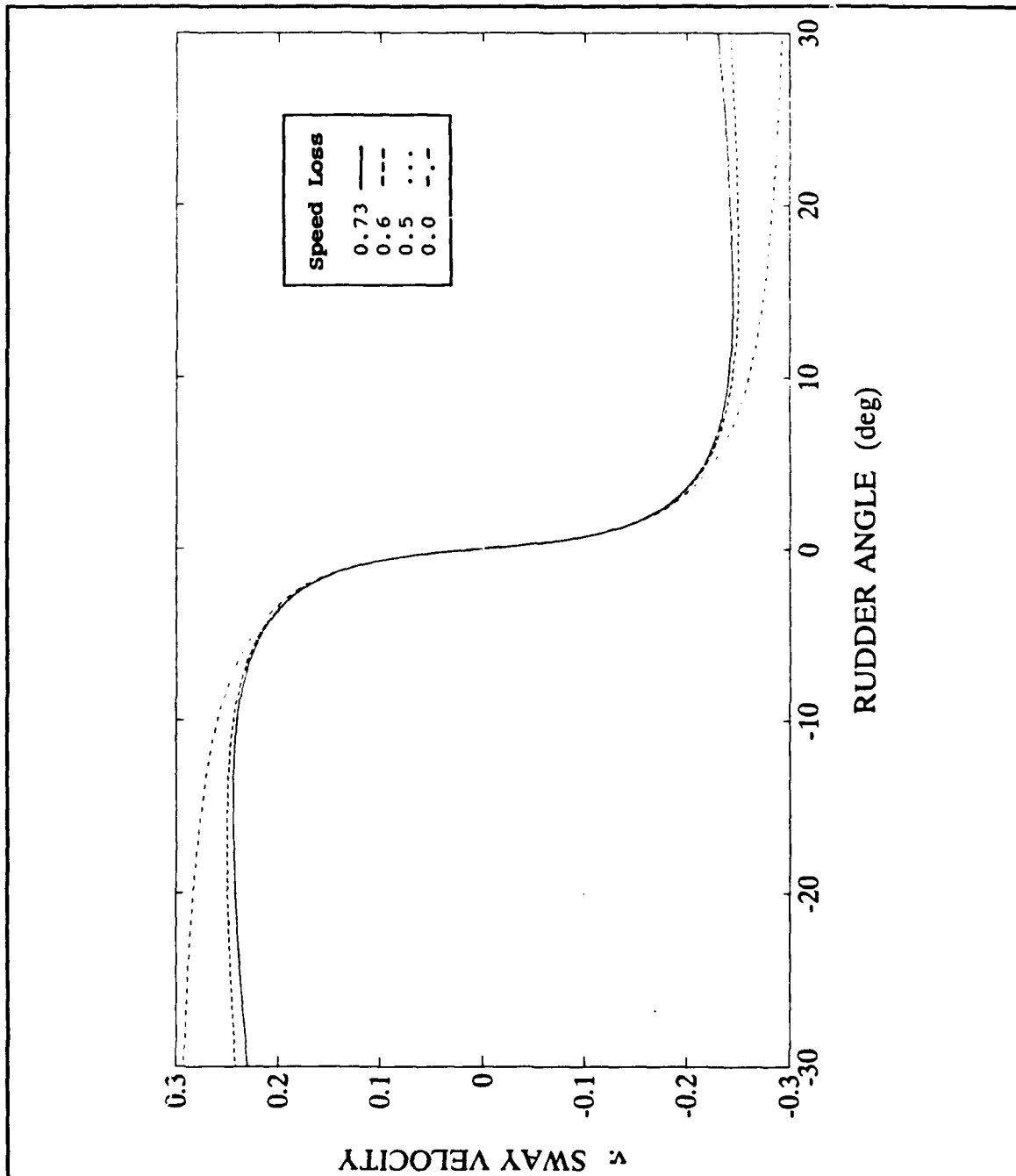B.12: Effect of Speed Loss on Coupled Model Root Locus
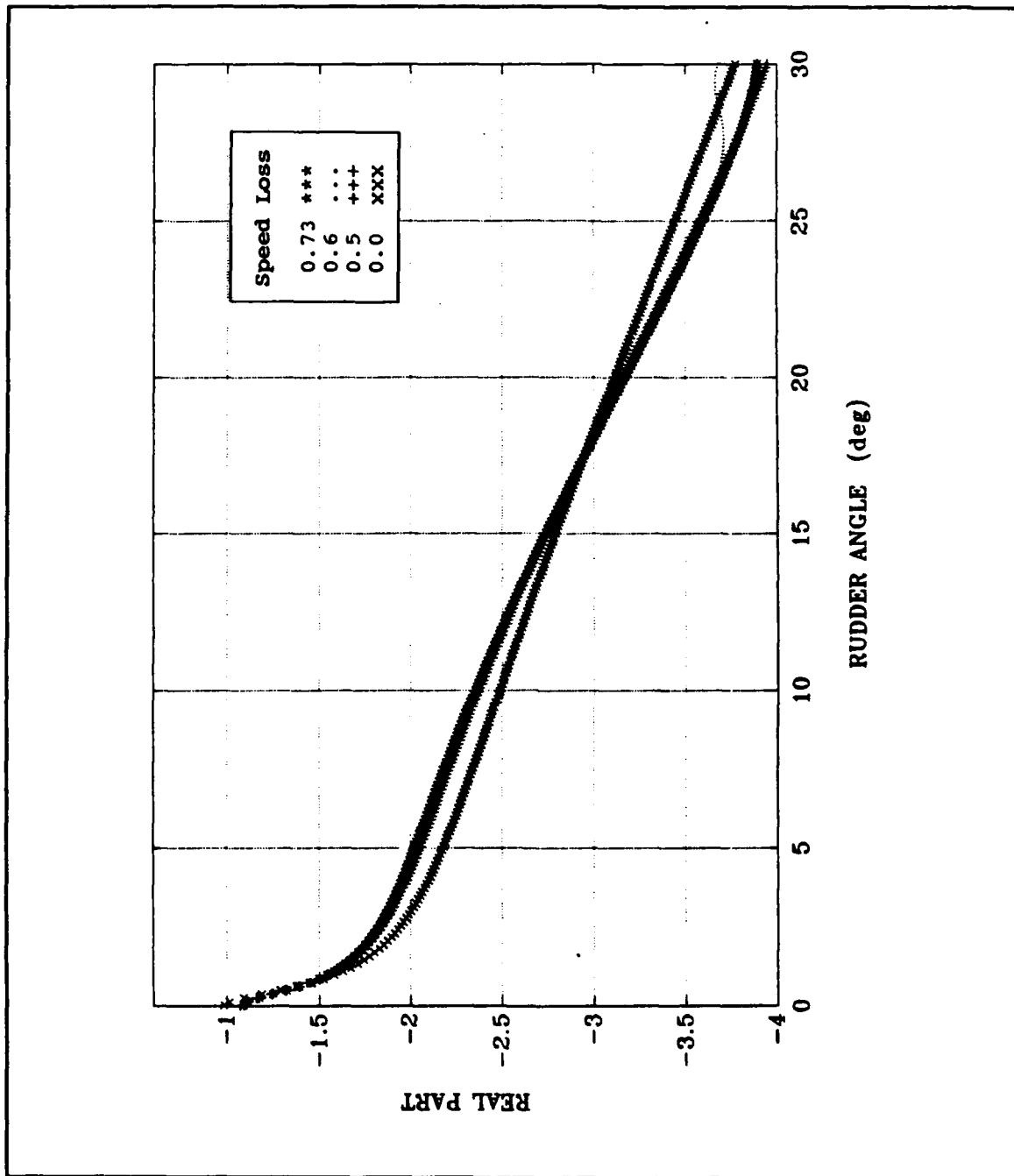
B.13: Effect of Speed Loss on Coupled Model Upper Steering Eigenvalues
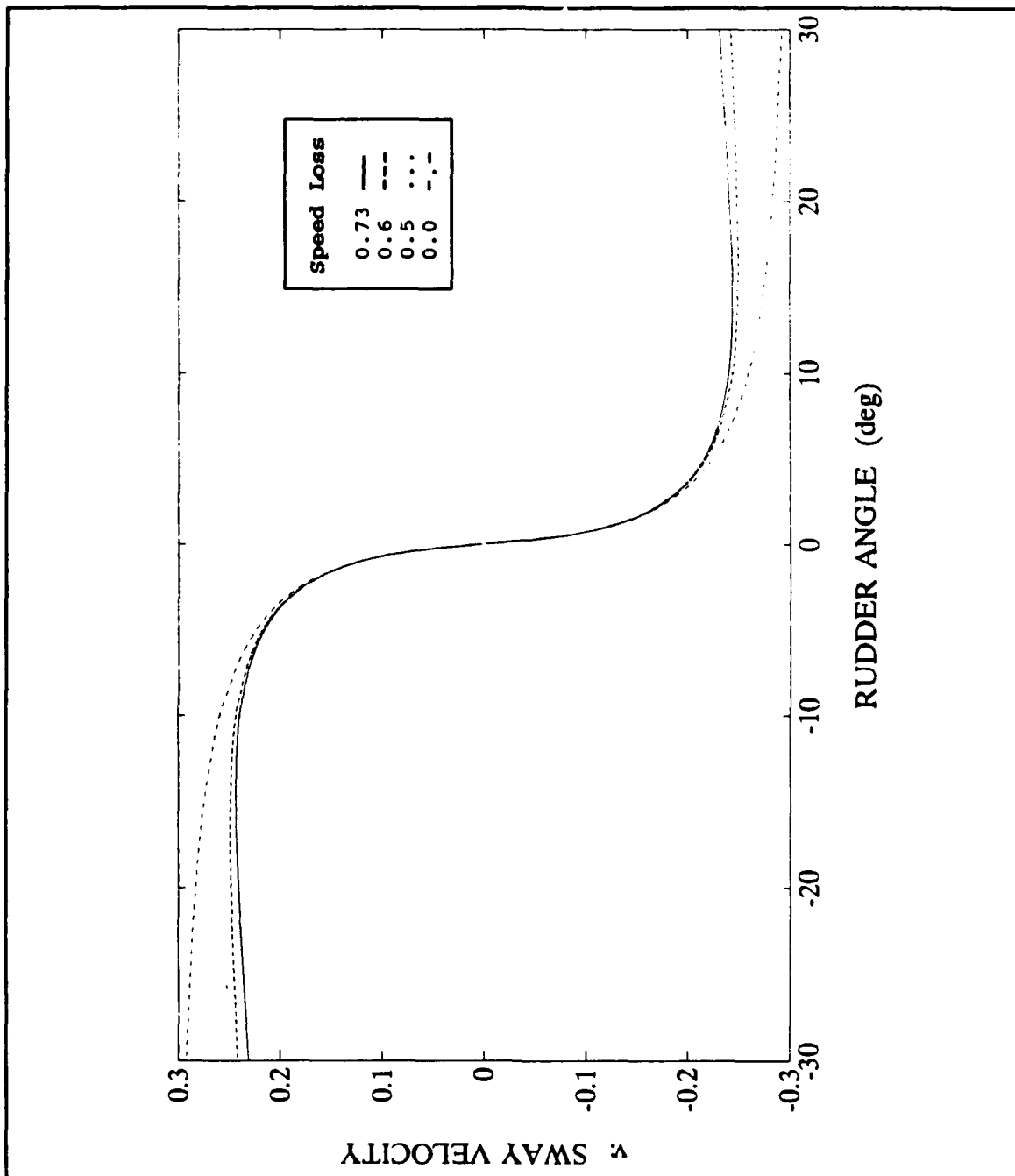
GM = 0.3 m and Fn = 0.3

B.14: Effect of Speed Loss on Coupled Model Lower Steering
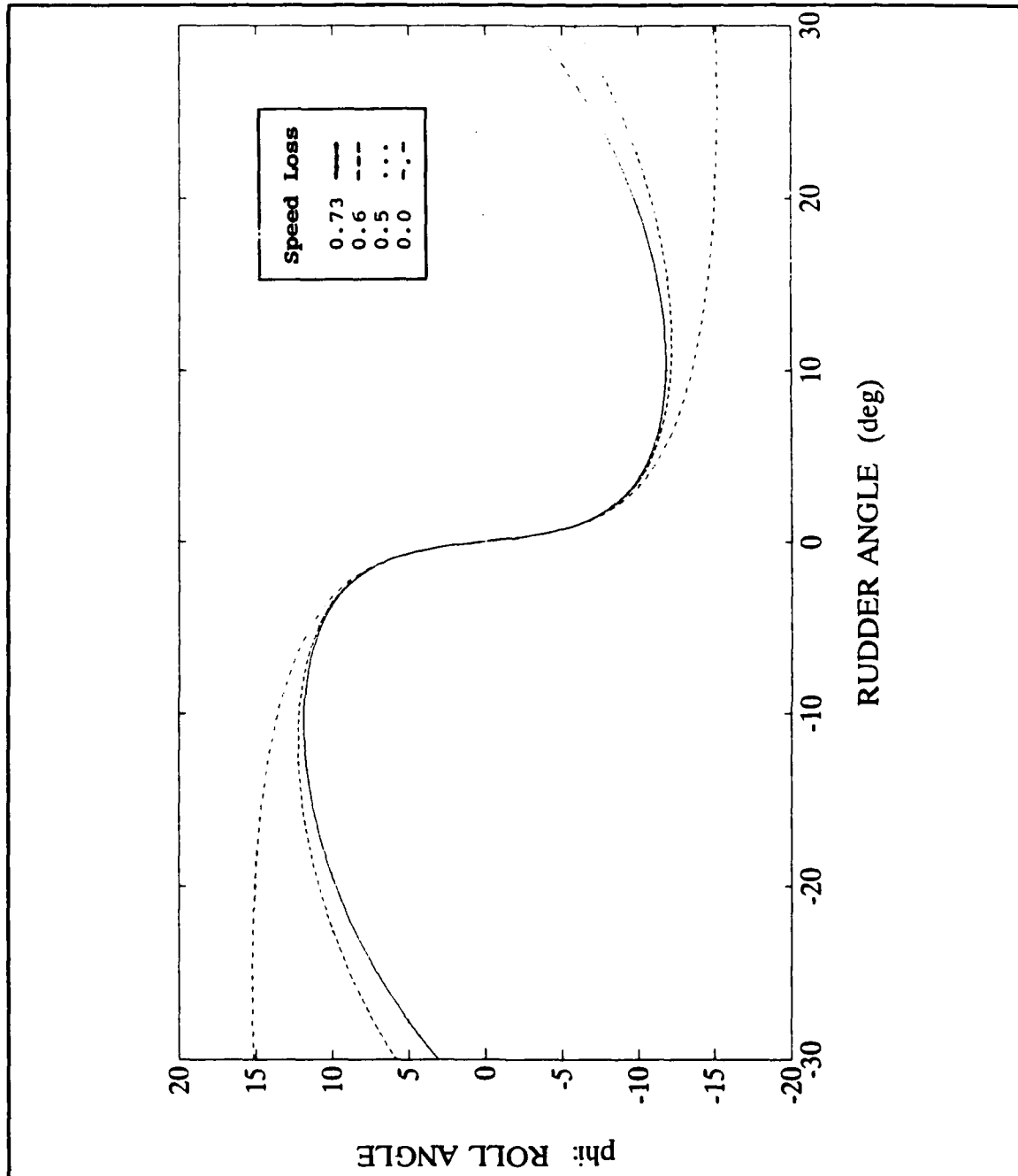Eigenvalues

Fn = 0.3

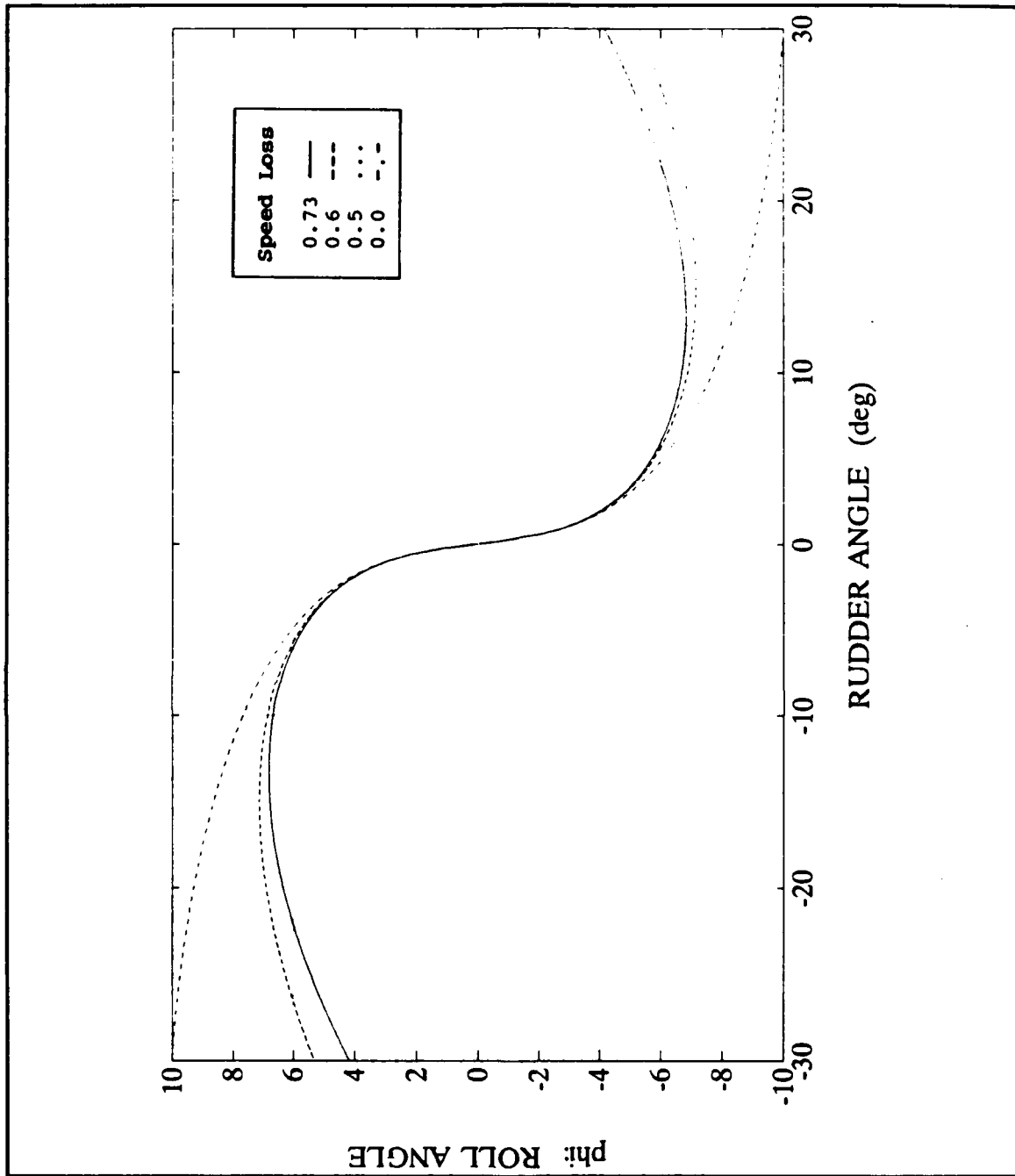B.15: Effect of Speed Loss on Coupled Model Sway Velocity with GM = 1.0 m

Fn = 0.3

B.16: Effect of Speed Loss on Coupled Model Sway Velocity with GM = 3.0 m
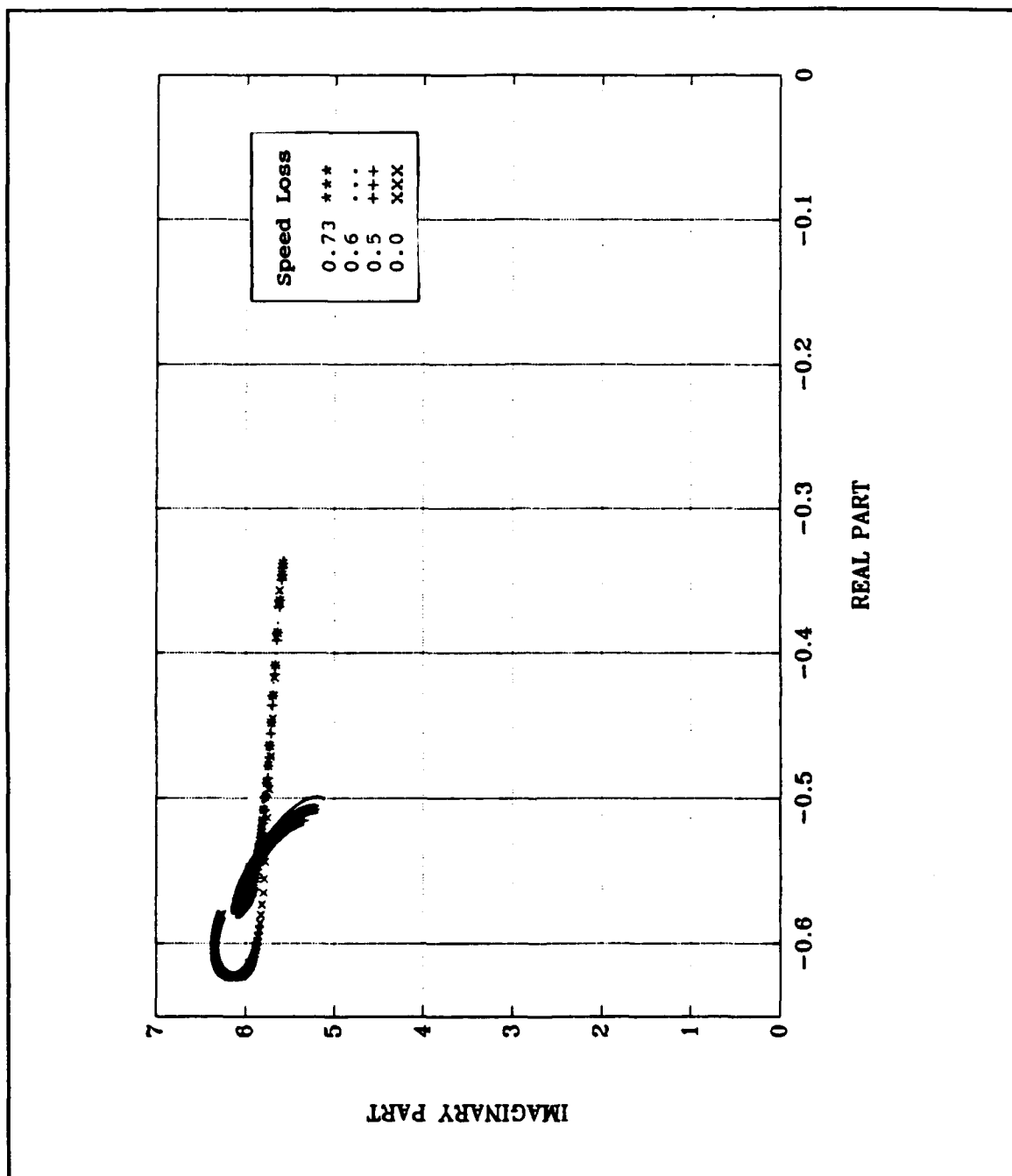
Fn = 0.3

B.17: Effect of Speed Loss on Coupled Model Roll Angle with GM = 1.0 m

99

Fn = 0.3

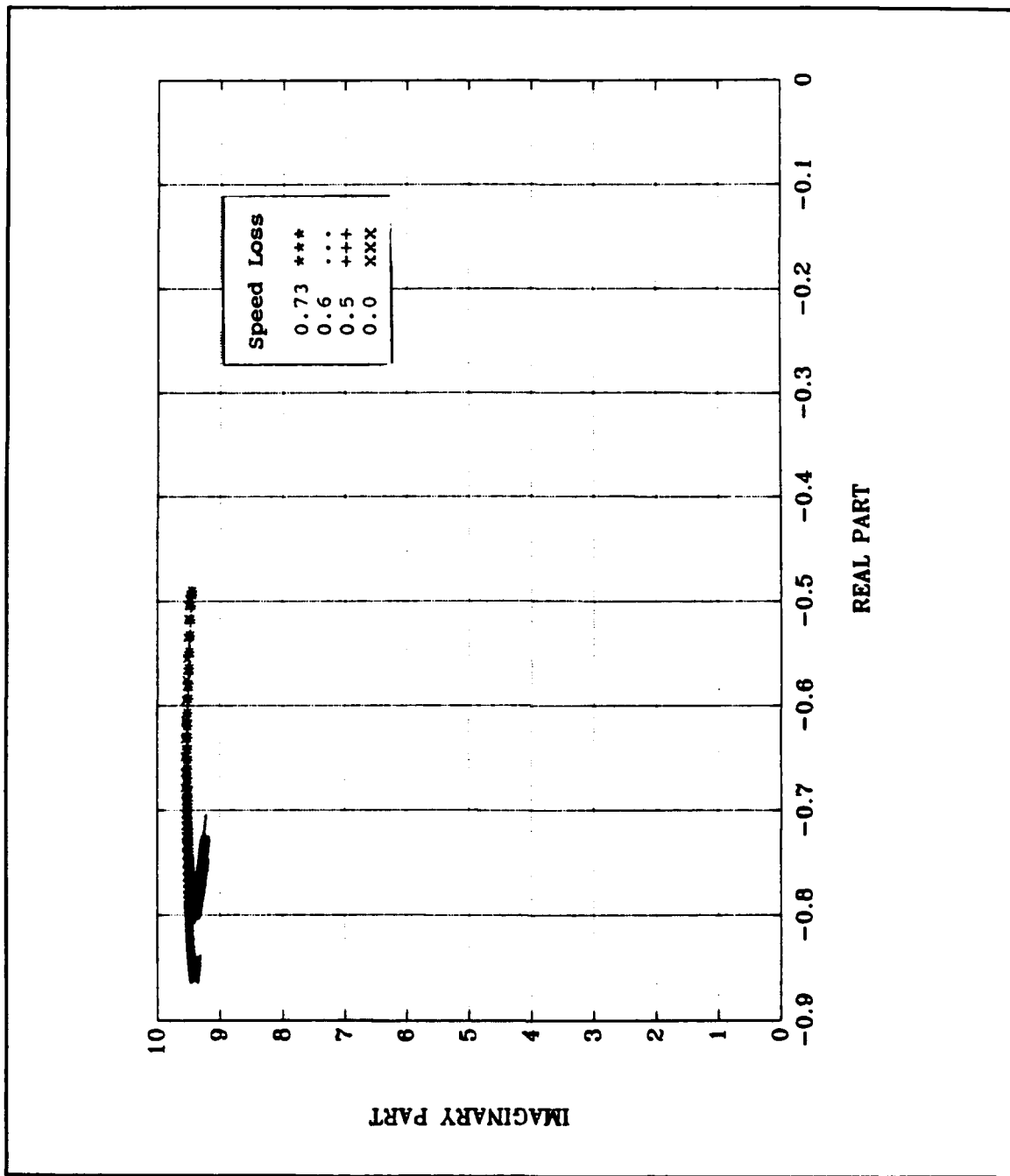**B.18: Effect of Speed Loss on Coupled Model Roll Angle with GM = 3.0 m**

Fn = 0.3

B.19: Effect of Speed Loss on Coupled Model Root Locus with GM = 1.0 m

Fn = 0.3

B.20: Effect of Speed Loss on Coupled Model Root Locus with GM = 3.0 m

LIST OF REFERENCES

1.   Abkowitz, M.A., "Stability and Motion Control of Ocean Vehicles," Initial Course Notes, MIT Press, Cambridge, MA, and London, England, May 1969.

2.   Lewis, E.V., ed., *Principles of Naval Architecture*, The Society of Naval Architects and Marine Engineers, Vol. III, Jersey City, NJ, 1989.

3.   Eda, H., Falls, R. and Walden, D.A., "Ship Maneuvering Safety Studies," *Transactions*, The Society of Naval Architects and Marine Engineers, Vol. 87, pp 229-250, 1979.

4.   Chadwick, J.H., "On the Stabilization of Roll," Annual Meeting of the Society of Naval Architects and Marine Engineers, New York, NY, November, 1955.

5.   Bishop, R.E.D., Burcher, R.K., and Price, W.G., "Directional Stability Analysis of a Ship Allowing for Time History Effects of the Flow," *Proceedings*, The Royal Society of London, A. 335, pp. 341-354, 1973.

6.   Cox, G.G., and Lloyd, A.R., "Hydrodynamic Design Basis for Navy Ship Roll Motion Stabilization," *Transactions*, The Society of Naval Architects and Marine Engineers, Vol. 85, pp. 51-93, 1977.

7.   Baba, E., Asai, S., and Toki, N., "A Simulation Study on Sway-Roll-Yaw Coupled Instability of Semi-Displacement Type High Speed Craft," Second International Conference on Stability of Ships and Ocean Vehicles, Tokyo, Japan, October 1982.

8.   Rutgersson, O., and Ottosson, P., "Model Tests and Computer Simulations: An Effective Combination for Investigation of Broaching Phenomena," *Transactions*, The Society of Naval Architects and Marine Engineers, Vol. 95, pp. 263-281, 1987.

9.   Son, K., and Nomoto, K., "On the Coupled Motion of Steering and Rolling of a High Speed Container Ship," *Journal of the Society of Naval Architects of Japan*, Vol. 150, pp. 232-244, December 1981. (In Japanese)

10.   Vassalos, D., and Spyrou, K., "An Investigation into the Combined Effects of Transverse and Directional Stabilities on Vessel Safety," Strathclyde Marine Center, University of Strathclyde, Glasgow, 1984.

11. Inoue, S., Hirano, M., Kijima, K., and Takashima, J., "A Practical Calculation Method of Ship Maneuvering Motion," *International Shipbuilding Progress,* Rotterdam, Netherlands, Vol. 28, No. 325, September 1981.

12. Bass, D.W., and Haddara, M.R., "Nonlinear Models of Ship Roll Damping," *International Shipbuilding Progress,* Vol. 35, No. 401, pp. 5-24, 1988.

13. Haddara, M.R., and Bennet, P., "A Study of the Angle Dependence of Roll Damping Moment," *Ocean Engineering,* Vol. 16, No. 4, pp. 411-427, 1989.

14. Clarke, D., Gedling, P., and Hine, G., "The Application of Maneuvering Criteria in Hull Design Using Linear Theory," *The Royal Institute of Naval Architects,* Vol. 125, pp. 45-68, 1983.

15. Inoue, S., Hirano, M., and Kijima, K., "Hydrodynamic Derivatives on Ship Maneuvering," *International Shipbuilding Progress,* Rotterdam, Netherlands, Vol. 28, No. 321, 1981.

16. Lewis, E.V., ed., *Principles of Naval Architecture,* The Society of Naval Architects and Marine Engineers, Vol. I, Jersey City, NJ, 1988.

17. More, Jorge, Garbow, B., and Hillsrom, K., "User Guide for MinPack-1," *Argonne National Labs Report,* ANL-80-74, Argonne, IL, 1980.

18. Himeno, Y., "Prediction of Ship Roll Damping-State of the Art," University of Michigan Report No. 239, 1981.

19. Golub, G.H., and VanLoan, C.F., "Matrix Computations," The John Hopkins University Press, Baltimore, MD, 1983.

20. Harding, L.J., "Numerical Analogy and Applications Software Abstracts," The University of Michigan Computing Center, Memo 407, Ann Arbor, MI, p. 94, September 1979.

INITIAL DISTRIBUTION LIST

No. Copies

1. Defense Technical Information Center
   Cameron Station
   Alexandria, Virginia 22304-6145

   2

2. Library, Code 52
   Naval Postgraduate School
   Monterey, California 93943-5002

   2

3. Department Chairman, Code ME
   Department of Mechanical Engineering
   Naval Postgraduate School
   Monterey, California 93943-5000

   1

4. Professor Anthony J. Healey
   Code ME/Hy
   Department of Mechanical Engineering
   Naval Postgraduate School
   Monterey, California 93943-5000

   4

5. LT Mary J. Logsdon
   242 Codell Dr.
   Lexington, Kentucky 40509

   2

6. Naval Engineering Curricular Officer, Code 34
   Department of Mechanical Engineering
   Naval Postgraduate School
   Monterey, California 93943-5004

   1